CHALMERS

Prestress losses in railway sleeper production with long bed systems

Master of Science Thesis in the Master's Programme Structural Engineering and Building Technology

ARNÓR MÁR GUÐMUNDSSON
FREYR GUÐMUNDSSON

Department of Civil and Environmental Engineering
Division of Structural Engineering
Concrete Structures
CHALMERS UNIVERSITY OF TECHNOLOGY
Göteborg, Sweden 2014
Master's Thesis 2014:81

Prestress losses in railway sleeper production with long bed systems

Master of Science Thesis in the Master's Programme Structural Engineering and Building Technology

ARNÓR MÁR GUÐMUNDSSON

FREYR GUÐMUNDSSON

Prestress losses in railway sleeper production with long bed systems
Master of Science Thesis in the Master's Programme Structural Engineering and Building Technology
ARNÓR MÁR GUÐMUNDSSON
FREYR GUÐMUNDSSON

Department of Civil and Environmental Engineering
Division of Structural Engineering
Concrete Structures
Chalmers University of Technology
SE-412 96 Göteborg
Sweden
Telephone: + 46 (0)31-772 1000

Cover:
Overview of a long line casting bed in Vislanda

Prestress losses in railway sleeper production with long bed systems
Master of Science Thesis in the Master's Programme Structural Engineering and Building Technology

ARNÓR MÁR GUÐMUNDSSON
FREYR GUÐMUNDSSON
Department of Civil and Environmental Engineering
Division of Structural Engineering
Concrete Structures
Chalmers University of Technology

ABSTRACT

The design and production of concrete railway sleepers requires optimization to fulfil increasing demands for faster and larger trains and to minimize safety margins. The sleepers are pretensioned to avoid cracking and increase durability. Measurements in factories situated in Vislanda and Marijampolé have shown that unexplained, large prestress losses take place in the first 20 hours after the casting of concrete sleepers with the "Long line method". More knowledge is needed to understand why these prestress losses take place, and therefore be able to meet the increasing demands for the sleepers.

The aim of this master's project was to understand why prestress losses take place during the curing of pretensioned concrete railway sleepers in a long casting bed. In order to achieve that knowledge, a literature study was carried out and a finite element model of the sleepers in a long bed was developed. The analyses were based on linear elastic analysis. The temperature change during the curing was given as an input based on measurements. Prestress losses due to thermal effects were assumed to be of most importance; losses due to other effects were not included. The bond between concrete and steel was modelled as a function of time in the numerical modelling; this was implemented through a user-supplied subroutine. The bond model assumed low bond stresses and a constant stiffness at each time step.

The numerical model could describe the prestress loss behaviour in Vislanda and Marijampolé. However, the magnitude of the losses in Marijampolé was not fully explained. The results showed an accumulation of prestress losses towards the end of the bed, where measurements had been carried out, while the other end did not experience this accumulation effect. The analyses showed that the accumulation occurred due to the bond development, casting sequence and temperature variation along the bed. The greatest prestress losses were obtained when a large temperature increase occurred in the bed before bond developed in the last cast end. From the results it can be concluded that the prestress losses can be decreased by minimizing the casting time and having the same temperature conditions along the entire bed.

Key words: Pretensioned concrete sleeper, prestress loss, long line method, early age concrete, thermal properties of concrete, thermal stresses, bond stress – slip model, transmission length, accumulation of stresses, time dependant linear FE analysis.

II

Contents

Preface

In this thesis, prestress losses that occur during the production of pretensioned railway sleepers were studied. A numerical model was developed to predict the phenomenon. The project was carried out between January and June 2014 at the Department of Civil and Environmental Engineering, Division of Structural Engineering, Concrete structures, Chalmers University of Technology, Sweden. The thesis was a continuation of another thesis by Simon Carlsson and Erik Holmbom from 2012 and initiated by Abetong AB.
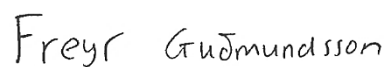
This project was carried out by Arnór Már Guðmundsson and Freyr Guðmundsson. The literature study and the development of the model were carried out to an equal amount by both. However, Arnór took the main responsibility for generating the results and Freyr for writing about them.

We would like to thank our supervisors Ph. D Rikard Bolmsvik, Abetong and Professor Karin Lundgren for their support and excellent guidance throughout the project work. Furthermore, we would like to thank our opponents Guðjón Ólafur Guðjónsson and Jón Grétar Höskuldsson for their feedback during this project.

Göteborg, June 2014

Arnór Már Guðmundsson   Freyr Guðmundsson

Notations

Roman upper case letters

A_c	Area of concrete cross section
A_I	Area of transformed concrete section
A_s	Area of steel cross section
C_m	Moisture correction factor
E	Apparent activation energy
E_c	Young's modulus of concrete
E_s	Young's modulus of steel
F_{cT}	Internal restraint force, case 1
F_{cTF}	Internal restraint force in case of full restraint, case 1
F_{sT}	Internal restraint force, case 2
F_{sTF}	Internal restraint force in case of full restraint, case 2
N_c	External restraint force, case 1
N_{Fc}	External restraint force in case of full restraint, case 1
N_{Fs}	External restraint force in case of full restraint, case 2
N_s	External restraint force, case 2
R	Universal gas constant
R_{ext}	External restraint degree
R_{int}	Internal restraint degree
T	Average absolute temperature of concrete during time interval Δt
T_r	Absolute reference temperature
ΔT	Change in temperature
V_{agg}	Volume of aggregates in mix
V_{conc}	Total volume of concrete mix
V_{paste}	Volume of cement paste in mix

Roman lower case letters

a_i	Constant that depends on concrete composition
b_i	Constant that depends on concrete composition
f_c	Compressive strength of concrete
f_c^{28d}	Compressive strength of concrete at the age of 28 days
f_{ct}	Tensile strength of concrete
l	Length of member

t	Age of concrete
t_e	Equivalent age

Greek letters

α	Ratio of Young's modulus
$\alpha_{agg,i}$	CTE of ith aggregate
α_{cTc}	Coefficient of thermal contraction of concrete
α_{conc}	Coefficient of thermal expansion of concrete
α_{mTx}	Coefficient of thermal expansion
α_{paste}	CTE of cement paste
α_{sTc}	Coefficient of thermal contraction of steel
ε_c	Stress dependent strain, case 1
ε_{cT}	Stress independent strain, case 1
ε_{mT}	Thermal strain
ε_s	Stress dependent strain, case 2
ε_{sT}	Stress independent strain, case 2
σ_c	Concrete stress, case 1
σ_s	Final prestress change
σ_{s1}	Steel stress, case 1
σ_{s2}	Steel stress, case 2

1 Introduction

The railway system is an important part of modern transportation. Trains have had a great influence on the industry, human expansion and the ability to travel over the last 200 years. Ever since it was invented, this way of transportation has always been a technical issue and constantly improving. In the beginning, steam trains were used with timber sleepers. With time, concrete sleepers have become more widely used due to durability, the tracks being more stable and other reasons. A great amount of concrete sleepers is produced around the world every day. Therefore, an optimization of the production is an important task to reduce costs and the use of materials (Train history, n.d.).

1.1 Background

With time, demands for railway sleepers increase with increased speed and loads on the railway tracks. Railway sleepers have been designed with large safety margins since the knowledge about the mechanical behaviour during the production has lacked. With increasing demands this safety margin decreases. Now, the production almost utilises the full prestress capacity in order to fulfil the load requirement set for the sleepers.

One solution to increase the prestress capacity of the sleepers would be to invest in new casting moulds. That is not a favourable choice for Abetong AB since that would be a very expensive investment. Therefore it is important to increase the knowledge of the mechanical behaviour of the concrete during production, keeping the same moulds. Along with being less expensive, an optimisation of the present method of production would be more sustainable since less material would be used.

Measurements have shown that unexplained prestress losses take place in the concrete curing process and vary between the ends of the casting bed. The losses also vary between factories that have different production conditions.

The results of these measurements have been evaluated in previous master's studies (Carlsson, Holmbom, 2012). Those studies didn't manage to develop a proper finite element (FE) model to capture the behaviour that takes place, but the results indicate that a better knowledge regarding the development of the bond between concrete and steel during curing would be needed to capture the phenomena.

1.2 The long line method

The casting method used by Abetong is called "The long line method" in the production of railway sleepers. This method was invented in 1960 and licenced six years later. Today there are 35 licenced sleeper plants all around the world using the long line method.

Figure 1.1.   Licenced plants using the long line method around the world, modified from Abetong (2014).

The idea of producing sleepers with the long line method is to create high quality sleepers in a safe, efficient and reliable process. To obtain good quality, the sleepers have to meet various requirements.

Railway sleepers play a vital role in the structural demands for railways. They contribute to distribution of vertical load and lateral movements induced by trains. The most commonly used sleeper today is the prestressed mainline monoblock sleeper, see Figure 1.2. The railway sleepers have demanding technical requirements combined with strict dimensional requirements. To reduce the maintenance and increase the lifetime of the sleepers, they are prestressed to decrease the risk of cracking. Prestressing protects the sleeper from the risk of corrosion and damage due to fatigue loading which is a high risk (Gustavson, 2002).
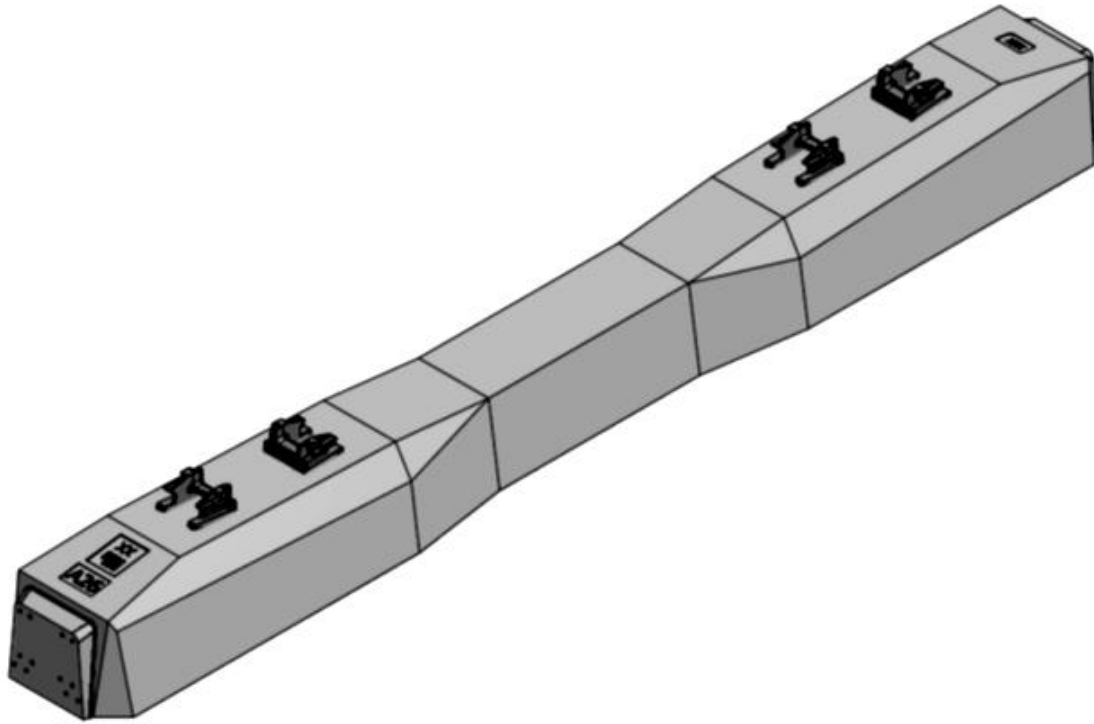
Figure 1.2.   Prestressed mainline monoblock sleeper, from Carlsson, Holmbom (2012).

The long line method is a production where sleepers are cast in a line using 100 to 150 m long beds. Typically in a sleeper production plant there are four or more casting beds in which a number of casting moulds are placed (Abetong, 2013).

The production of sleepers is done in certain casting steps. The first step is preparation of the moulds for casting by cleaning and oiling. The cast-in fastening components are placed in the mould. Then a specific number of steel wires are placed in a predetermined position in each line. They are then pre-tensioned by a hydraulic jack to give a certain initial prestress force. Before casting, the mould has to be lifted to an upper casting position. Then the casting can start, it is performed with an automatic casting machine that guaranties a continuous process. The casting process can take from 1 up to 3 hours from one end of the bed to the other. The casting time varies between plants but is most commonly 2 hours. After casting, the moulds are covered with tarpaulins to preserve the heat and humidity in the concrete (Bolmsvik, 2013).

The sleepers are allowed to cure in the moulds for approximately 16 hours until the bond capacity between the concrete and steel has reached sufficient strength. The sufficient bond capacity is checked by testing the compressive strength of the concrete and monitoring the temperature rate. When the temperature starts to decrease and the compressive strength has reached 35 MPa, the sleepers are safe for release of the prestressing force. After release of prestress, the sleepers are de-moulded by lowering the moulds to a lower position. The sleepers are then transferred to a cutting machine where they are cut to exact length with a diamond saw. The sleepers then go through a final treatment where the fastening components are assembled and the sleepers are inspected before they are ready for delivery to the costumer (Bolmsvik, 2013).

Figure 1.3.   Production equipment used in "The long line method" from Carlsson, Holmbom (2012).

1.3   Purpose and objectives

The purpose of this master's project is to understand why prestress losses take place during the curing of pretensioned concrete railway sleepers in a long casting bed. The aim is to establish a FE model including the following:

- Early age behaviour of concrete
    - o Temperature change with time due to hydration of concrete.
    - o The development of bond between steel and concrete.
    - o Other concrete mechanical properties
- The casting sequence in "The long line method".
    - o Casting time
    - o Length of casting bed
- Boundary conditions

Then, the most important parameters influencing the thermal stresses can be identified and a parameter study performed to investigate the influence of varying parameters. This can lead to an optimization of the production process.

1.4   Scope and method

Analytical and numerical models were established along with a theoretical study. The analytical model was used only to verify the numerical model by simple checks. The numerical model was the main tool used to be able to include all important factors in the process. First, a small scale numerical model was established to gain understanding and to simplify the modelling procedure. A user-supplied subroutine for including the increasing bond stiffness was developed for the FE analysis. Then, the model was extended to a full scale model that had the same dimensions as the real structure. All effects that possibly arise due to the length of the bed could be included in the full scale model. Thermal stresses representing the prestress losses could then be obtained as a function of time and compared with the measured stress values.

1.5   Limitations

The thesis was focused on the prestress changes taking place during hardening of the concrete; therefore the process of tensioning the tendons was not included. To decrease the complexity of the model, the simulation of the transient heat analysis was excluded, instead measured temperature values were used as an input. Shrinkage of the concrete and stress relaxation of the steel along with other factors affecting the steel wire were not included in this work, because the previous thesis work on this subject concluded that these properties do not have much effect on the prestress (Carlsson, Holmbom, 2012). Also, the prestress losses caused by the release of prestress were not of interest.

The bond strength development for early age concrete has not been researched much. Therefore, further studies are needed on how the bond develops with time, which is not within the scope of this report.

1.6   Outline of contents

Introduction to the subject including: background, purpose and objects, scope and limitations can be found in Chapter 1. In Chapter 2, the general material and mechanical behaviour along with an analytical model are presented. The measured data that this work is based on is presented in Chapter 3. The development and verification of the numerical model are presented in Chapter 4. Chapter 5 presents the input data used for the analysis imitating the measured data, and the results are presented in Chapter 6. The knowledge gained through a parameter study is presented in Chapter 7. Final remarks can be found in the last chapter.

2   Materials and mechanical behaviour

This study focuses on what drives the prestress changes in the tendons and the main parameters limiting the stress change. The most affecting properties in these studies have been found to be the deformation caused by temperature change in concrete. This temperature change is assumed to occur in the tendon as well since the steel has high conductivity. It has also been noticed that the concrete acts as a restraint to the steel, therefore affecting the stress change taking place. The focus in this study was for the first hours after casting of concrete, therefore it was vital to study the development of the following properties from the start. The following subchapters explain the most important factors.

2.1   Temperature development

2.1.1   Hydration

Concrete is a complex material consisting of several heterogeneous components, water, cement, aggregates and admixtures. Mechanical and thermal properties of concrete are affected by various factors, such as types of material used and volume ratios of aggregate, concrete temperature, water content, porosity, etc. (Kim, Kim, Yang, 2000).

The key component of concrete mixture is cement. When hydrated it binds the aggregates together to form the hard, strong and monolithic whole (Domone, Illston, 2010). Hydration of cement is the reaction between cement particles and water, including chemical and physical processes. The fresh concrete properties, such as setting and hardening, are the direct results of hydration. The properties of hardened concrete are also influenced by the process of hydration. Cement hydration is a complex physical–chemical process. During the process, a cement–water mixture is changed from a fluid state to a porous solid state called cement paste (Li, 2011).

In the hydration process silicates and aluminates in the cement is hydrated with time to make a firm and hard mass of solid concrete (Neville, 2003).

The hydration process can be split up to three main chemical reactions, expressed as:

$$2C_3S + 6H \rightarrow C_3S_2H_3 + 3Ca(OH)_2$$

$$2C_2S + 4H \rightarrow C_3S_2H_3 + Ca(OH)_2$$

$$C_3A + 6H \rightarrow C_3AH_6$$
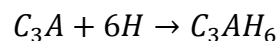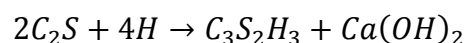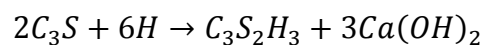
The chemical reaction for Tricalcium silicate (C_3S) has a fast exothermic reaction at the early stage. It contributes most to early strength of the concrete. The Dicalcium silicate (C_2S) reaction on the other hand reacts very slowly and contributes little heat. It contributes most to the long-term strength of concrete (Li, 2011).

Calcium silicate hydrate ($C_3S_2H_3$), often referred to as gel, is assumed to be the final production of Di- and Tricalcium silicates. For Portland cement it is believed to provide major strength, due to its small scale and amount. The gel occupies about 50% of the structural components in a cement paste (Li, 2011).

The Tricalcium aluminate (C_3A) is a more complex reaction than the calcium silicate reactions. Rate of Tricalcium aluminate reaction is controlled by the amount of gypsum added to the mix. The reaction is exothermic and contributes to the early strength (Neville, 2003).

Figure 2.1 shows the strength development of constituents with time.

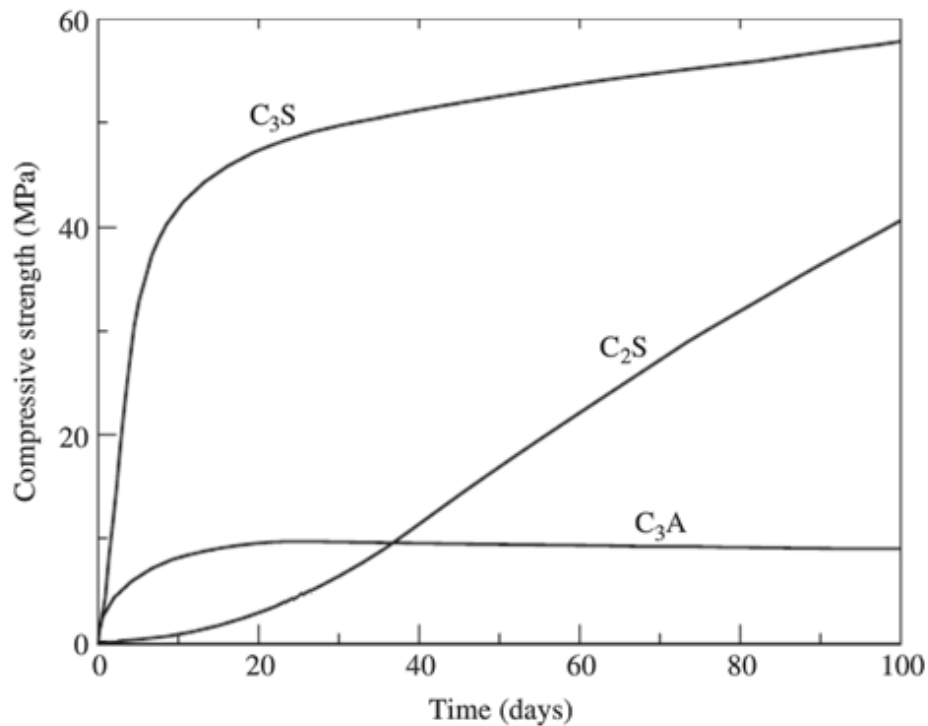*Figure 2.1.   Strength development of constituents in cement. C_3S, C_3A contribute to early strength of the concrete and C_2S affects the final strength of the concrete. Modified from Li (2011).*

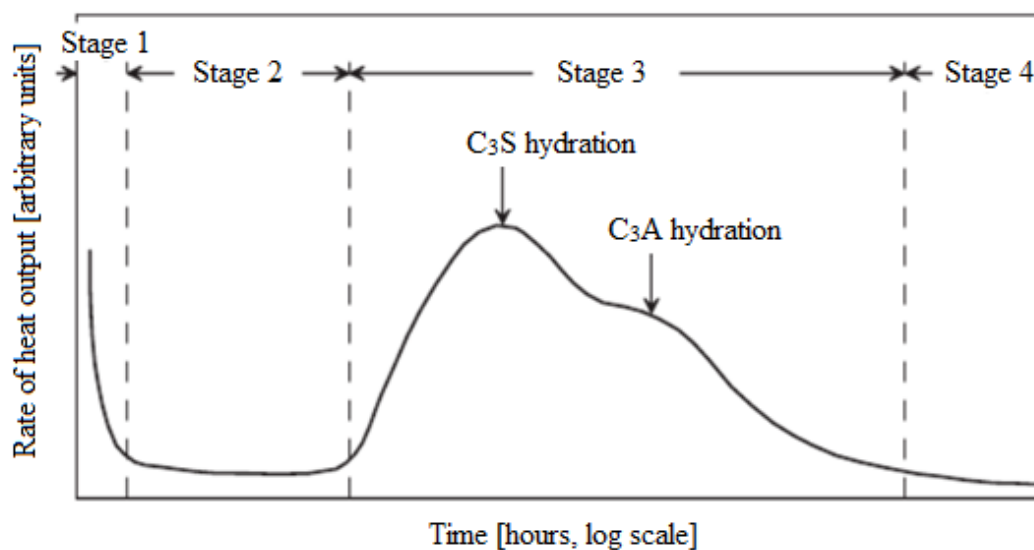Figure 2.2 shows the rate of heat output during the hydration process.

Figure 2.2.   Rate of heat output, different stages show where different exothermic reactions occur. Modified from Li (2011).

Stage 1 in Figure 2.2, is a reaction of gypsum and is not significant to any early strength formation in the concrete. This short peak lasts only few minutes during the mixing of the concrete. Stage 2 in Figure 2.2 is called dormant period, when the cement is relatively inactive (Domone, Illston, 2010).

The (C_3S) hydration is very exothermal as mentioned before. The reaction starts to increase rapidly at a time corresponding to the initial set, between stage 2 and 3 in Figure 2.2. The strength gain does not happen until after the final set which happens some hours later before the heat development reaches a peak, when most of the (C_3S) has hydrated and the concrete is ready to carry some load (stage 3 in Figure 2.2). Then the rate of hydration slows down. Another peak occurs somewhat after the (C_3S) peak. This second heat increase is due to (C_3A) hydration (Neville, 2003).

2.1.2 Rapid hardening

Portland cement type III is a rapid hardening concrete with great amount of (C_3S) and (C_3A). Those properties give high early strength as Figure 2.1 shows. As the name implies, rapid hardening cement develops strength faster and is described as high early strength cement. Rapid hardening cement gives higher rate of heat development, though the initial set is not changed from ordinary cement (Neville, 2003).

2.1.3 Maturity

Strength of concrete depends on both time and temperature. Maturity is an expression of how strength changes with time and temperature. It is defined as the equivalent time the concrete has been curing. Equivalent age gives an estimation of how old the concrete would be if cured at a reference temperature. Ambient temperature affects the rate of the chemical hydration process. By using recorded temperature history the equivalent age can be estimated (Carino, Lew, 2001).

$$t_e = \sum_0^t e^{\frac{-E}{R} \cdot \left(\frac{1}{T} - \frac{1}{T_r}\right)} \cdot \Delta t \qquad (2.1)$$

Where
t_e = The equivalent age at the reference temperature

E = Apparent activation energy

R = Universal gas constant

T = Average absolute temperature of concrete during time interval Δt

T_r = Absolute reference temperature

2.2 Concrete strength development

The concrete develops its strength and stiffness during the hydration process. During the dormant period, the concrete is in a plastic, workable phase and will deform very easily. 1 to 3 hours after casting, at time corresponding to the initial set, needle like hydration products start to grow outwards from the cement grain surface to form a three dimensional network in the mixture. This network will gradually hinder the movements of the particles in the cement paste, making it stiffer, but no strength has developed yet. After the final set of the mixture, the amount of hydration products increases and consequently the concrete hardens and linking forces become stronger.

When the linking forces become stronger, the skeleton of hydration products becomes more stable and the concrete strength increases (Lundgren 2005).

2.2.1 Compressive strength

The concrete strength development depends on complex interactions between different factors. For simplification, these factors can be discussed separately under the following three different categories:

- Characteristics and proportions of materials
- Curing conditions
- Testing parameters

The first category involves the actual concrete mixture ingredients, the second involves the temperature and humidity during curing and the third involves how concrete strength tests are influenced by parameters in the tests. The second category is considered to be the most relevant for this thesis and will therefore be looked at in more detail (Metha, Monteiro, 2001).

Curing of concrete involves controlling three factors immediately after the placing of concrete to the formwork. Those factors are: time, humidity and temperature.

The change of concrete strength with age can be estimated by the following empirical equation, see Byfors (1980):

$$f_c = \frac{a_1 \cdot t^{b_1}}{1 + \frac{a_1}{a_2} t^{b_1 - b_2}} \cdot f_c^{28d} \qquad (2.2)$$

Where t = Age of concrete

f_c = Compressive strength of concrete at age, t.

f_c^{28d} = Compressive strength of concrete at the age of 28 days

a_i, b_i = Constants that depend on the concrete composition

Equation (2.2) is based on experiments carried out to be able to describe the strength gain during the first hours after casting and is assumed to capture the behaviour better than the relations in Eurocode, EC2. The constants, a_i and b_i were chosen for rapid hardening Portland cement and final compressive strength of 60 MPa (Springenschmid, 1998), which is close to the properties of the sleepers; see Table 3.1 and Table 3.2. The relation between concrete compressive strength and age can be seen in Figure 2.3.

Figure 2.3.   Compressive strength as a function of concrete age.

Figure 2.3 shows that the strength is very low until around 7 hours after casting when it starts to increase quite rapidly.

Generally, time-strength relationships assume moist curing conditions and normal temperatures. For concrete cured at different temperature than 20°C, the age, t must be adjusted with the equivalent time function, (2.1) (Byfors, 1980).

Ambient humidity can have a large influence on the development of the concrete strength. The highest ultimate strength is obtained when the concrete is moist-cured for the entire curing time. However, it can be assumed that the curing relative humidity does not affect the strength gain during the first 3-4 days for a curing temperature of 20°C (Byfors, 1980). Therefore, it can be concluded that the relative humidity is not of importance in this study.

The curing temperature influences the hydration process considerably and therefore influences the strength development. This influence is often taken into account through maturity functions like the previously mentioned equivalent time. Experimental results show a clear difference in strength growth at different curing temperatures, the strength development starts earlier for higher curing temperatures and therefore the strength is higher during the first hours for higher temperatures. With time, this behaviour is reversed and higher ultimate strength is reached for lower curing temperatures (Byfors, 1980).

2.2.2   Young's modulus

The elastic behaviour of concrete is characterised by the volume fraction, the density and the modulus of elasticity of the cement paste and aggregates along with the characteristics of the transition zone. Usually, the elastic modulus is expressed with a direct relation to the strength and the density. The relation to the strength is reasonable since both factors are directly related to the porosity of the constituent phases in the concrete (Metha, Monteiro, 2001).

The relation between Young's modulus and compressive strength can be described by the following empirical equation, see Byfors (1980).

$$E_c = \frac{9.93 \cdot 10^3 \cdot f_c^{2.675}}{1 + 1.370 \cdot f_c^{2.204}} \qquad (2.3)$$

Where $\quad E_c$ = Young's modulus of concrete

$\qquad\qquad f_c$ = Compressive strength of concrete

Equation (2.2), which gives the relation between the compressive strength and age, can be used with equation (2.3) to obtain the Young's modulus as a function of age. Figure 2.4 shows the Young's modulus as a function of age:
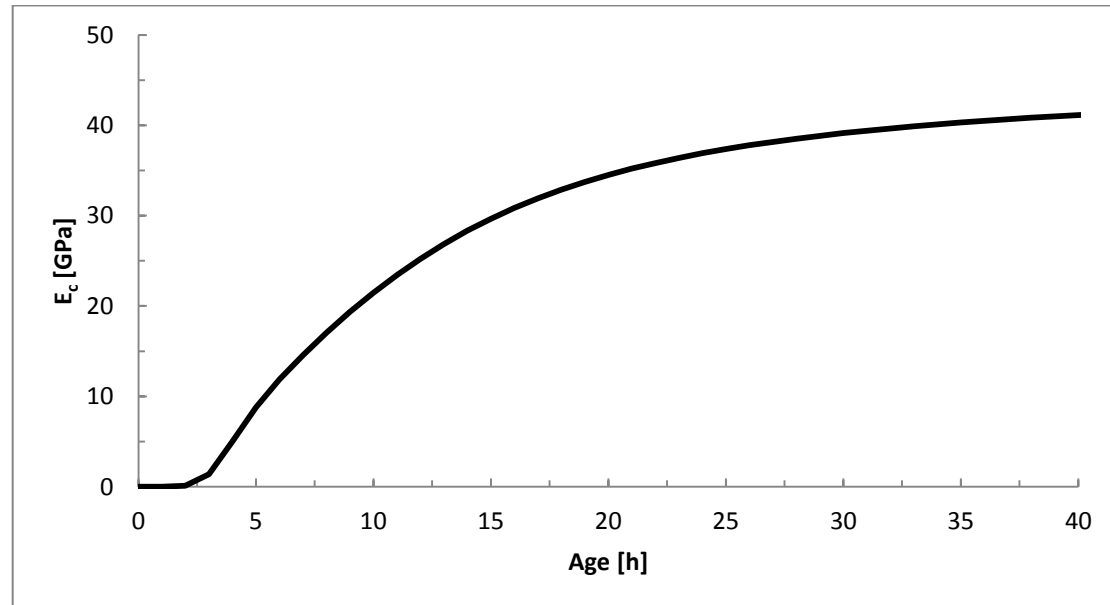

Figure 2.4.   Young's modulus as a function of concrete age.

The graph shows that the stiffness is developing from 3 hours after casting when the value is around 1 GPa up to 20 hours when a high value is reached (around 35 GPa). No great changes will occur after that.

2.2.3   Tensile strength

The main influencing factors for the tensile strength development at early ages are the same as for the compressive strength development. For that reason, the shapes of the curves for the compressive- and tensile strengths are expected to be similar. The relation between the compressive- and tensile strengths has been studied in many different researches, from which the tensile strength as a function of age can be obtained using equation (2.2). Such a relation has been presented by Byfors (1980), with the following expression which has been shown to provide a good adaptation:

$$f_{ct} = \begin{cases} 0.082 \cdot f_c^{1.09} & f_c \leq 20 MPa \\ 0.105 \cdot (f_c - 20) \cdot 0.839 + 2.28 & f_c > 20 MPa \end{cases} \qquad (2.4)$$

Where $\quad f_{ct}$ = Tensile strength of concrete

Equations (2.2 and 2.4) have been used to obtain the graph in Figure 2.5, which shows the tensile strength as a function of the concrete age:
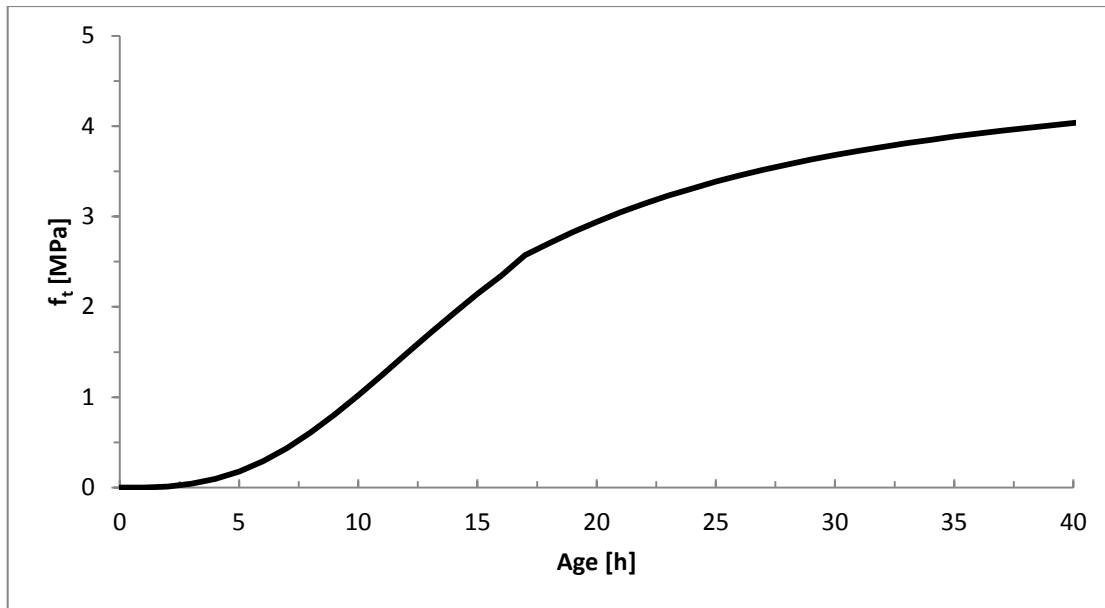
Figure 2.5. Tensile strength as a function of concrete age. Obtained from equations (2.2 and 2.4).

The figure shows that the tensile strength starts to develop at around 5 hours after casting and develops rapidly up to around 20 hours where the slope changes and the strength gain becomes slower. This will be particularly useful when the bond strength development will be estimated later on in the thesis.

2.3   Bond behaviour

The bond between concrete and steel arises from friction, adhesion and mechanical interlocking between the two materials. A critical property affecting the bond strength is the tensile strength of the concrete. The bond for hardened concrete is usually expressed as being proportional to the square root of the tensile strength (Neville, 2003). For that reason it can be assumed that the bond strength starts to develop at the same time as the tensile strength, i.e. around the time of initial set.

The prestress force is transferred from the tendon to the concrete surrounding it by bond stresses within a certain length called the transmission length (Engström, 2011a). The transmission length is affected by the prestress force and the bond strength and stiffness between the concrete and the steel.

The bond stress-slip relationship is commonly measured with a pull-out test. This test measures the bond stress-slip relationship with certain properties. Since the focus in the report is on the first hours the general pull-out test does not describe fully how the bond stress-slip develops over time; still, such tests can show how the final bond stress-slip relationship is. Therefore a linear increase of bond stiffness was assumed, see Section 5.3.

2.4   Thermal coefficient

The thermal coefficient is a ratio of how much temperature change affects deformations in a material, it can be expressed in the following way, see Engström (2011b):

$$\varepsilon_{mT} = \alpha_{mTx} \cdot \Delta T \qquad\qquad (2.5)$$

Where ε_{mT} = Thermal strain, m for material

α_{mTx} = Coefficient of thermal expansion, m for material and x for expansion or contraction

ΔT = Change in temperature

The coefficient of thermal contraction (CTC) is assumed to be of minor importance since the prestress losses occur during the heating phase. Therefore, it is assumed for simplification that the CTC is equal to the coefficient of thermal expansion (CTE). The resulting strain will be the same with opposite directions. Thus, temperature decrease results in contraction and temperature increase in expansion.

The coefficient of thermal expansion varies for different steel types. CTE for high strength steel varies between $9.9 - 13 \cdot 10^{-6} \, 1/°C$ (ASM, 2002).

The knowledge of the CTE of concrete is vital to know the stresses from thermal changes that arise from the hydration process of concrete. The CTE of hardened cement paste varies due to concrete age and the moisture content (Domone, Illston, 2010).

The CTE of cement paste is a function of several factors such as age, moisture content and cement fineness.
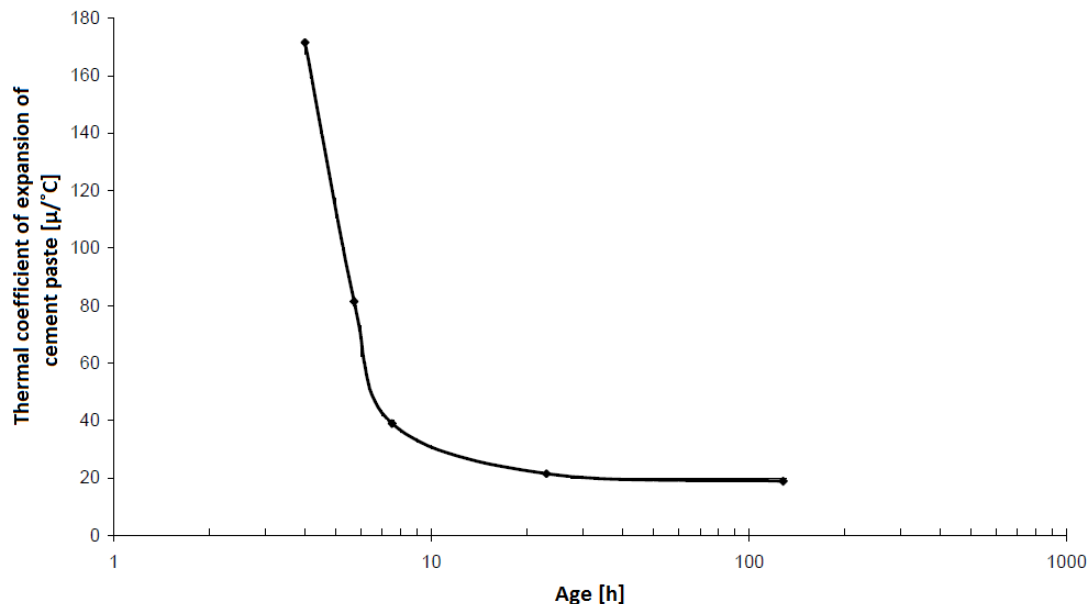

Figure 2.6.   Thermal coefficient of thermal expansion of cement paste as a function of concrete age. Modified from McCullough, Rasmussen (1998).

Figure 2.6 shows the age dependency of the CTE, where the CTE is very high in the first hours and decreases rapidly to a constant value after 11 hours.

Typically CTE of hardened cement paste is larger than the aggregates. Therefore the cement paste usually governs the total expansion of concrete. The CTE for aggregates is constant with age and is dependent on chemical and mineral composition of the aggregates. Aggregates can have thermal coefficient of $4 - 12 \cdot 10^{-6} \, 1/°C$ (McCullough, Rasmussen 1998).

The ratio and combination of aggregates and cement paste control the final CTE of concrete. The following expression can be used to determine the CTE for concrete, see McCullough, Rasmussen (1998):

$$\alpha_{conc} = C_m \left[\sum_{i=1}^{\# \, of \, aggs} \left(\alpha_{agg,i} \cdot \frac{V_{agg,i}}{V_{conc}} \right) + \alpha_{paste} \cdot \frac{V_{paste}}{V_{conc}} \right] \qquad (2.6)$$

Where C_m = Moisture correction factor

$\alpha_{agg,i}$ = CTE of ith aggregate

α_{paste} = CTE of cement paste

V_{agg} = Volume of aggregate in mix

V_{paste} = Volume of cement paste in mix

V_{conc} = Total volume of concrete mix

2.5   Analytical model

To describe the phenomenon of the prestress losses in a simple way an analytical calculation model was established. It is based on the model in Engström (2011b); internal- and external restraint degrees are used along with other material parameters. A restraint degree is a ratio that gives an expression to what extent a free movement of a structure is restrained. For full prevention of movements, the ratio equals 1, while the ratio is 0 when the structure can move completely freely. The restraint degree can be expressed in the following way:

$$restraint \, degree = \frac{actual \, imposed \, strain}{imposed \, strain \, in \, case \, of \, full \, restraint} \qquad (2.7)$$

Where *the actual imposed strain* is the stress-dependent strain that is created when the need for movement is prevented. *The imposed strain in case of full restraint* is the strain that would be created in the structure if the movements would be fully prevented (Engström, 2011b).

The restraint degree is dependent on the stiffness of the boundaries and the structural member. The external restraint degree represents the prevention of free movements that is provided by the external boundaries. The internal restraint degree arises if different parts of the cross-section of the member have different stress-independent strains (due to thermal- or stiffness properties for instance) and a tendency to move separately while being connected to each other. That creates stresses since the parts will then try to prevent each other from moving. Concrete and steel have different stiffness properties and at a certain point, also different thermal properties.

Because the temperature in the concrete is changing, the temperature of the steel wire changes as well, due to high conductivity of steel. Thus, both materials will try to deform at the same time because of the temperature changes. The deformations change the stresses of the materials. In this model it is assumed that the deformations

for the different materials can be considered to work independent of each other as for two load cases which are then combined by superposition. The easiest way to explain how the model works is to look at the cooling phase of the process. Then full bond can be considered and material parameters considered constant.

2.5.1   Case 1: Concrete cooling

The following figure can be considered to explain the concrete cooling process. The 5 steps in the figure are used to develop the equations presented nedan. Steps 1a and 1b show the initial state of concrete (1a) and steel (1b) before any stresses have developed in the materials. Step 2 represents the free concrete contraction where the concrete is deformed but doesn't experience any stresses. Since the steel should have the same deformations due to strain compatibility, step 3 shows the internal restraint force F_{cT} that is applied to the steel in order for the deformations to fit. Now, the materials are combined and the force that was previously applied in compression to the steel is released and will act in tension to the transformed concrete section. That is shown in step 4, which then represents the internal restraint (bond). The last step shows how an external restraint force would pull the whole section back to its original position if full external restraint would be present.
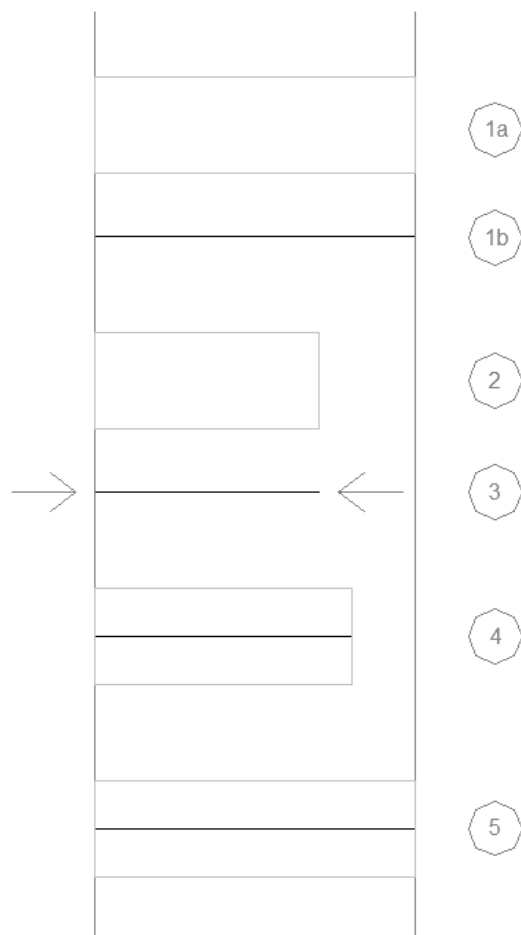

Figure 2.7.   Scheme to understand concrete cooling

Different deformations must fit and therefore, compatibility must be fulfilled. The compatibility condition can be established by adding up all different deformations in the combined concrete and steel material. For full external restraint and without including prestress, the deformations must equal 0 and the compatibility condition becomes:

$$\varepsilon_c \cdot l + \varepsilon_{cT} \cdot l = 0 \qquad (2.8)$$

Where ε_c = Stress dependent strain

l = Length of member

ε_{cT} = Stress independent strain

The stress independent strain develops due to the temperature decrease. Using equation (2.5), the strain can be expressed in the following way:

$$\varepsilon_{cT} = \alpha_{cTc} \cdot \Delta T \qquad (2.9)$$

Where α_{cTc} = Coefficient of thermal contraction for concrete

ΔT = Temperature change, time dependent

The stress dependent strain develops because the strain due to temperature change must be counteracted by restraint forces. That creates stresses in the material and therefore, also strain, which can be expressed as:

$$\varepsilon_c = \frac{N_{Fc} + F_{cT}}{E_c \cdot A_I} \qquad (2.10)$$

Where N_{Fc} = External restraint force in case of full restraint

F_{cT} = Internal restraint force

E_c = Young's modulus of elasticity of concrete

A_I = Area of transformed concrete section

The internal restraint force results from step 3 in Figure 2.7. When the concrete contracts, the steel acts as an internal restraint on the concrete. Therefore, the restraint force is considered to be acting on the steel. In the case of full internal restraint, the restraint force becomes:

$$F_{cTF} = E_s \cdot \varepsilon_{cT} \cdot A_s \qquad (2.11)$$

Where E_s = Young's modulus of steel

A_s = Area of steel cross section

In the general case, the bond could be less than full. The actual internal restraint force can therefore be expressed as:

$$F_{cT} = R_{int} \cdot F_{cTF}$$

Where R_{int} = Internal restraint degree, constant for cooling

The transformed concrete section represents the transformation of the steel cross section to concrete material, through the ratio of Young's modulus, α.

$$A_I = A_c + (\alpha - 1) \cdot A_s \qquad (2.12)$$

Where A_c = Area of concrete cross section

$$\alpha = \frac{E_s}{E_c}, \text{ratio of Young's modulus}$$

Now, combining equations (2.8) and (2.10) gives:

$$\frac{N_{Fc}+F_{cT}}{E_c \cdot A_I} = -\varepsilon_{cT} \qquad\qquad (2.13)$$

This gives an expression for the external restraint force in case of full restraint:

$$N_{Fc} = -\varepsilon_{cT} \cdot E_c \cdot A_I - F_{cT} \qquad\qquad (2.14)$$

The external restraint degree will be partial since the steel is fully fixed to the boundary but the concrete is not. However, the restraint degree can only be varied with this parameter, thus the two materials must have the same restraint degree. To vary it, N_{Fc} should be multiplied by the external restraint degree:

$$N_c = R_{ext} \cdot N_{Fc} \qquad\qquad (2.15)$$

Where $\qquad R_{ext}$ = External restraint degree

Knowing the restraint forces, the concrete stress can be expressed as (from steps 4 and 5 in Figure 2.7):

$$\sigma_c = \frac{N_c+F_{cT}}{A_I} \qquad\qquad (2.16)$$

The steel stress will react in proportion to the stiffness ratio, α and internal restraint R_{int}, along with the stress from step 3 in Figure 2.7.

$$\sigma_{s1} = \frac{-F_{cT}}{A_s} + R_{int} \cdot \alpha \cdot \sigma_c \qquad\qquad (2.17)$$

In this case, during concrete cooling, the steel will be subjected to compressive stress since it needs to be compressed to have strain compatibility with the concrete when it contracts. That results in prestress losses. In the case of full external restraint, no change will occur in the steel stress, but in reality, the external restraint will not be full and prestress losses will therefore occur from this case.

2.5.2 Case 2: Steel cooling

The steel cooling can be explained with Figure 2.8 which works in the same way as Figure 2.7 for concrete cooling. Steps 1a and 1b are the same. Now the steel is contracting freely in step 2 and the internal restraint force, F_{st} will be applied to the concrete in step 3 for strain compatibility. Then, steps 4 and 5 are the same as before.
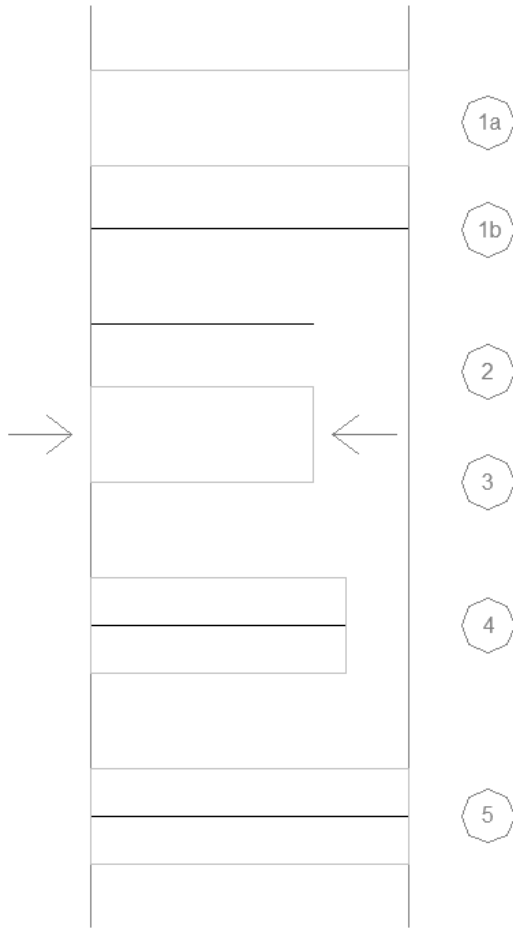
Figure 2.8.   Scheme to understand steel cooling

In the same way as case 1, equation (2.8) the compatibility condition must be fulfilled.

$$\varepsilon_s \cdot l + \varepsilon_{sT} \cdot l = 0 \qquad\qquad (2.18)$$

Where ε_s = Stress dependent strain

              l = Length of member

              ε_{sT} = Stress independent strain

The stress independent strain develops due to the temperature decrease. The strain can be expressed in the following way, using equation (2.5):

$$\varepsilon_{sT} = \alpha_{sTc} \cdot \Delta T \qquad\qquad (2.19)$$

Where α_{sTc} = Coefficient of thermal contraction of steel

              ΔT = Temperature change, time dependent

The internal restraint force results from step 3 in Figure 2.8. When the steel contracts the concrete acts as an internal restraint on the steel. Therefore the restraint force is considered to be acting on the concrete. In the case of full internal restraint, the restraint force becomes:

$$F_{sTF} = E_c \cdot \varepsilon_{sT} \cdot A_c \qquad\qquad (2.20)$$

The actual internal restraint force can be expressed as:

$$F_{st} = R_{int} \cdot F_{sTF} \tag{2.21}$$

The external restraint force in case of full external restraint N_s is expressed as:

$$N_{Fs} = -\varepsilon_{sT} \cdot E_c \cdot A_I - F_{sT} \tag{2.22}$$

As for case 1, partial external restraint can be considered with:

$$N_s = R_{ext} \cdot N_{Fs} \tag{2.23}$$

That gives the steel stress for case 2 (from steps 4 and 5 in Figure 2.8):

$$\sigma_{s2} = \alpha \cdot \frac{N_s + F_{sT}}{A_I} \tag{2.24}$$

For steel cooling, steel will try to contract but will be pulled back by the restraints. Therefore, it will experience tension which results in prestress increase.

2.5.3 Load cases combined using the principle of superposition

These two load cases act together and are added up to obtain the final prestress change:

$$\sigma_s = \sigma_{s1} + \sigma_{s2} \tag{2.25}$$

Inserting the contribution from each case using equations (2.17) and (2.24) gives:

$$\sigma_s = \frac{-F_{cT}}{A_s} + R_{int} \cdot \alpha \cdot \sigma_c + \alpha \cdot \frac{N_s + F_{sT}}{A_I} \tag{2.26}$$

2.5.4 Modifying model for heating process

The model can be used in the same way for the heating process, except the internal bond will be time dependent, i.e.

$$R_{int} = R_{int}(t)$$

Other parameters in the model will be considered to be constant, see further discussion about input parameters in Chapter 5.

2.5.5 Discussion concerning analytical model

The hand calculation model cannot describe the actual behaviour of the beam. It can only be used as a tool to verify the FE model. The reason for this is that the external boundary conditions can't be included properly. The boundary conditions will always act in such a way that the concrete and the steel will have the same restraint degree. That will not be the case in reality, since the steel will always be fully fixed at its ends but the concrete will either be free or with a low external restraint. This means that the FE model will be tested with either fully fixed ends for both concrete and steel or free ends for both materials to enable comparison with the hand calculation model and thus verify the analyses.

3 Measurements

Measurements have been made by Abetong AB to investigate how the prestress varies in the steel wires during the sleeper production. The wires in all of the tests were tensioned up to around 1400 MPa from one end of the bed, the active end. The wires were fixed the whole time at the other end, the passive end. Casting of the concrete took place from the passive end to the active end. The prestress was measured at 0.5 m inside the concrete at the active end. The results from these measurements along with production conditions at two different factories will be presented here. The factories are situated in Vislanda (Sweden) and in Marijampolé (Lithuania) (Bolmsvik, 2013).

3.1 Vislanda

3.1.1 Properties and conditions

The concrete and steel properties in Table 3.1 were present in the tests made at Vislanda implemented from Bolmsvik (2013).

Table 3.1.   Concrete and steel properties at Vislanda.

Concrete	
Cement type	CEM I 52.5 R (Skövde)
Concrete	SH
w/c - ratio	0.42
Density of mature concrete	2400 kg/m^3
Admixtures	None
Compressive strength after 17 h	35 MPa
Ballast type	Granit
Cube compressive strength at 28 days	73 MPa
Tensile strength at 28 days	5.2 MPa
E-modulus at 28 days	38 GPa
Prestressed steel strand	
Steel strand type	3x3.15 mm, low relaxation
Number of steel strands	14
Total area of steel strands	3.2731·10^{-4} m^2
Perimeter of all steel strands*	0.249 m
Initial steel stress	1343 MPa

*The actual perimeter of the steel strands is reduced by 40 % because they are twined together. This also applies for Marijampolé.

The conditions in the factory at Vislanda are as follows:

- The bed in Vislanda consists of 11 moulds along the 110 m long concrete beam. There are 4 sleepers in each mould, which makes 44 sleepers in the bed along each line of sleepers, in total 176 sleepers in the bed along 4 lines. Between each mould is a 0.05 m gap of "naked" steel wires, i.e. the concrete is

discontinuous. Furthermore, "naked" steel wires are also at both ends, 0.5 m each. Total length of the bed is therefore 111.5 m.

- The indoor temperature is 20°C, so the initial temperature of the steel wires is 20°C since they are stored in the same hall. The temperature of the fresh concrete is between 10°C and 20°C. No additional heating of the system is present. The bed is covered with tarpaulins directly after casting, so a part of the produced heat is kept inside the sleepers.
- The compressive strength that needs to be present at the release of the prestress is at least 35 MPa.

3.1.2 Results

Three test results from the factory in Vislanda are available. The tests were performed at 03/02/2010, 16/02/2010, and 12/03/2010. Strain of the wires at the active end along with the concrete temperature also at the active end was measured in all of the tests.

The test from 03/02/2010 monitored the strain of one wire at the rail seat section of the first sleeper (active end) during the first 48 hours after tensioning of the wires. Casting of the concrete at the active end took place just before 3 hours and the prestress force was released at around 18 hours. Casting time was around 1 hour. The results can be seen in Figure 3.1, see Andersen, Bolmsvik (2011).
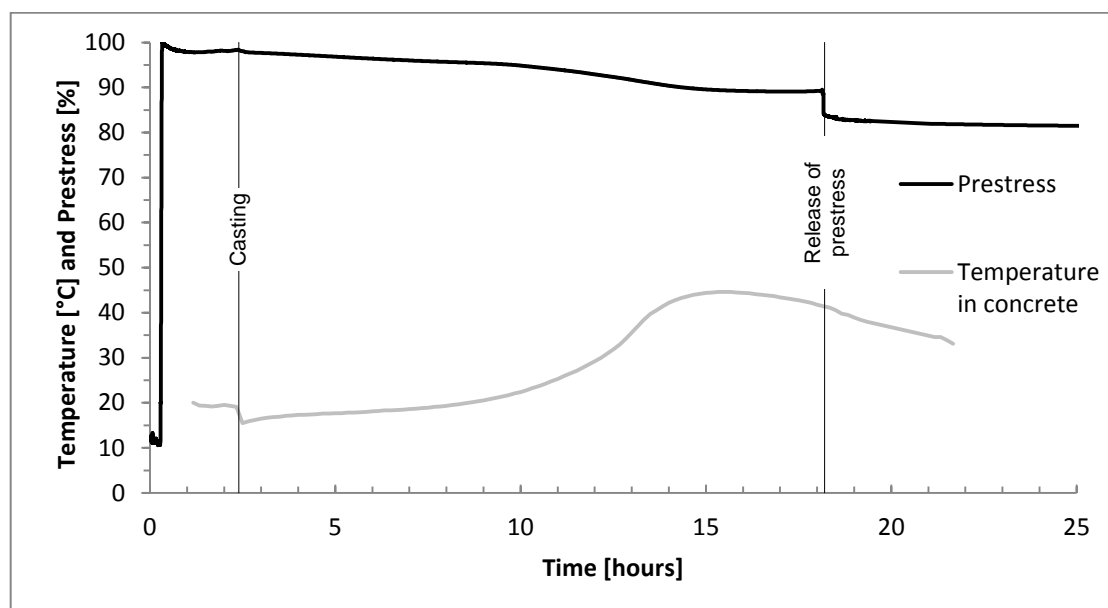

Figure 3.1. Variation of prestress and concrete temperature at Vislanda. Measurements made at 03/02/2010, modified from Andersen, Bolmsvik (2011).

The test from 16/02/2010 also monitored the strain at the rail seat section of the first sleeper (active end) but now the data covered the first 24 hours after tensioning of the wires. Casting took place earlier than before; at around 1 hour at the active end and the release of prestress was at around 19 hours. Casting time was around 1 hour. The results can be seen in Figure 3.2, see Andersen, Bolmsvik (2011).
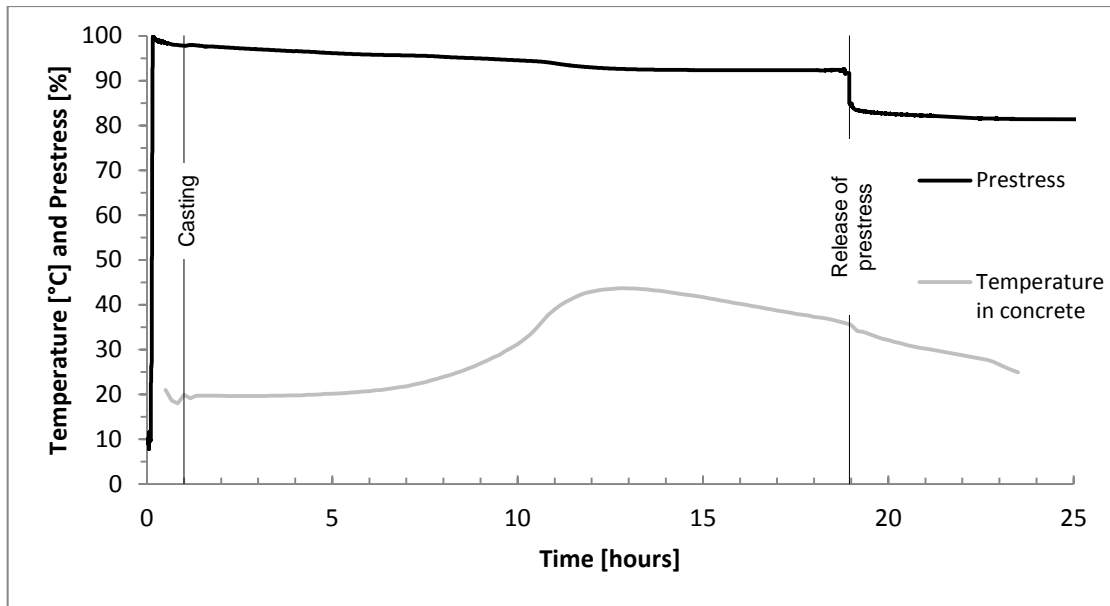
Figure 3.2   Variation of prestress and concrete temperature at Vislanda. Measurements made at 16/02/2010, modified from Andersen, Bolmsvik (2011).

The test from 12/03/2010 monitored the strain both inside- and outside of the concrete on a single wire at the active end. The casting at the active end took place at around 3 hours, but the release of prestress was much later than in the other two tests, at around 66 hours. Casting time was around 1 hour. The aim with this test was to determine when the two measurements started to deviate. That time could then be interpreted as the time when the bond between the steel and the concrete started to influence the prestress. The results can be seen in Figure 3.3, see Andersen, Bolmsvik (2011).
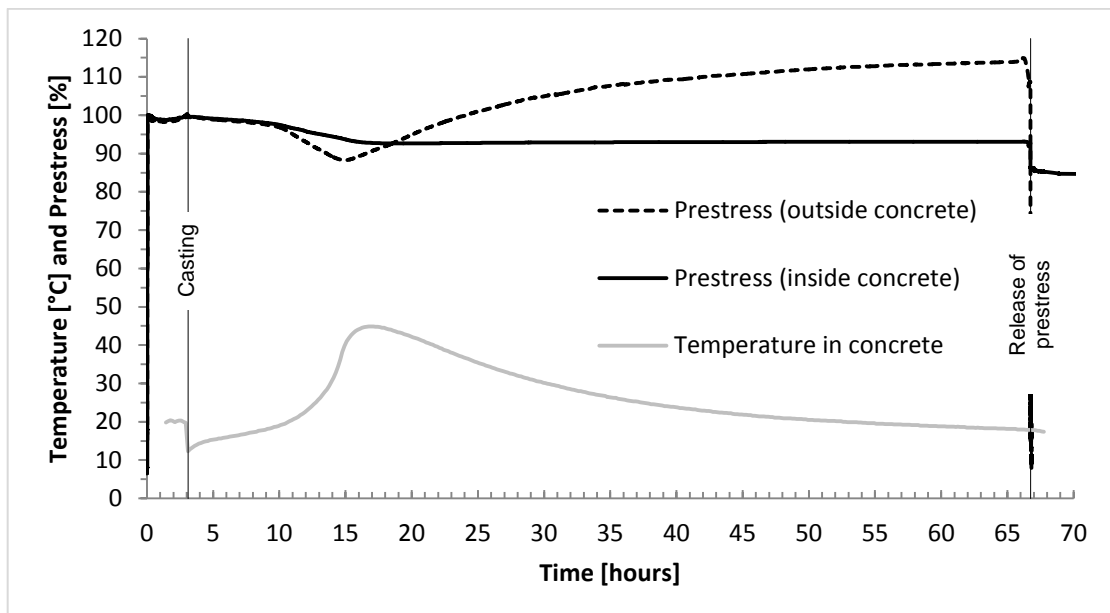

Figure 3.3.   Variation of prestress and concrete temperature at Vislanda. Measurements made at 12/03/2010, modified from Andersen, Bolmsvik (2011).

The measurements from Vislanda all show similar behaviour. The temperature increase caused by the hydration is 25°C - 30°C. The prestress loss is rather small and seems to have the same shape as the temperature curve up to around 7 hours after casting. Then, the temperature increases rapidly up to around 45°C and the prestress loss also becomes greater. Hence, the same mechanism seems to be affecting the temperature and the strain at that time.

The measurements shown in Figure 3.3 show that the part of the wire outside the concrete shows a different behaviour at around 7 hours after casting. That means that the concrete and the wire start to act as one structure at that time and strains start to accumulate towards the parts of the wires outside of the concrete, i.e. bond has formed between the concrete and the steel.

Then, when the temperature reaches its maximum, the prestress inside the concrete approaches a constant value around 89% and remains almost constant after that, with only a small increase. The prestress outside the concrete shows a great increase after the maximum temperature. That can be explained by the difference in length of the parts outside the concrete and parts inside the concrete. The parts inside are around 110 m, while the parts outside are only around 1 m. That means that when full bond is reached, for the same deformation, the strain reading outside the concrete will be 110 times greater than the reading within the concrete. During the cooling phase, the bond will be close to being fully developed and therefore the strain readings outside the concrete are much larger than inside.

Finally, the prestress is released which creates a drop of around 6-8% which is close to the theoretical value of 4% (Andersen, Bolmsvik 2011).

3.2   Marijampolé

3.2.1   Properties and conditions

The concrete and steel properties in Table 3.2 were present in the tests made at Marijampolé implemented from Bolmsvik (2013).

Table 3.2.   Concrete and steel properties at Marijampolé.

Concrete	
Cement type	CEM I 52.5 R
Concrete	C50/60
w/c - ratio	0.37
Density of mature concrete	2400 kg/m^3
Admixtures	BASF/ACE 30 1.9 l/m^3
Compressive strength after 17 h	37 Mpa
Ballast type	Granit
Cube compressive strength at 28 days	65 MPa
Tensile strength at 28 days	4.8 MPa
E-modulus at 28 days	38 GPa
Prestressed steel strand	
Steel strand type	3x3.15 mm indented 1860 S3
Number of steel strands	12
Total area of steel strands	$2.806 \cdot 10^{-4}$ m^2
Perimeter of all steel strands	0.214 m
Initial steel stress	1395 MPa

The conditions in the factory at Marijampolé are as follows:

- The bed in Marijampolé is 109 m and is continuous. It consists of 40 sleepers in a line and they have a length of around 2.7 m each. At each end, "naked" steel wires of 0.5 m are present, as in Vislanda. The total length of the bed is thus 110 m.
- The indoor temperature is 6°C; i.e. the initial temperature of the steel wires is also 6°C, since they are stored in the same hall. That is much colder than in Vislanda, thereby the wires will experience a greater temperature increase when the concrete is cast. The temperature of the fresh concrete is increased up to 17°C by heating the aggregates and using hot water, to make the hydration start earlier. Furthermore, a heating system is placed under the casting bed which is switched on during the whole time of the measurements and the bed is covered with tarpaulins directly after casting.
- Two concrete cubes are tested in compression before releasing the prestress force and in these measurements they showed a capacity of 43 MPa and 44 MPa, which is sufficient.

3.2.2   Results

One test result is available from the factory in Marijampolé. The test was performed at 22/03/2011 and monitored the strain in the wire inside- and outside of the concrete at the active end of the bed. The temperature was also measured, both at the passive and the active end along with the temperature of the air between the first sleeper at the

active end and the anchor plate at the support. Casting took place at around 2.8 hours and the release of prestress at around 21.5 hours. Casting time was 2.5 hours. The results can be seen in Figure 3.4, see Andersen (2011).
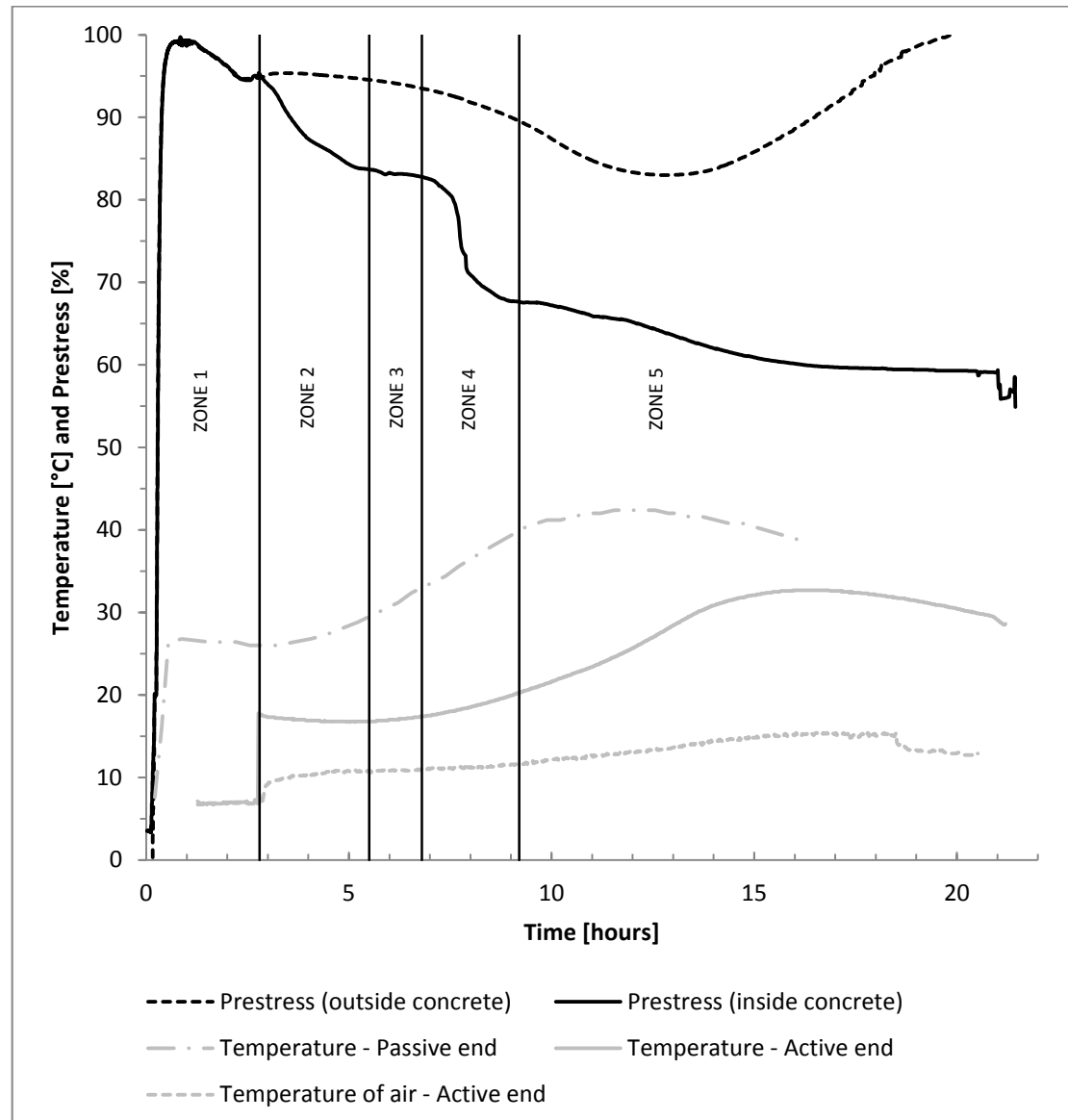

Figure 3.4.   Variation of prestress and concrete temperature at Marijampolé. Measurements made at 22/03/2011, modified from Andersen (2011).

The results from Marijampolé are quite different from the ones in Vislanda, although similarities can also be seen. The prestress losses are much greater in Marijampolé, the final prestress is around 59% just before the release. The temperature starts from 7°C and goes up to around 33°C, which is an increase of 26°C. The graph has been divided into 5 zones to be able to understand it better.

Zone 1 shows a drop of about 5% which occurs before the casting at the active end. That is most likely due to the temperature increase in the beginning when the concrete is poured on the wires.

Zones 2 and 4 both show very large drops that were not seen in Vislanda. The drop in zone 2 is around 11% and occurs gradually over a period of 3 hours. The temperature at the active end is nearly constant while the temperature at the passive end starts to

increase in the beginning of this zone. This happens soon after a great temperature increase at the active end, when the concrete was poured on the wires.

The drop in zone 4 is around 15% and occurs quite rapidly over a period of around 2 hours. The temperature at the active end starts to increase in the beginning of this zone and increases quite slowly during the period. The temperature at the passive end is increasing more rapidly at the same time.

The drop in zone 5 is around 8% and occurs over a period of around 8 hours and the prestress remains nearly constant after 17 hours. The behaviour during this period is very similar to the one in Vislanda and the loss begins at around 7 hours after casting, just like in Vislanda. Also, the drop in the part of the wire outside the concrete starts at around 7 hours after casting and is greater than the drop inside at the same time. Then, it starts to increase again after the maximum temperature is reached, just as in Vislanda (Andersen, 2011).

3.3   Summary

The results for the measured prestress losses in Vislanda performed at 12/03/2012 and Marijampolé have been summarized in Figure 3.5:
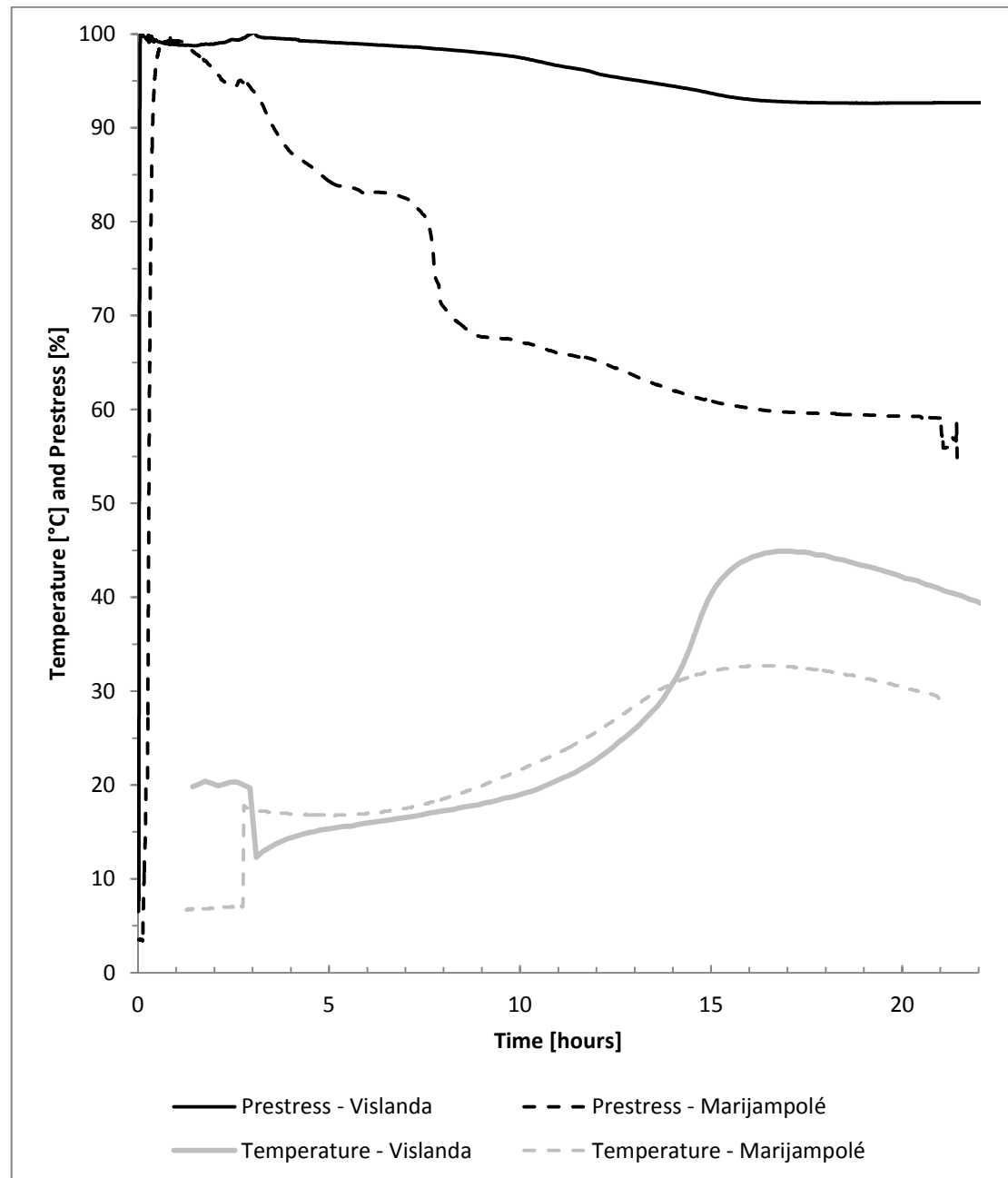

Figure 3.5.   Summary of prestress losses at Vislanda and Marijampolé.

The difference between the two factories is very clear. The prestress losses are much greater in Marijampolé while the temperature due to hydration doesn't increase as much. The total temperature increase is similar though, since the surrounding temperature is much lower in Marijampolé. The similarities between the factories that were mentioned earlier can be seen by comparing the two prestress curves after 10 hours where the losses are very similar.

4 Numerical modelling

4.1 Setup of small scale model

The process of developing a small scale model before going to a full size model was done to obtain a better knowledge of different parameters influencing the real behaviour. The model was tested for different input and the results checked to see if the model responded in a reasonable way. The input that was used for the checks is based on the measurements made in Vislanda at 12/03/2010 (see Section 3.1) but doesn't represent the correct values. It is only a way of testing the model; the real input for the two factories will be discussed in detail in Chapter 5. The small scale numerical model was 10 m long and the calculations were performed on the basis of linear elastic analysis. The concrete and steel had the same geometry properties as the actual sleeper, see Section 4.2.1. Later, this model was expanded to simulate the behaviour of the real, full size line of sleepers.

The model had to take into account the concrete, steel, the interface between them and the boundary conditions. The steel was modelled as a single steel wire in the middle of the cross-section and extended half a meter out of the beam on each side where the ends were fixed in both horizontal and vertical direction, see Figure 4.1. Theoretically, only the horizontal direction is needed to be fixed but in order to avoid rigid body motions in the vertical direction, that direction was also fixed. No prestress was applied and negative stress on steel element does therefore represent prestress losses.
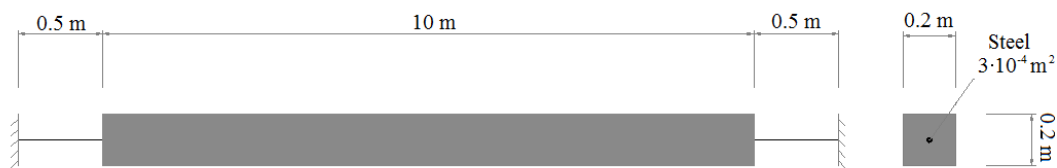

Figure 4.1.   Dimensions, boundary conditions and cross-section of small scale model.

4.1.1 Choice of elements

Since the variation of the bond properties was an important factor, interface elements that give the possibility to vary its properties were needed between the concrete and the steel. Element type L8IF is such an element, which has a two dimensional configuration. Diana recommends using 2D plane stress elements for concrete along with these interface elements; therefore concrete elements were chosen as the type Q8MEM, which is a four-node quadrilateral isoparametric plane stress element. For the purpose of prestress losses, only stress in the longitudinal direction is needed, so a truss element could be used to model the steel. The element L2TRU is a two-node truss element and was used to model the steel. The connections between different elements were modelled as Figure 4.2 shows (DIANA, 2011).
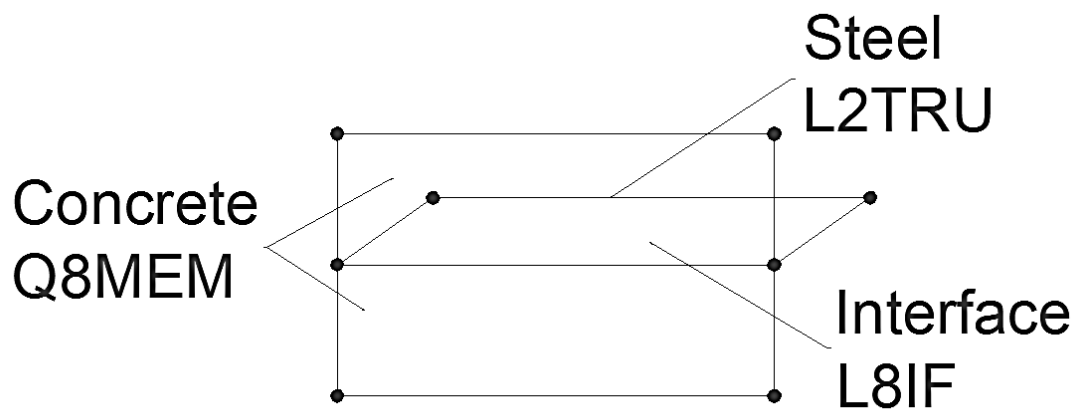
Figure 4.2.   Connections between elements

This configuration ensures that the concrete and the steel are both connected to the interface element through separate points that have the same coordinates; in this way the concrete and the steel are connected only through the interface element.

4.1.2   Convergence study

A convergence study was performed in order to know how many elements were needed to get sufficient accuracy of the results. The study was performed by assuming the input parameters from Table 4.1, constant bond stiffness (see Figure 4.8); and a single temperature change of 33°C to both the concrete and the steel was applied. The steel stress at half a meter inside the beam and in the centre was studied. The numbers of steel elements considered were the following: 10, 50, 80 and 99. The results for the convergence study are shown in Figure 4.3:
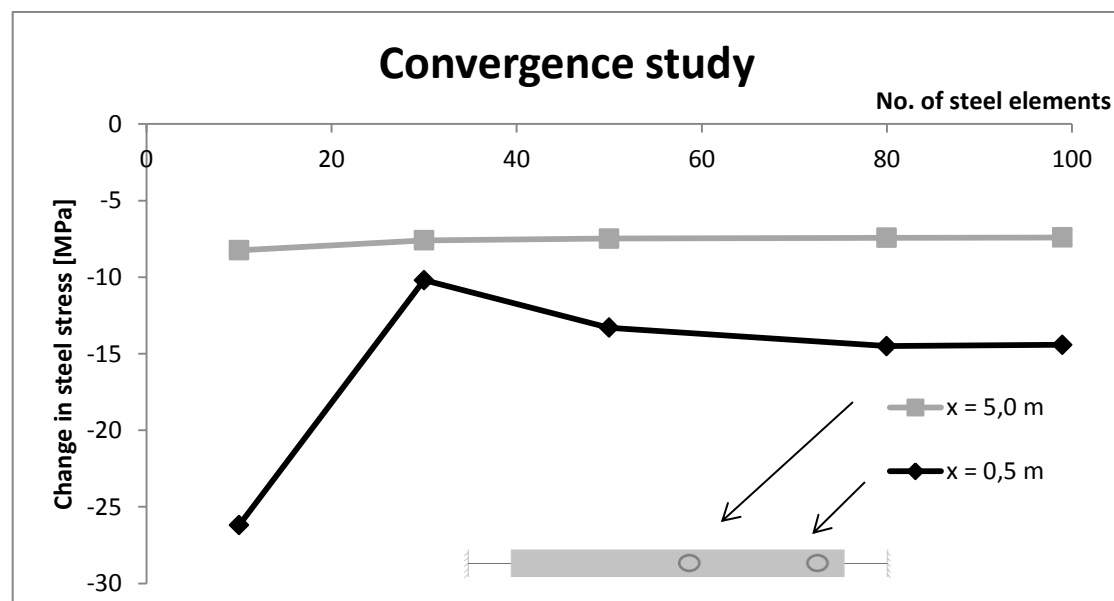

Figure 4.3   Convergence for steel stress at specific points in the small scale model.

For the steel stress at the centre point, convergence was reached with relatively few elements. However, for the steel stress at half a meter from the edge, around 80 elements were needed to have a converged solution. This point was of major interest because all measurements were done half a meter from the edge. For a discussion why these two points have different stresses, see Section 4.2.3.

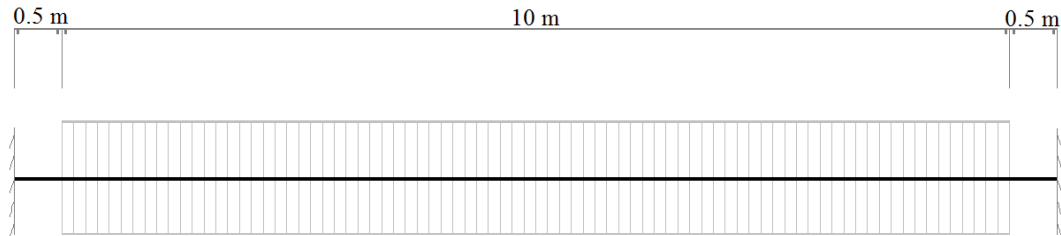The resulting model can be seen in Figure 4.4.

Figure 4.4.   Overview of the numerical small scale model.

4.2   Input

4.2.1   General input parameters

The following material parameters were used in the development of the numerical small scale model.

Table 4.1.   General constant input parameters for the small scale model.

Parameter	Concrete	Steel	Interface
Thickness [m]	0.2	-	0.057
Area [m^2]	0.04	$3.00 \cdot 10^{-4}$	-
Young's modulus [GPa]	38	205	-
Poisson's ratio [-]	0.2	0.3	-
Coeff. thermal expansion [1/°C]	$12 \cdot 10^{-6}$	$12 \cdot 10^{-6}$	-

These parameters were obtained from the previous master's thesis related to this subject (Carlsson, Holmbom, 2012). They were all considered to be constant with time, see Sections 4.2.4, 4.2.5 and 5.1 for motivations.

4.2.2 Temperature curve

The measured temperature curve from the Vislanda measurements at 12/03/2010 was used in the model. The effect of the temperature drop in the first 3 hours, due to casting of concrete over the measuring equipment was ignored, since it's not necessary for the verification of the model.
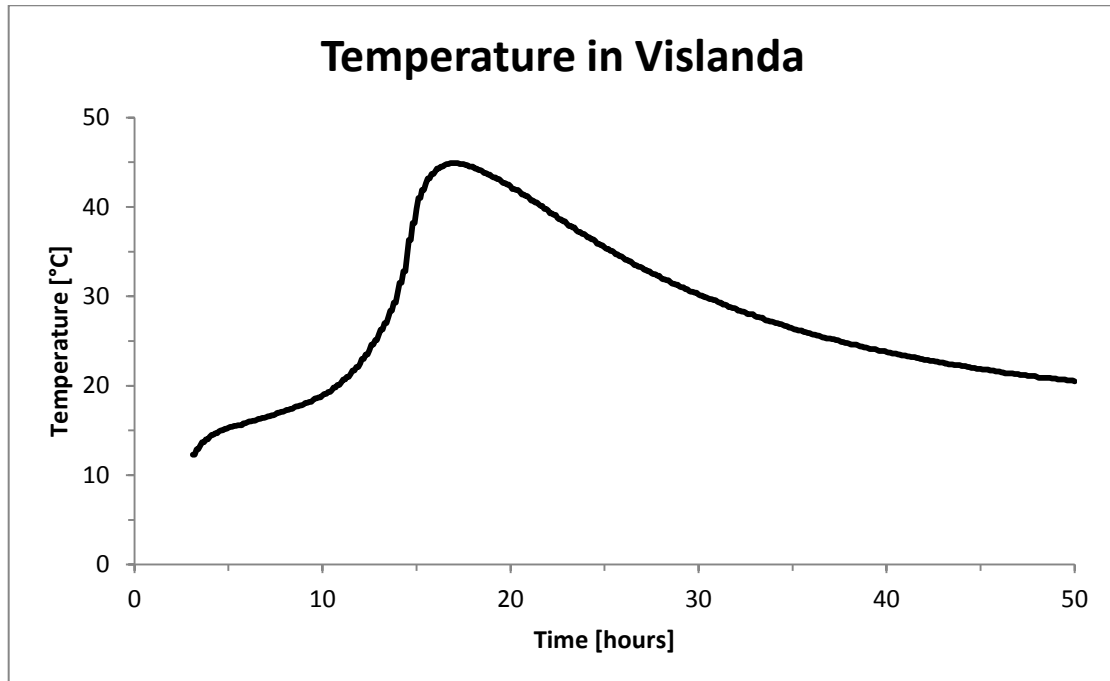
Figure 4.5.   Temperature input, from Vislanda measurements 12/03/2010.

The conduction in the steel was assumed to be infinite. Therefore, the same temperature curve was applied to both the steel and concrete elements as an input.

To verify that the temperature was correctly applied to the model, a naked steel strand was modelled; temperature input was applied on the steel wire and no concrete was included. Figure 4.6 shows the model.

Figure 4.6.   Naked steel strand.

Figure 4.7.   Change in steel stress in naked steel strand due to temperature change.

The stress on the naked steel has perfect correlation with the temperature input but with opposite sign, compare Figure 4.5 and Figure 4.7. This confirms that the temperature was correctly applied in the model. It also confirms that increasing the steel temperature gives prestress loss and that temperature decrease increases the prestress.
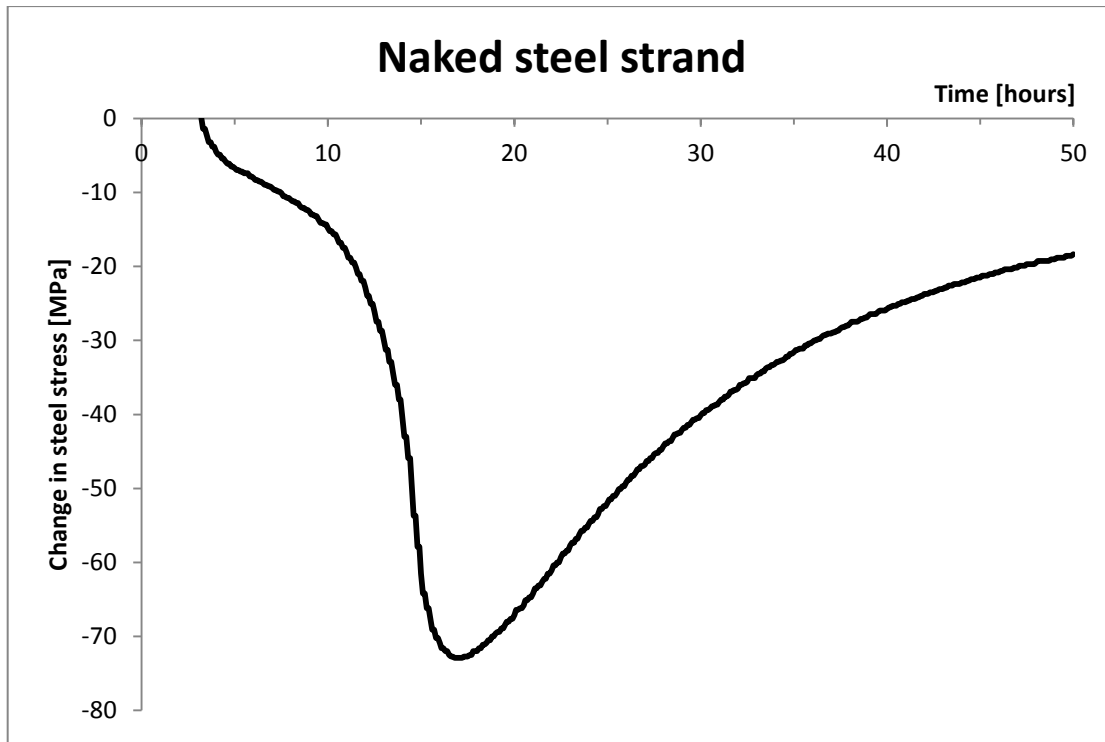
4.2.3   Bond between steel and concrete

The bond between concrete and steel was modelled with the interface elements. Typically, the input is modelled as a bond-slip curve where the bond would fail after a certain slip. For these analyses, small bond stresses were assumed and therefore only a linear curve with a constant stiffness was used. This assumption can be made if the values of bond stresses are low enough for the bond-slip curve to still have the shape of the initial stiffness. Therefore, the bond stresses obtained from the analysis must be checked and compared to a bond capacity; this was done for the results obtained for the full size model, see Chapter 6.

The bond stiffness was modelled in three different ways: 1) with a very small value, in practice zero; 2) with a constant value, and 3) to be increasing with time since the concrete was in the process of hardening. The assumed bond stiffness development with time can be seen in Figure 4.8. A final bond stiffness value of 100 GPa/m was chosen in the small scale analyses. The bond development with time was based on the measurements from Vislanda performed at 12/03/2010. Further discussions on this item can be found in Section 5.3.

The varying bond stiffness was modelled in Diana by using a user-supplied subroutine, see appendix B.2.

Bond stiffness variation
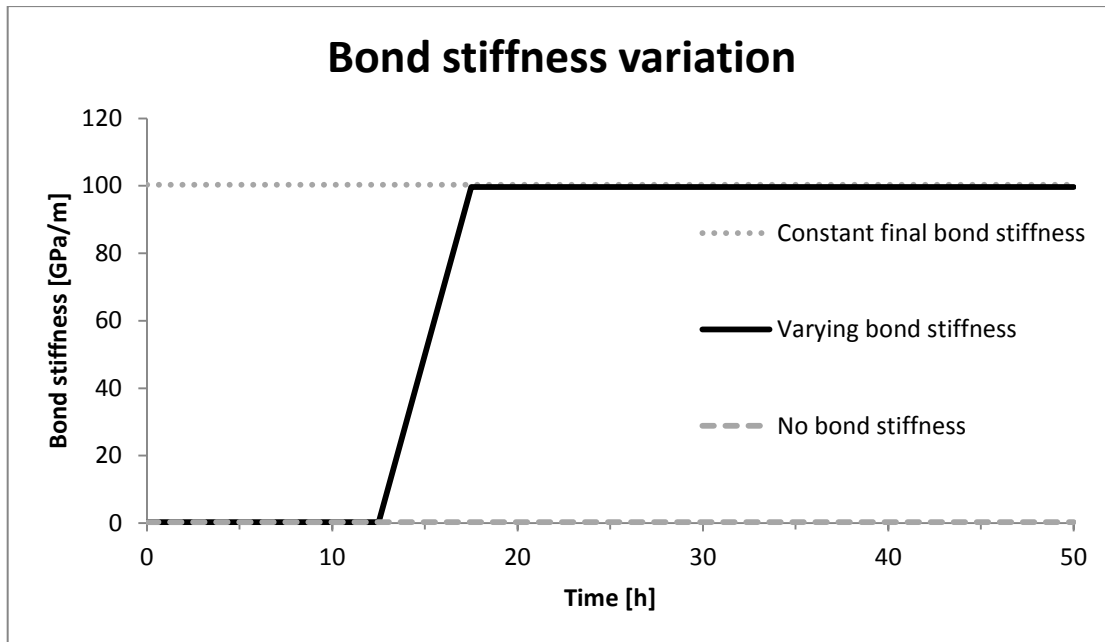
Figure 4.8.   Bond stiffness of interface element variation with time.

The results from the different bond configurations applied (Figure 4.8) can be seen in Figure 4.9.
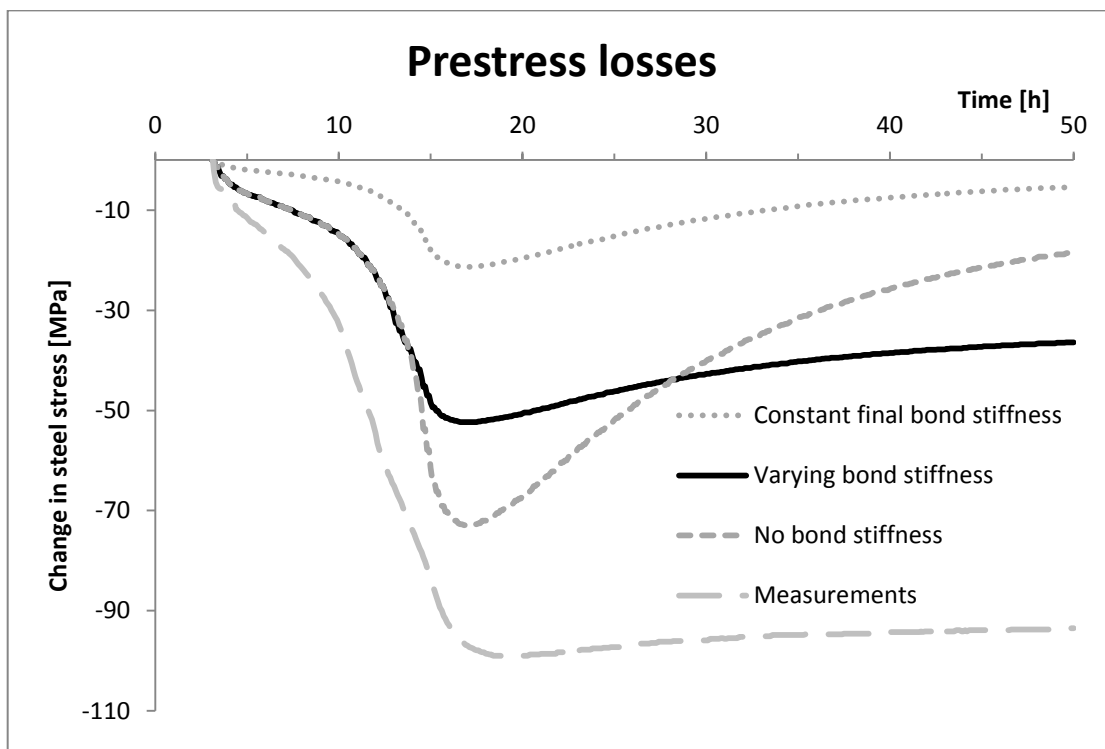
Prestress losses

Figure 4.9.   Prestress loss with variations of bond stiffness as shown in Figure 4.8.

The results showed that the model was responding to the applied bond development in a reasonable way. The curve for no bond was the same as the curve in Figure 4.7 which showed the stresses for a wire without including any concrete. The curve for having a final stiffness value of 100 GPa/m the whole time, resulted in less prestress losses. That is also reasonable since the steel was then surrounded by concrete and a part of the stresses was transferred to the concrete so the stresses in the steel should

decrease. The curve showing the stresses resulting with varying bond showed similar behaviour. The stresses followed the curve without bond up to 12.5 hours when the bond was applied, then those curves started to deviate and between 12.5 h and 17.5 h, the stress change was less since the bond was increasing. After 17.5 h, the bond had reached the final value and the stress increase followed the curve that had the final value the whole time, perfectly. That resulted in quite low prestress increase during the cooling phase. The shape of this curve was similar to the measurements but the magnitude was not the same which could be due to various reasons that will be discussed later.

The results showed a large prestress drop at both ends of the sleeper while the prestress was constant in the middle. This is reasonable; the length where this drop occurs is the transmission length, i.e. the length needed to transfer the stresses from equilibrium inside the concrete to the naked wire outside of the concrete. The magnitude of the bond stiffness has a great influence on this length. If the stiffness is high, then the interface elements at the end are capable of transferring more stresses and therefore less distance is needed for the transfer. The results seen in Figure 4.9 were obtained at 0.5 m from the edge of the concrete which is the same place as the measurements were made. At that point, equilibrium has been reached and the transmission length does not affect the stresses. If the bond stiffness would have been less, the transmission length would have affected the results and the prestress losses would have been greater. This can be seen in Figure 4.10, where the transmission length is approximately 0.5 m.
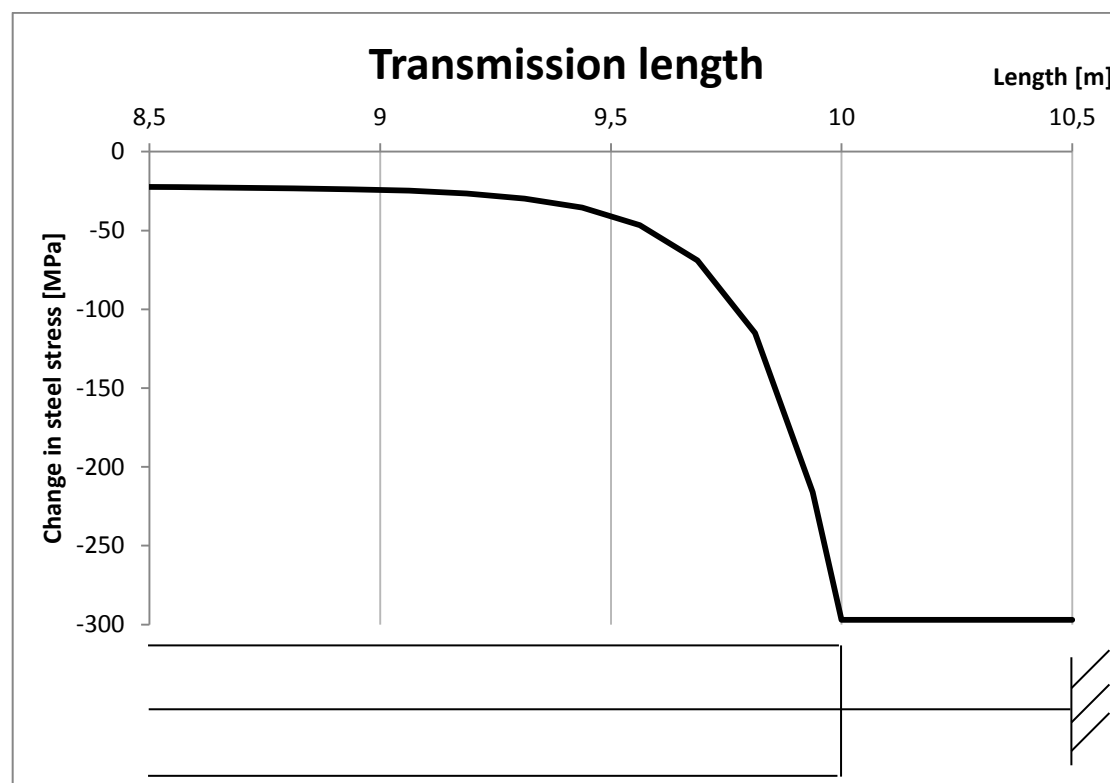

Figure 4.10. The transmission length of steel stresses is approximately 0.5 m or at 9.5 m, which is the point where the results in Figure 4.9 are obtained from.

4.2.4 Thermal coefficient of concrete

As mentioned in Section 2.4, the thermal coefficient of concrete varies in the early stages during hydration. The coefficient is very high in the beginning and decreases rapidly to a constant value. To investigate whether varying thermal coefficient with age was relevant for this analysis, different constant thermal expansion coefficients were employed. Furthermore, different values of bond stiffness, constant with time were used. The maximum steel stress values are compiled in Figure 4.11.
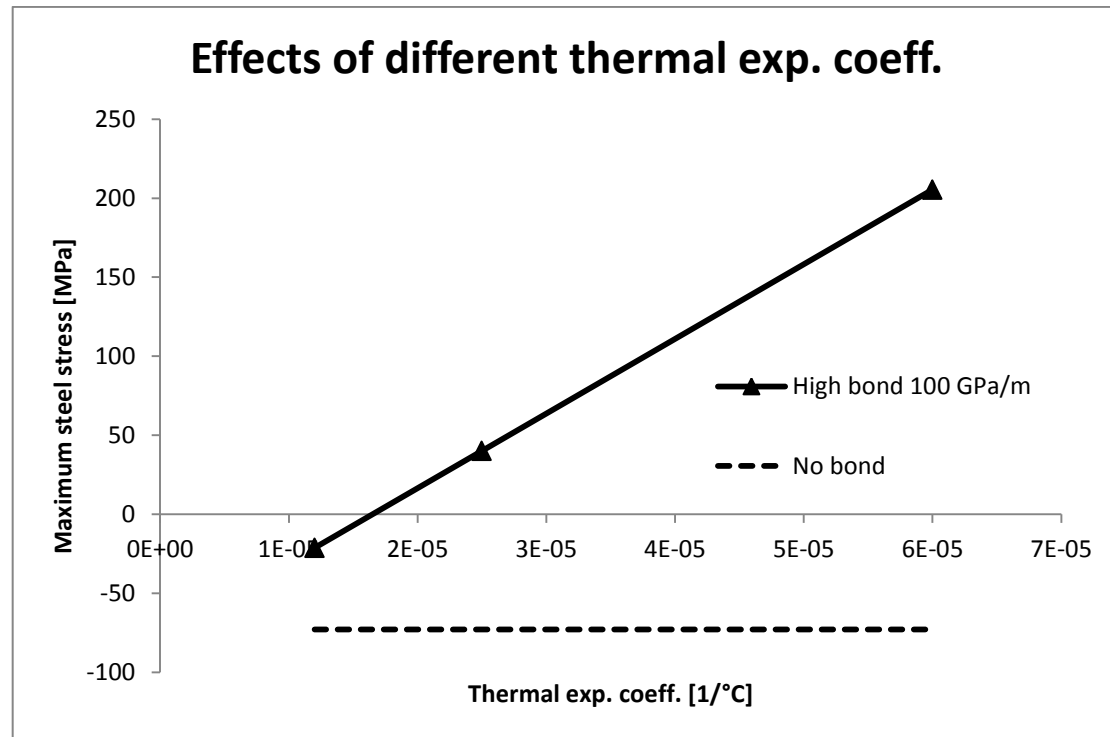

Figure 4.11.   Result of thermal coefficient of expansion of concrete.

The results show that when there is no bond, the thermal coefficient doesn't affect steel stress as can be expected since the concrete cannot influence the steel stresses without bond. Figure 4.11 also shows that for high bond stiffness, the variation in thermal coefficient affects the stress. By comparing how the thermal coefficient of expansion varies with time (Figure 2.6) to the variation of bond stiffness with time (Figure 4.8), it can be seen that the thermal coefficient is decreased to a low value before the bond is established. Therefore, it can be concluded that the development of the thermal coefficient of concrete will not have much influence on the steel stresses and may be kept constant during the whole process. Still, it should be noted that if the coefficient has a high value when bond is established, it can have an influence. That will not be considered in the general modelling in this thesis.

4.2.5 Young´s modulus of concrete

To investigate whether the change in Young's modulus during the hardening of the concrete has an influence on the results, the model was tested for different values of E-modulus, constant with time. The model was also tested for different values of bond, constant with time. The maximum steel stress values are compiled in Figure 4.12.
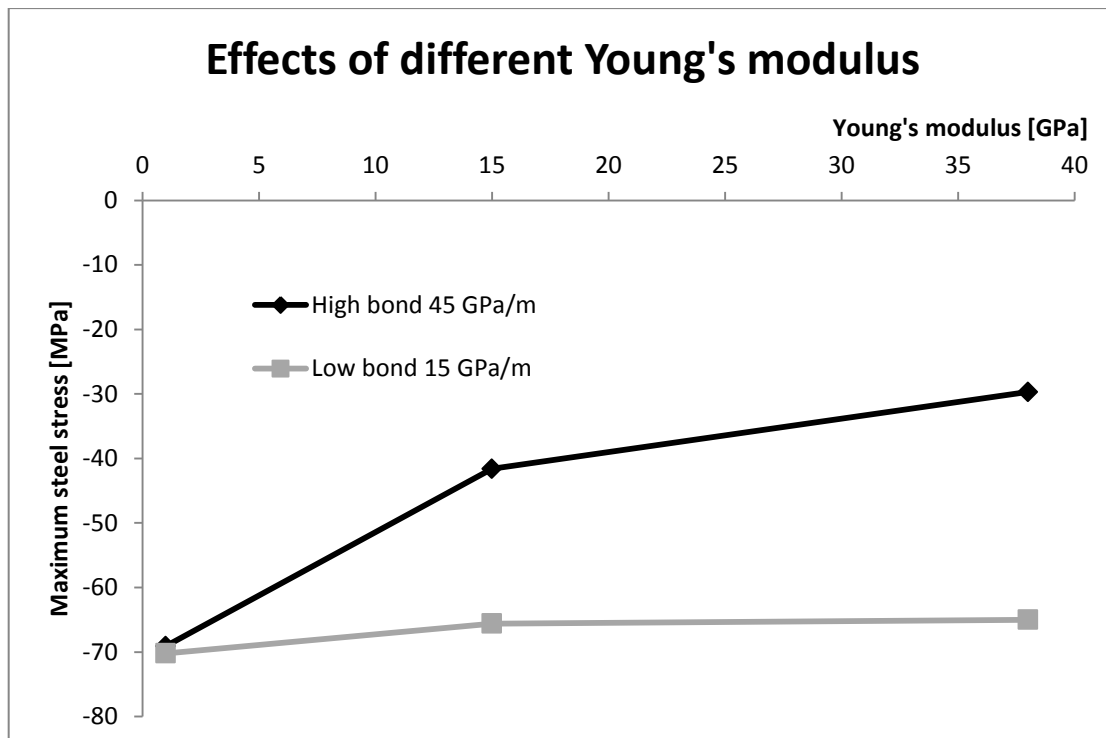
Effects of different Young's modulus

Figure 4.12. Results for different Young's modulus of concrete with low and high bond stiffness.

The results show that for low bond values, the effect of decreasing the Young's modulus is little, but for high bond values the effect is much larger. That is reasonable since if there is no/little connection between the concrete and the steel, the concrete can't have much influence on the steel; while if there is a stiffer connection between them, the concrete will be able to affect the steel more. This means that the Young's modulus could only affect the results to a great extent if, at the same time, the bond would be high and the Young's modulus would be low. That is not considered to be a realistic case since bond stresses can't be transferred if the concrete is in nearly liquid state. For these reasons, the effect of the development of the Young's modulus during the hardening process was considered to be negligible in the analysis and the Young's modulus was kept constant to 38 GPa.

4.2.6   External boundary on concrete

The concrete will be externally restrained due to friction with the surrounding moulds. The moulds will then be restrained by friction to the underlying bed. However, for simplification, this was not taken into account directly in the model. The only parameter that restrained the steel was the bond between steel and concrete. Since the concrete was assumed to have a constant, high Young's modulus during the whole process, that stiffness increased the restraint on the steel and therefore had similar effect as the external restraint would have. Also, the stiffness of the internal bond was chosen to have a quite high value (see Section 5.3) which also added restraints to the steel. For these reasons, it was assumed that the external restraint acting directly on the concrete could be neglected and was not considered to be necessary for the modelling of prestress losses within the concrete. It should be noted that this assumption can have large effects on the stress in the part of the wire outside the concrete since the external boundary equilibrium is changed. Thus, the stress results

for that part of the wire will not be correct, and accordingly, the stress inside the transmission length will not be correct either, since stresses will be transferred from equilibrium inside the concrete to a wrong value outside.

4.2.7   Accumulation effects

Accumulation of stresses is an effect that happens due to the casting sequence from one end to the other. The casting takes place over a certain period of time which means that the concrete in one end will start to hydrate and mature before the other end. Then, the temperature- and bond development will be delayed between the ends. This effect was tested in the model by assuming a total casting time of 1 hour and dividing the model up to 10 parts, 1 m each which gives a 6 minute delay between adjacent parts. Then, for each 1 m part the casting was assumed to take place at the same time. This was taken into account by delaying the temperature- and bond development input by 1 time step for each part. The input can be seen in appendix B.3 where the user-supplied subroutine for the bond model can also be seen. Figure 4.13 and Figure 4.14 show the input for the two end parts, casting starts from the passive end and ends at the active end:
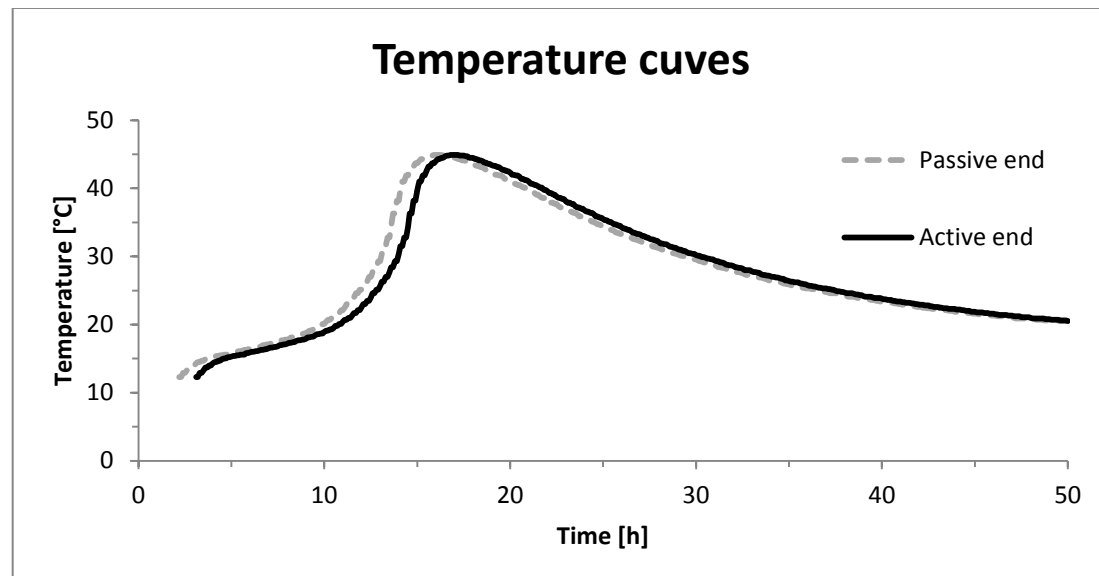

Figure 4.13.   Temperature curves for accumulation effects, showing only the ends.
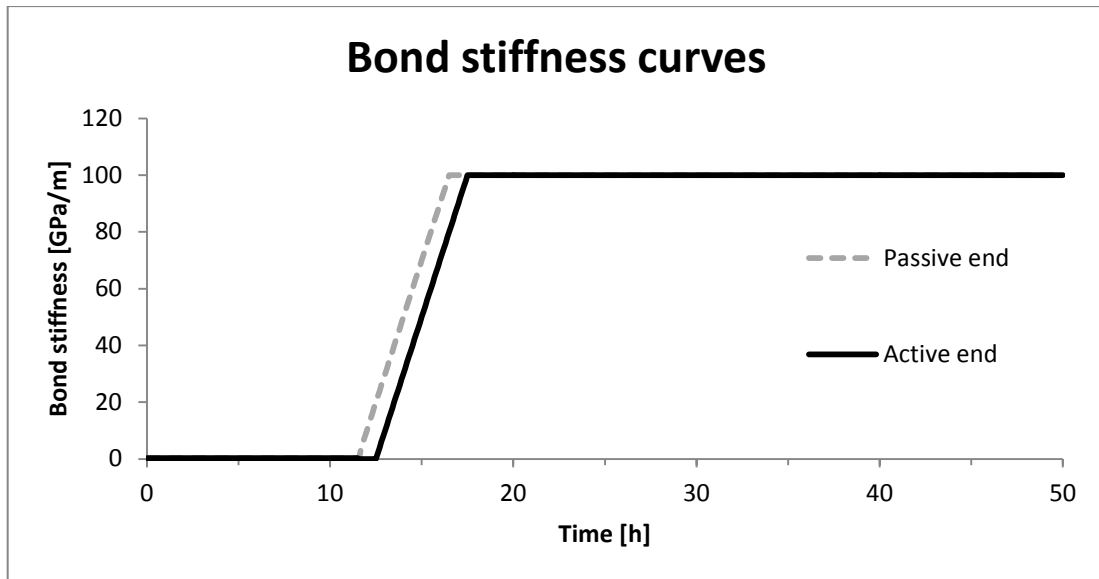
Figure 4.14.   Varying bond stiffness curves for accumulation, showing only the ends.

Results showing the effects of accumulation can be seen in the figures nedan.
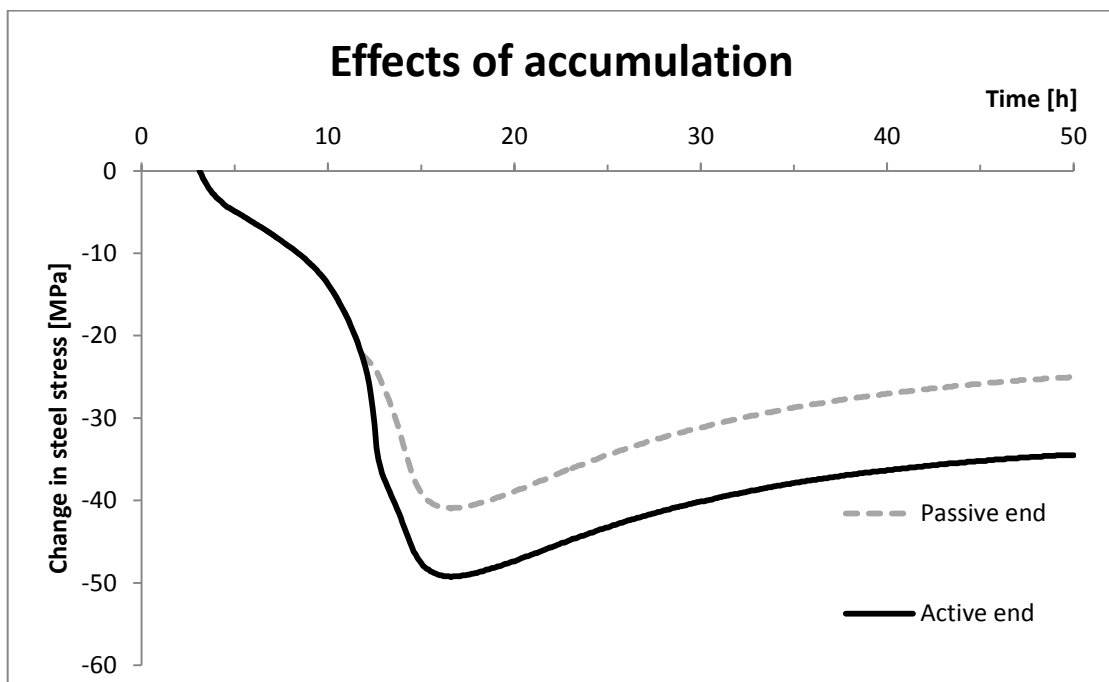
*Figure 4.15.   Results at 0.5 m from the concrete edges, showing accumulation effects
in small scale model.*
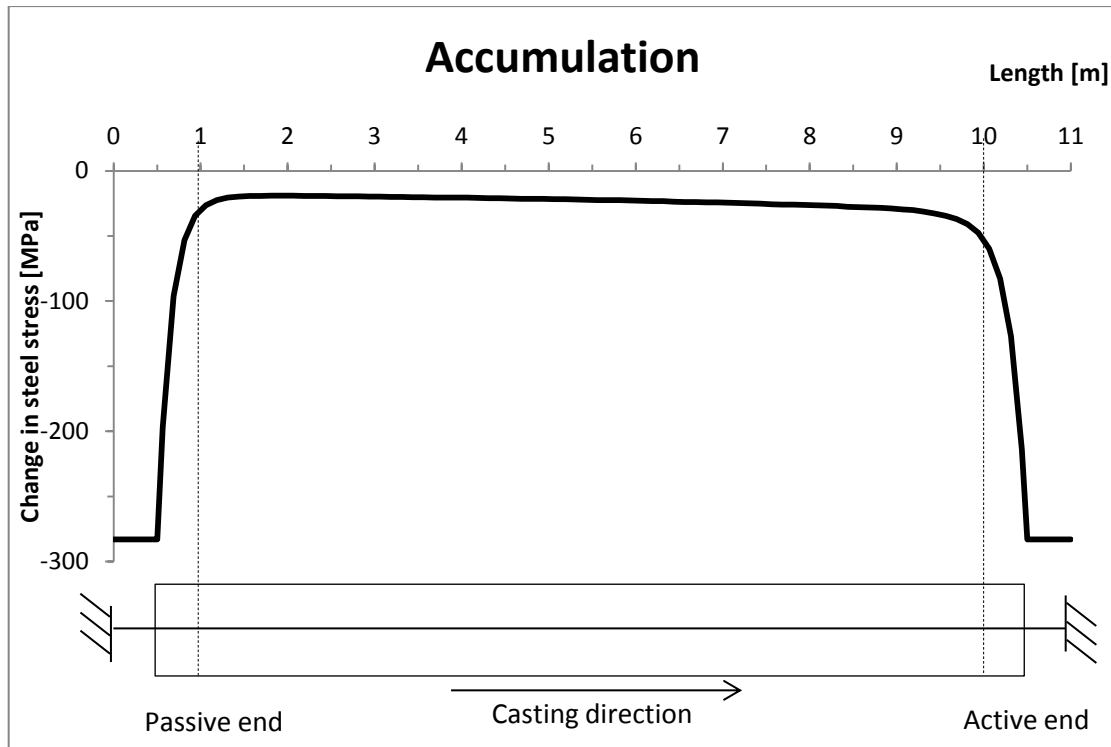
Figure 4.16. Steel stress showing the accumulation effect along the model at 17.5 h. The model is cast from the passive end to the active end. With 1 hour casting time.

The results show that the accumulation did have an effect on the stresses along the model. The change of stress was higher in the active end which indicates that stresses were accumulated towards that end. In the passive end, the change of stress was lower, which indicates that stresses were accumulated from the passive end to the active end. Thus, the maximum prestress loss was obtained in the active end.

4.3 Verification of the numerical small scale model

The analytical model presented in Section 2.5 was used as a tool to verify the numerical small scale model. As stated in Section 2.5.5, the analytical model has some restrictions for the boundary conditions. The model can only be used with free- or fully fixed boundaries which can be expressed as Figure 4.17 shows:
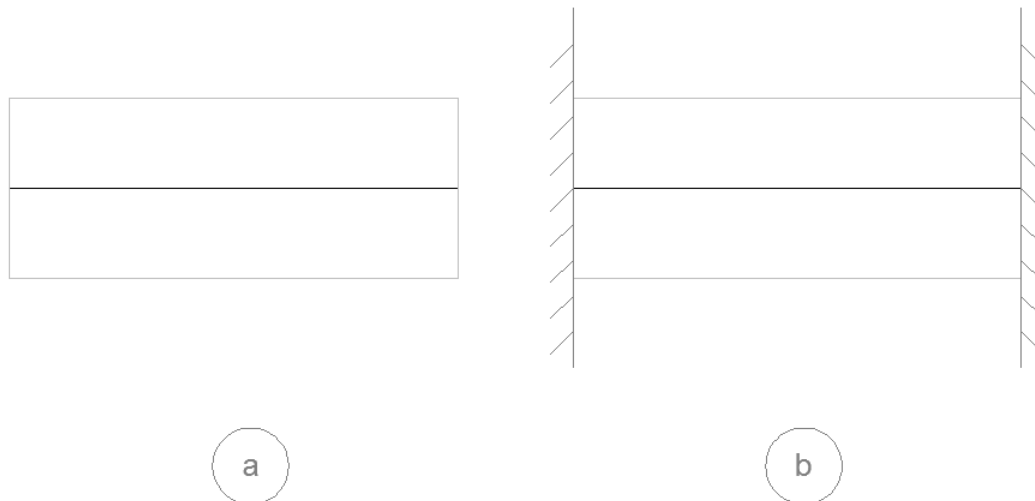
Figure 4.17. Boundaries for verification, a) Model with free ends b) Model with ends fully fixed.

The boundaries of the numerical small scale model were modified in the same way so it could be compared to the analytical model. The bond stiffness varied as the varying bond curve in Figure 4.8, both for the numerical- and analytical model. The input for the temperature development and other input were as in Sections 4.2.2 and 4.2.1 respectively. The results of the verification can be seen in Figure 4.18.
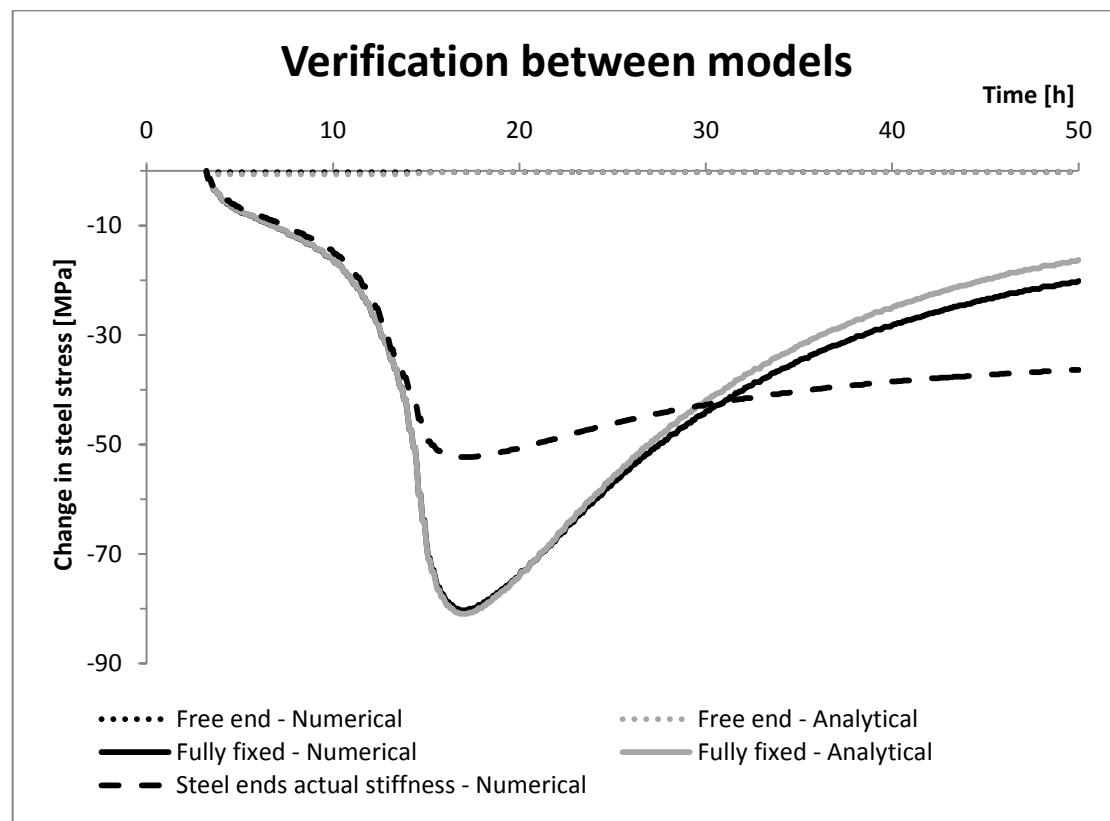
Figure 4.18. Verification between analytical model and numerical model.

The results clearly show that there is a good correlation between the analytical model and the numerical small scale model for free ends and fully fixed ends.

The results for free ends show that there was almost no steel stress, both for the analytical model and the numerical model. That is reasonable since deformations can occur freely and the need for movements is the same for both materials since the coefficient of thermal expansion is the same and the temperature development also.

The fully fixed case had almost perfect correlation to the temperature curve and the curves for the two models are nearly identical. Since, in this case, both concrete and steel were fully fixed and, as before, both materials had the same thermal coefficient the steel had the same need for deformations as for the naked steel strand test, see Figure 4.18. The results are the same as in that case, which is reasonable.

As mentioned before, the analytical model couldn't be modified for the actual boundary conditions of a short steel wire outside of the concrete. Still, the results from the numerical analysis with the actual boundary conditions have been included in Figure 4.18 for comparison. Before the bond increases (12.5 h) there is no connection between the concrete and steel and therefore the steel could be assumed to be fully fixed. That can be seen by that the same shape and magnitude of steel stress at 12.5 h in Figure 4.18 for actual steel ends and the fully fixed case.

When bond started to develop at 12.5 hours, the concrete and steel started to act as one structure with only the steel ends as its boundary. The steel ends were not able to restrain the structure fully and experienced prestress losses. Then the combined concrete/steel structure had less stiff boundary than the fully fixed case and behaved more like the case with free ends. Thus, the temperature changes had less effect than for the fully fixed case and the prestress change was therefore less.

4.4 Full scale model

In order to simulate the real behaviour of the line of sleepers, the small scale model was expanded to a full scale model which had dimensions close to the real casting beds in the two factories. The model can be seen in Figure 4.19:
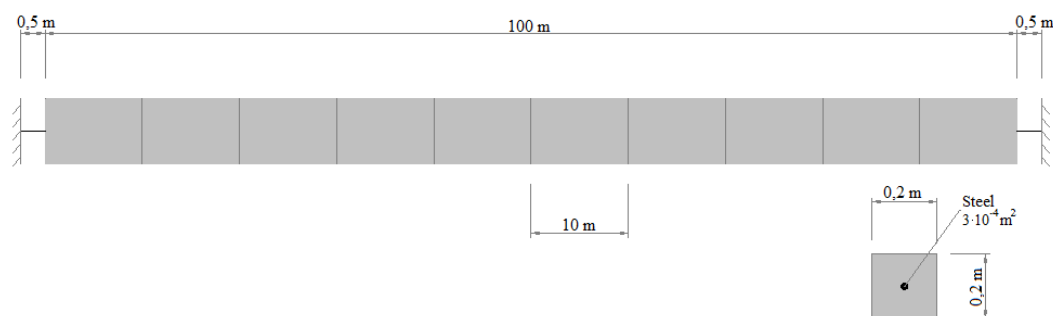

Figure 4.19. Geometry, boundary conditions and cross-section of full scale model.

The model was divided in 10 sections of 10 m each. The same element types as for the small scale model were used, and the number of elements was chosen according to the elements needed in the small scale model for convergence, i.e. 80 elements for every 10 m section.

5 Input

The input used in the full scale model to compare to measurements for the factories in Vislanda and Marijampolé is described in the following sections.

5.1 General input

General input includes parameters that were assumed to be constant with time. The input can be seen in the following table. The values were obtained from Table 3.1 and Table 3.2.

Table 5.1.   General input used in the full scale model.

Parameter	Concrete		Steel	
	Vislanda	Marijampolé	Vislanda	Marijampolé
Thickness [m]	0.2	0.2	-	-
Area [m^2]	0.04	0.04	$3.273 \cdot 10^{-4}$	$2.806 \cdot 10^{-4}$
Young's modulus [GPa]	38	38	205	205
Poisson's ratio [-]	0.2	0.2	0.3	0.3
Coeff. thermal expansion [1/°C]	$12 \cdot 10^{-6}$	$12 \cdot 10^{-6}$	$12 \cdot 10^{-6}$	$12 \cdot 10^{-6}$

The value for the Young's modulus of concrete is the final 28 day value and was based on the assumption that the development of the concrete stiffness with time will not influence the results to a great extent and can be considered to be constant (see 4.2.5). The same applies for the coefficient of thermal expansion of concrete (see 4.2.4) which was assumed to have the same value as for steel. The variation of the Poisson's ratio was neglected; as 3D analysis was considered not to be needed, strains in other directions than longitudinal were assumed to be of minor importance. Other parameters in the table were considered to be constant with time without further investigation.

The casting time was of great importance and was assumed to be 1 hour for Vislanda and 2.5 hours for Marijampolé (Bolmsvik, 2013). That influenced the temperature input and the bond input, which can be seen in Sections 5.2 and 5.3. Casting took place from the passive end towards the active end.

5.2 Temperature

The hydration of concrete was not modelled as stated before. Instead, the measured temperature curves from the different factories were implemented explicitly to the model.

5.2.1 Vislanda

The temperature curve that was used as the input for Vislanda analysis was from the measurements performed at 12/03/2010 (see Section 3.1.2). The measurements were obtained at the active end of the bed. It was assumed that the same temperature curve could be used for all parts of the bed with a delay of 1 time step for every 10 m long part; i.e. for a time step of 0.1 hours, the total delay was 1 hour as the casting time. The applied temperature curves for the ends can be seen in Figure 5.1.
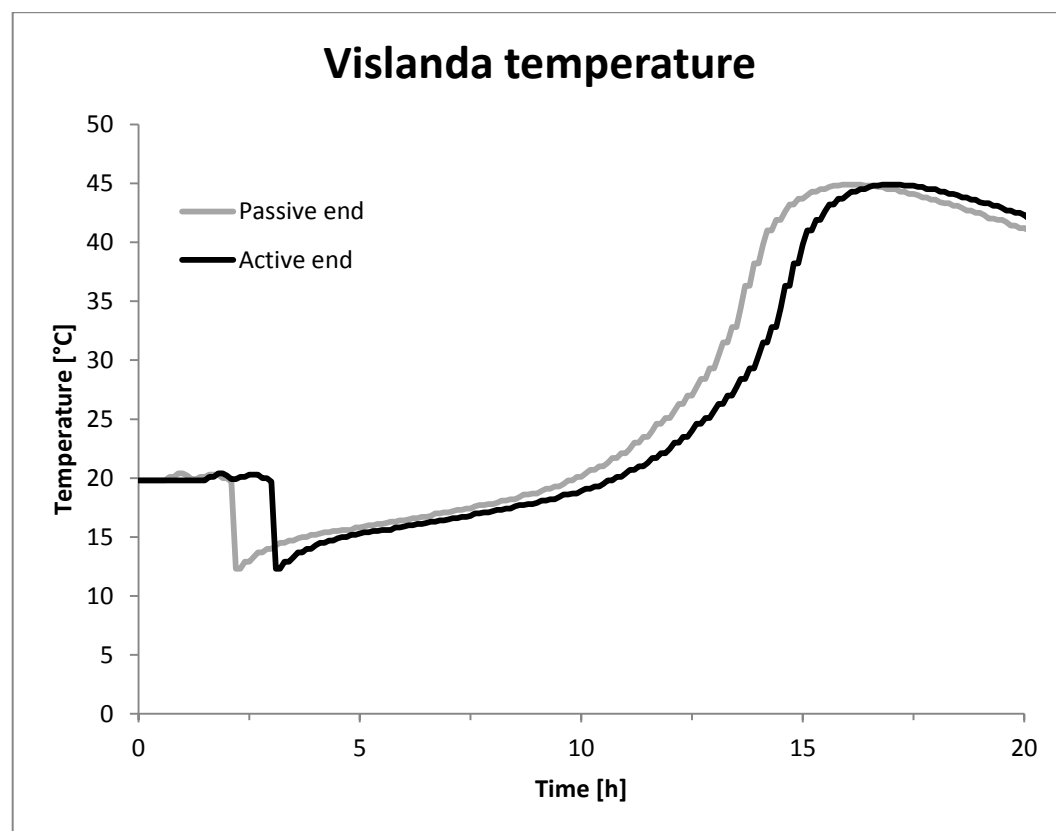
Figure 5.1.   Temperature curves in the passive and active end for Vislanda with 1 hour delay.

5.2.2 Marijampolé

Measurements for the temperature were available for Marijampolé both at the active- and passive ends; they showed quite a large difference between the ends (see Section 3.2.2). Each curve was applied to the corresponding end at the correct time, and linear interpolation was performed for every 10 m part in between. The delay of the temperature curves was 0.25 h between each part which resulted in a total delay of 2.5 hours between ends; i.e. the same as the casting time. The applied temperature curves can be seen in Figure 5.2.
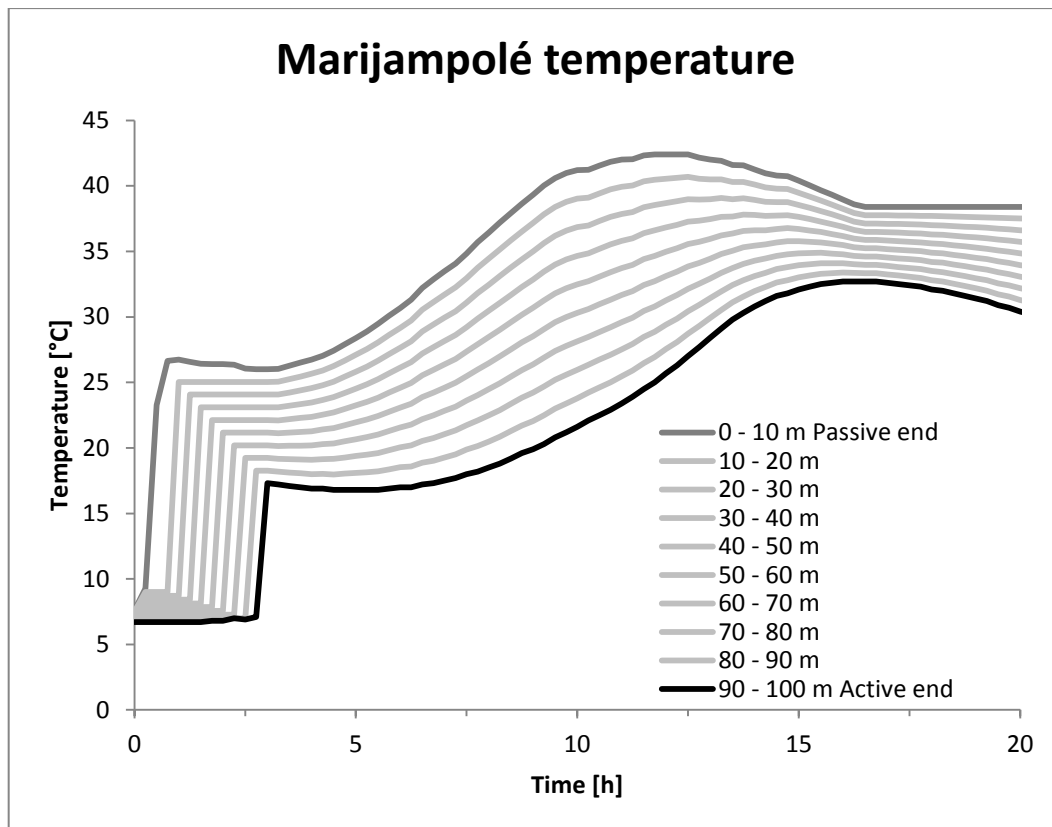
Figure 5.2.   Temperature curves in Marijampolé for each step from passive end to active end with 2.5 hours delay.

5.3   Bond

The bond between steel and concrete was modelled assuming bond stiffness only instead of using the whole bond-slip curve, see Section 4.2.3. The stiffness was then varied with time. Therefore, the input for the bond needs to include reasonable values for the bond stiffness at each point in time.

In order to obtain reasonable values for the bond stiffness, research made by Gustavson (2004) was used. The research included bond-slip curves from pull-out tests made 24 hours and 96 hours after casting of concrete, which gave an indication of the bond stiffness and strength at early ages. The bond-slip curves can be seen in Figure 5.3.
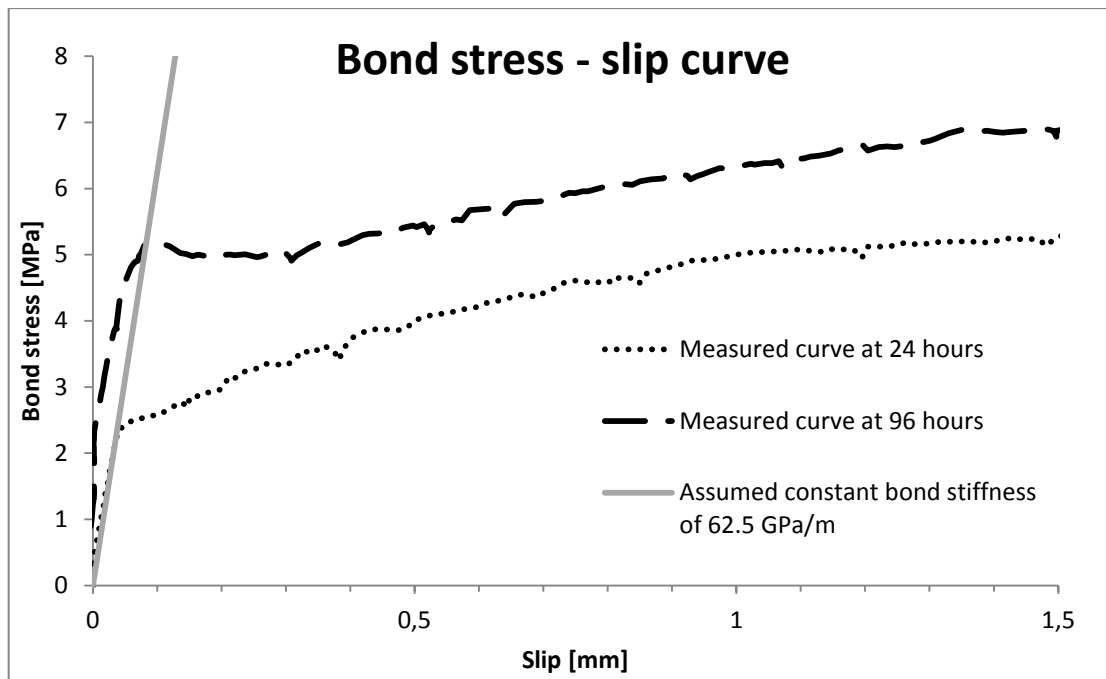
Figure 5.3. Assumed constant bond stiffness compared to measured bond stress – slip curves after 24 h and 96 h, from Gustavson (2004).

The bond strength was about 5 MPa but the stiffness decreased at 2.5 MPa for the 24 hours curve. The bond strength at 96 hours was about 7 MPa but the stiffness decreased at 5 MPa. The compressive strength at 24 hours was 27 MPa and 42 MPa at 96 hours.

The compressive strength at 17 h in the sleepers was supposed to be at least 35-40 MPa (see Sections 3.1.1 and 3.2.1). Therefore, the curve at 96 hours could give an approximation for the bond-slip curve in the sleeper production at around 20 hours. Thus, in order to see if the assumption of using a linear bond-slip curve holds, the maximum bond stress obtained in the analysis should not exceed 5 MPa. For bond stresses larger than 5 MPa, the stiffness should decrease to a large extent and therefore a more refined bond-slip curve would be needed for the modelling.

The bond stiffness in the analysis could be assumed to be 62.5 GPa/m at around 20 hours after casting. From Figure 5.3, it can be seen that 62.5 GPa/m is approximately the tangent stiffness at 24 hours after casting and the secant stiffness at 96 hours after casting. Therefore, it was assumed that 62.5 GPa/m was a reasonable value to use. The same final stiffness value was assumed for both Vislanda and Marijampolé.

Values for stiffness earlier than 24 hours are not known and need to be estimated. The estimation can be based on the measurements from the two different factories and the strength development discussion presented in Section 2.2. It was assumed that the bond started to develop at the same time as the concrete temperature started to increase. This is considered to be a reasonable assumption since the initial set, which corresponds to the start of the concrete stiffness development (see Section 2.2), occurs at that time. Then, the stiffness was assumed to reach the final value when the concrete temperature reached maximum with a linear relation from 0 GPa/m to 62.5 GPa/m. That is based on the assumption that the strength development was much slower after the maximum temperature had been reached and could be considered to

be constant. This behaviour can be seen in Figure 2.5, where the tensile strength gain decreases at around 20 hours. Tensile and bond strength are considered to be closely related (see Section 2.3). Also, the prestress losses to be evaluated occurred before the maximum temperature both in Vislanda and Marijampolé so the real value of the bond stiffness during the cooling was not of great importance.

Based on this discussion the bond stiffness in Marijampolé started to develop much earlier than in Vislanda. That can be seen in the following figures which show the bond development in the ends of the bed as a function of time for Vislanda and Marijampolé.
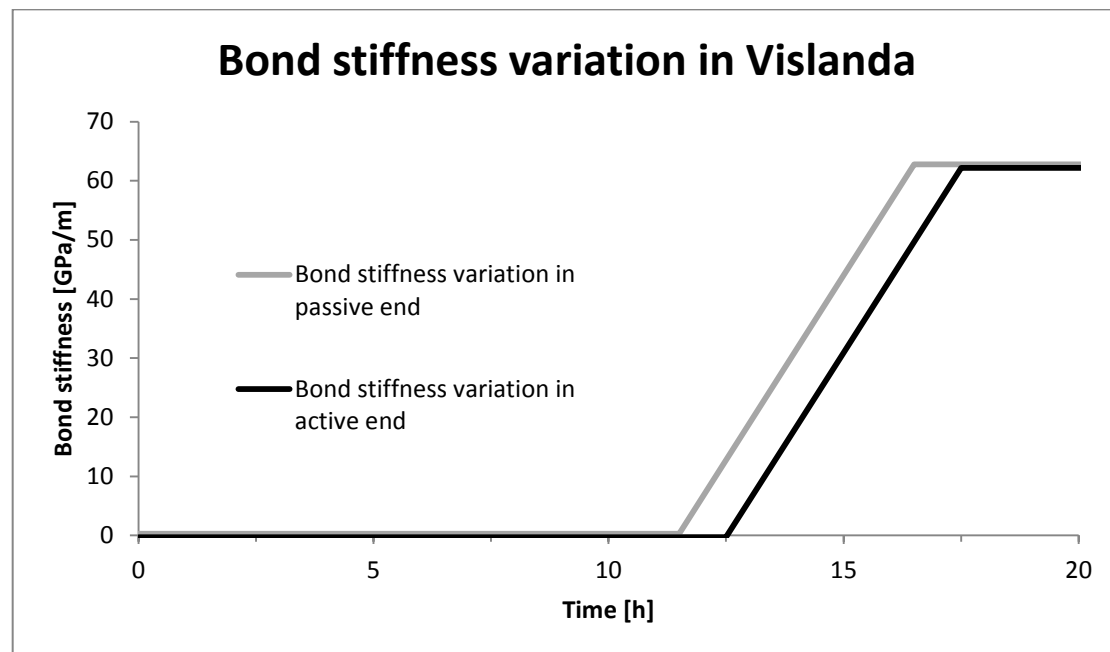
Figure 5.4.   Bond stiffness variation in Vislanda for passive and active end.
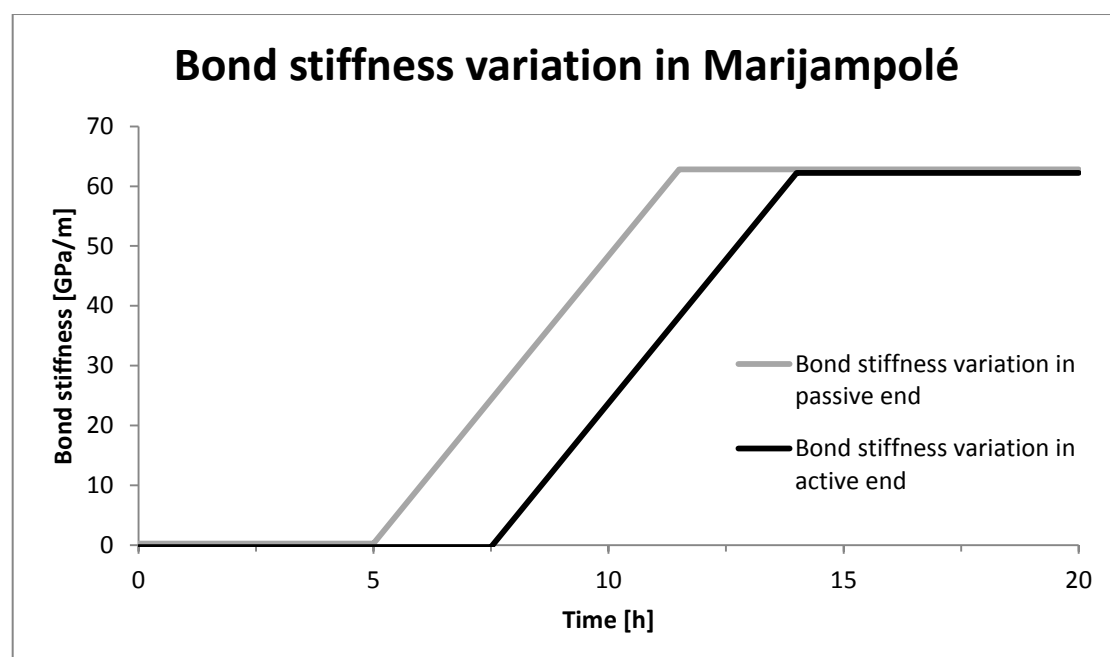
Figure 5.5.   Bond stiffness variation in Marijampolé for passive and active end.

In order to account for the casting time, the bond development was shifted towards the passive end for each 10 m part. Therefore, the bond in the passive end developed 1 h and 2.5 h ahead of the active end for Vislanda and Marijampolé respectively. This was modelled in a user-supplied subroutine, see appendix B.3.

Table 5.2. *Values regarding bond development in Vislanda and Marijampolé models.*

	Vislanda	Marijampolé
Final bond stiffness [GPa/m]	62.5	62.5
Bond dev. start in active end [h]	12.5	7.5
Bond dev. end in active end [h]	17.5	14
Bond stress limit [MPa]	5	5
Interface thickness [m]	0.213*	0.213
Casting time [h]	1	2.5

*The correct value is 0.249 m. However, due to a convergence error, the value from Marijampolé was used in the analyses. The effect of this was assumed to be negligible.

6   Results

The results from the numerical modelling were obtained from the full size model using the input from Chapter 5. The file showing the model geometry and input can be found in appendix C.

6.1   Vislanda

6.1.1   Prestress losses

The results for the prestress at 0.5 m from the edge of the concrete at the active end in Vislanda are presented in Figure 6.1. Measurements at the same position are also presented for comparison.
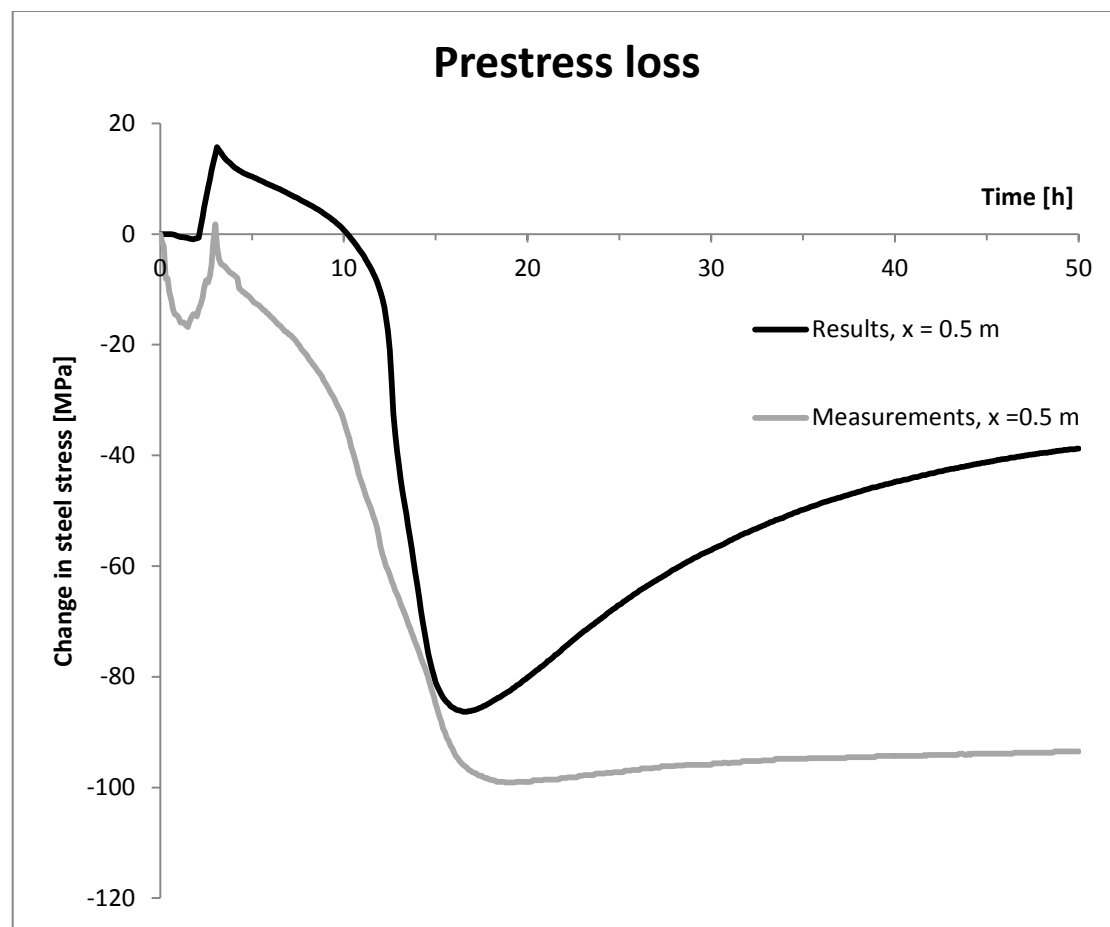
Figure 6.1.   Results for change in steel stress at 0.5 m from the concrete edge in the active end at Vislanda.

The results are similar to the measurements. The curves have a very similar slope between 3 and 10 hours, thereafter the slope of both curves changes and the prestress loss becomes more rapid between 10 and 17 hours. In this period, the greatest temperature increase takes place and the bond is increasing. After 17 hours, the concrete starts cooling and the results from the model show a prestress increase while the measurements almost show a constant prestress. This difference could be due to further increase of the bond which causes less prestress change (see Figure 4.9) or other factors like shrinkage of the concrete. However, the prestress losses during the

heating phase were the most important in this study, and therefore these other factors during the cooling phase were assumed to be negligible. Before casting, both curves show a prestress increase of a similar amount, which is due to the temperature drop in the wires during the period when the concrete is poured. Before the increase, a prestress loss can be seen in the measurements which the modelling results do not show. Reasons for these measured losses are unknown, but they could be due to relaxation of the wires, leakage in the hydraulic jack or other factors. This drop was added to the modelling results in Figure 6.2 to show only the prestress loss due to thermal effects. With this modification, the results simulate the measurements better in magnitude and the shape is still the same as before.
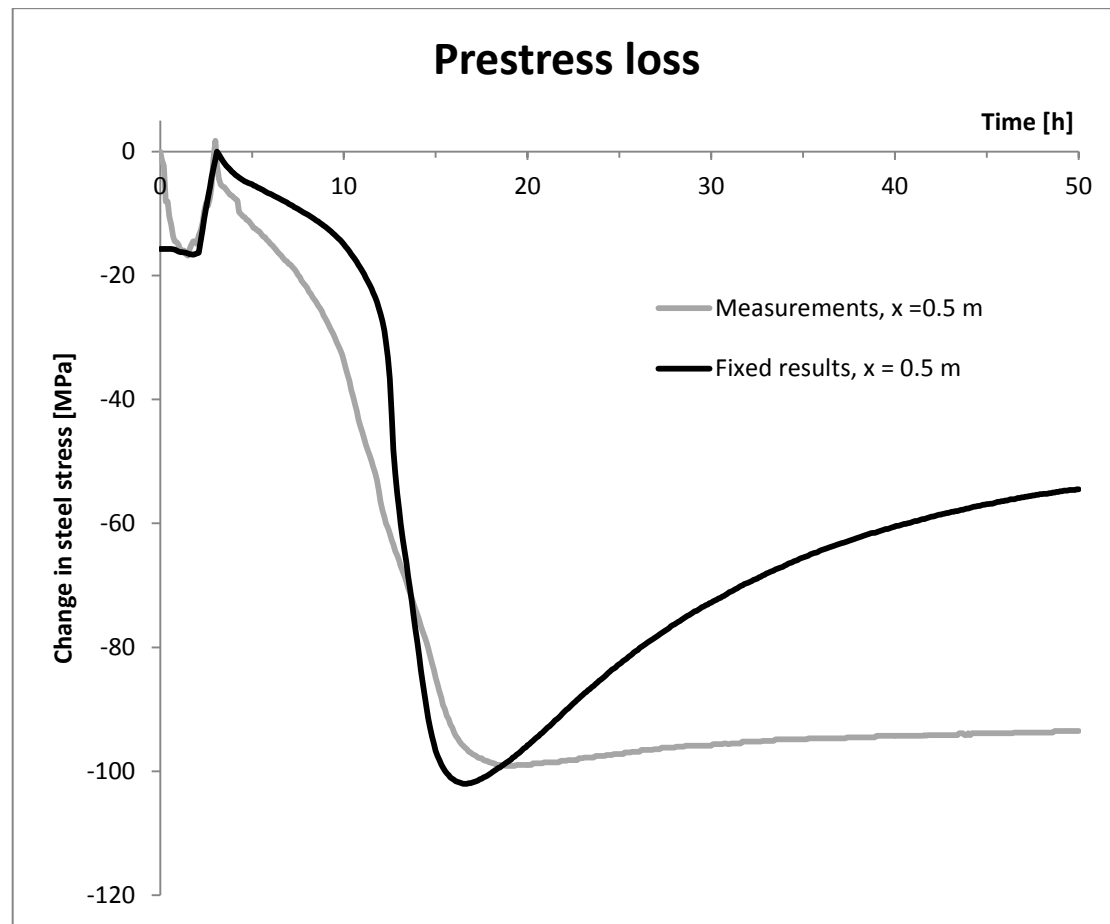
Figure 6.2.   Change in steel stress for Vislanda where the results have been modified to fit the initial drop.

Figure 6.3 below shows the prestress variation along the 100 m long bed at different times.
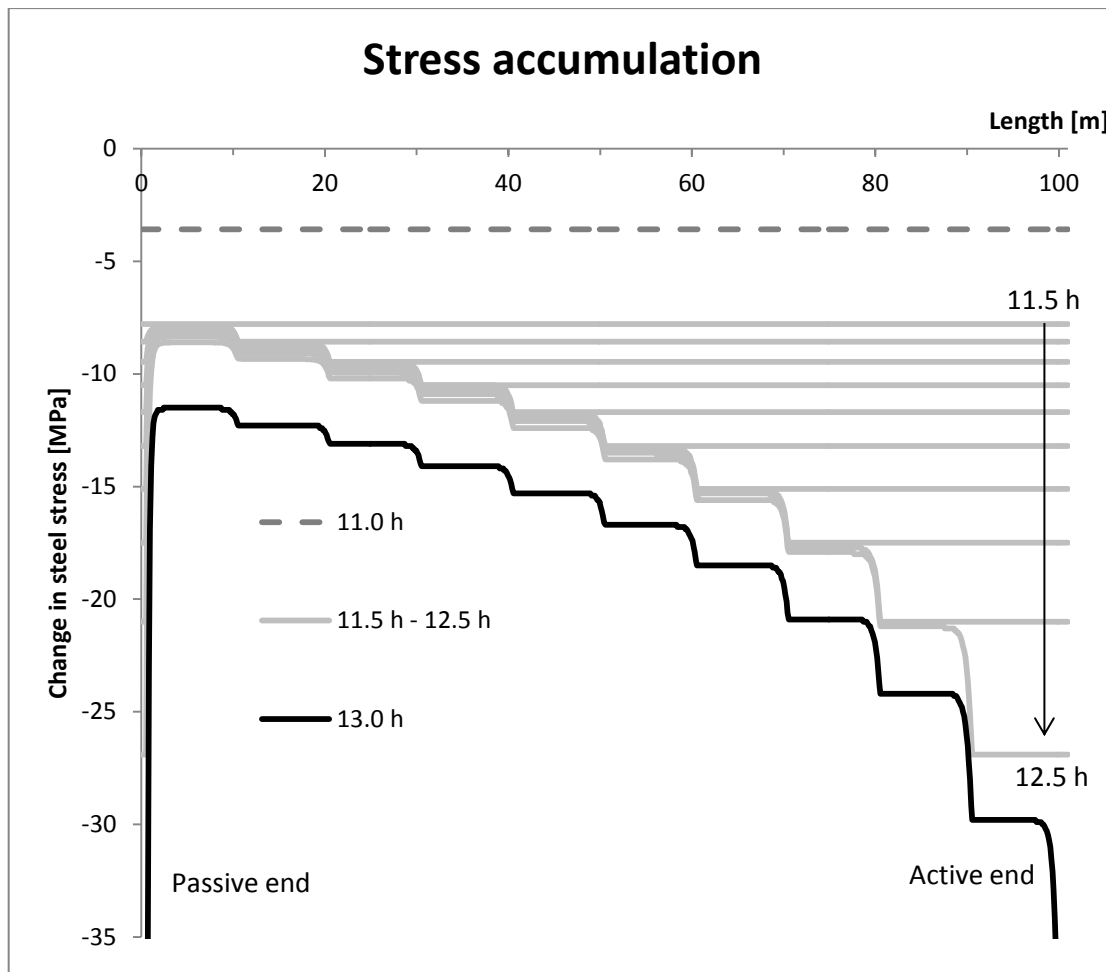
Figure 6.3. Stress accumulation along bed in Vislanda at different times. The concrete bed was 100 m from 0.5 m to 100.5 m and the wire outside the concrete was 0.5 m on each side of the bed.

The figure shows the effect of the application of the bond and the accumulation effect. The accumulation effect can be seen by the prestress losses being greater at the active end and the differences between the ends occur after application of the bond at the passive end (at 11.5 h). Each "jump" in the graph represents the application of bond at each part of the model, going from the passive end towards the active end increasing the prestress loss in the adjacent part in every step. After the application of bond, the prestress loss is much larger in the parts where bond has not been applied. Since the bond is applied the latest in the active end, the prestress loss will be largest there.

The difference between the ends increases with each step from 11.5 h to 12.5 h, and the length of the bed also increases this effect. If the bed would have been longer, this process would have kept on going and the difference between the ends would have been larger.

The difference between the curves for 12.5 hours and 13 hours show that the drop is the same along the bed, i.e. after the application of the bond at the active end at 12.5 hours the accumulation has stopped but prestress losses continue equally in all parts of the bed.

It should also be observed that the stress in the wire outside of the concrete ("naked") is the same at both ends during the whole process. This is correct due to force

equilibrium for the assumed model; however if the external restraint which is present in reality would be included (see Section 4.2.6), the stress in the "naked" wire would probably not be the same at both ends.

By excluding the external restraint, the prestress losses in the active side of the bed are most likely larger than in reality, since in the model the expansion of the parts with bond is evenly distributed between the total length of wire without bond. If an external restraint would be present, the expansion wouldn't necessarily be equally distributed between both ends. However, the general behaviour in terms of an accumulation of prestress losses along the bed should be the same, with different prestress losses at the ends.

The prestress loss in the "naked" wire and at 0.5 m from the edge as a function of time can be seen in Figure 6.4.
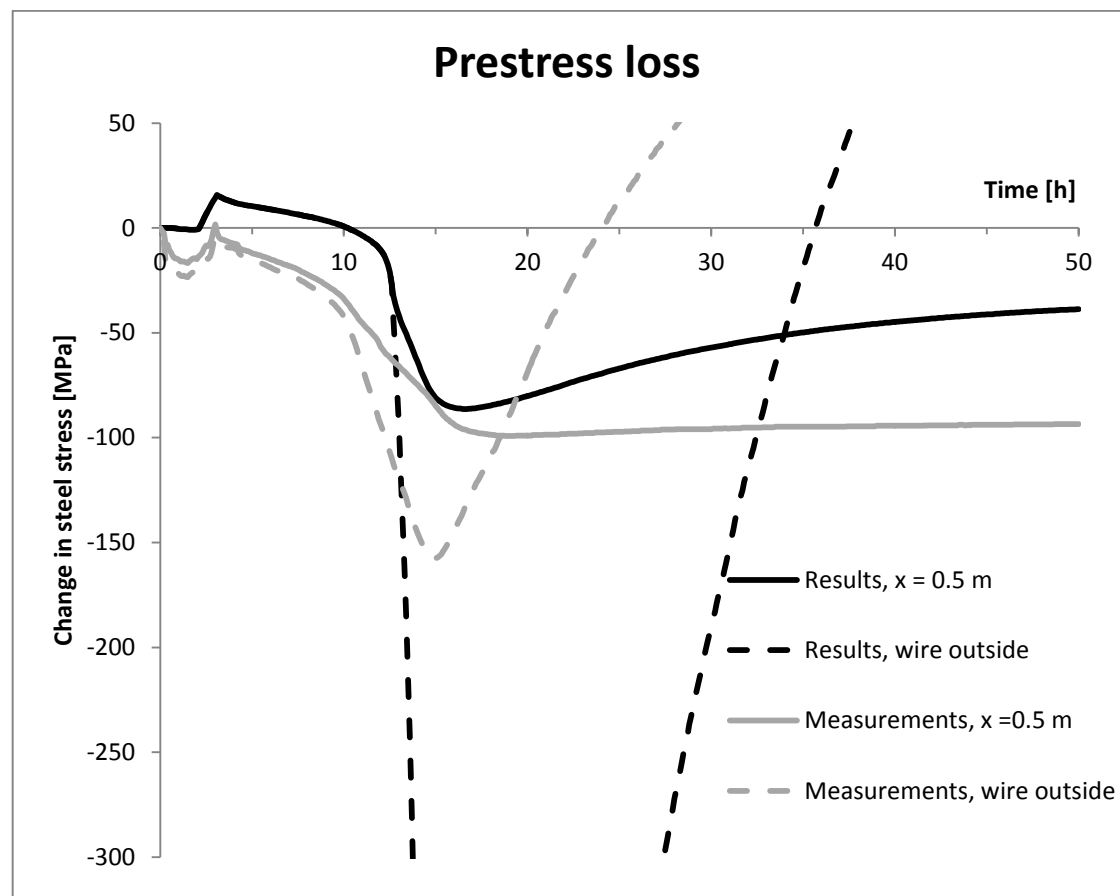
Figure 6.4.   Results for change in steel stress in Vislanda at 0.5 m from the concrete edge and the wire outside the concrete at the active end.

The behaviour of the "naked" wire in the analysis compared to the measurements is reasonable if the magnitude is ignored. The two curves in the analysis (at 0.5 m and "naked") start to deviate at 12.5 h when the bond was applied. However, the curves from the measurements start to deviate at 10 hours. That is assumed to be due to the bond starting to increase to a small amount in the measurements from 10 hours. If that were to be taken into account in the bond modelling, a more refined bond development should have been used. That was assumed to be of minor importance.

After 12.5 hours in the analysis, the prestress in the "naked" wire decreased much more than at 0.5 m from the edge until the cooling phase where a large increase can

be observed. This is exactly the same behaviour as the measurements show. Therefore, it can be concluded that the general behaviour of the "naked" wire has been captured but the magnitude is not correct.

6.1.2 Transmission length and bond stress

The transmission length must be checked to verify the results. Figure 6.5 shows the steel stresses along the bed at 17.5 hours (full bond) into the process and the stresses at the active end have been enlarged to study the transmission length.
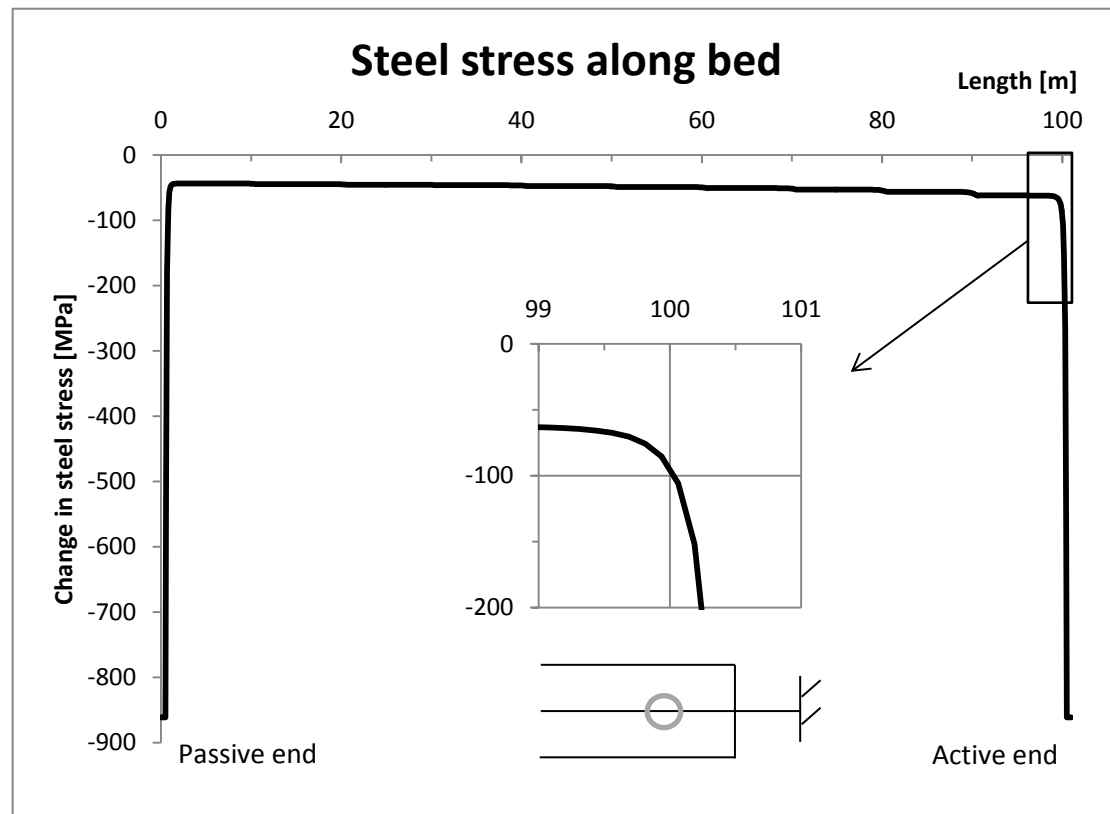
Figure 6.5.   Steel stress change along the bed in Vislanda at 17.5 hours.

The figure shows that the steel stresses have reached equilibrium at approximately 0.75 m from the edge of the concrete (99.75 m in the figure). The results in Figure 6.1 were obtained at 0.5 m from the edge at the active end. Thus, the transmission length has a slight effect on the results and the prestress losses are a bit higher than they should be. This is due to a convergence problem in the model which occurred because the interface thickness in Vislanda was too high. The interface thickness should be equal to the total perimeter of steel wires. The assumption of the same thickness as in Marijampolé was made and the bond was thereby lowered since the total perimeter of the wires was less in Marijampolé. The influence of this is considered to be negligible and the results therefore reliable.

Bond stresses were checked to see if they exceeded the limit of 5 MPa as discussed in Section 5.3. The bond stresses as a function of time at the very end, and at 0.5 m from the edge can be seen in Figure 6.6.

Bond stress over time
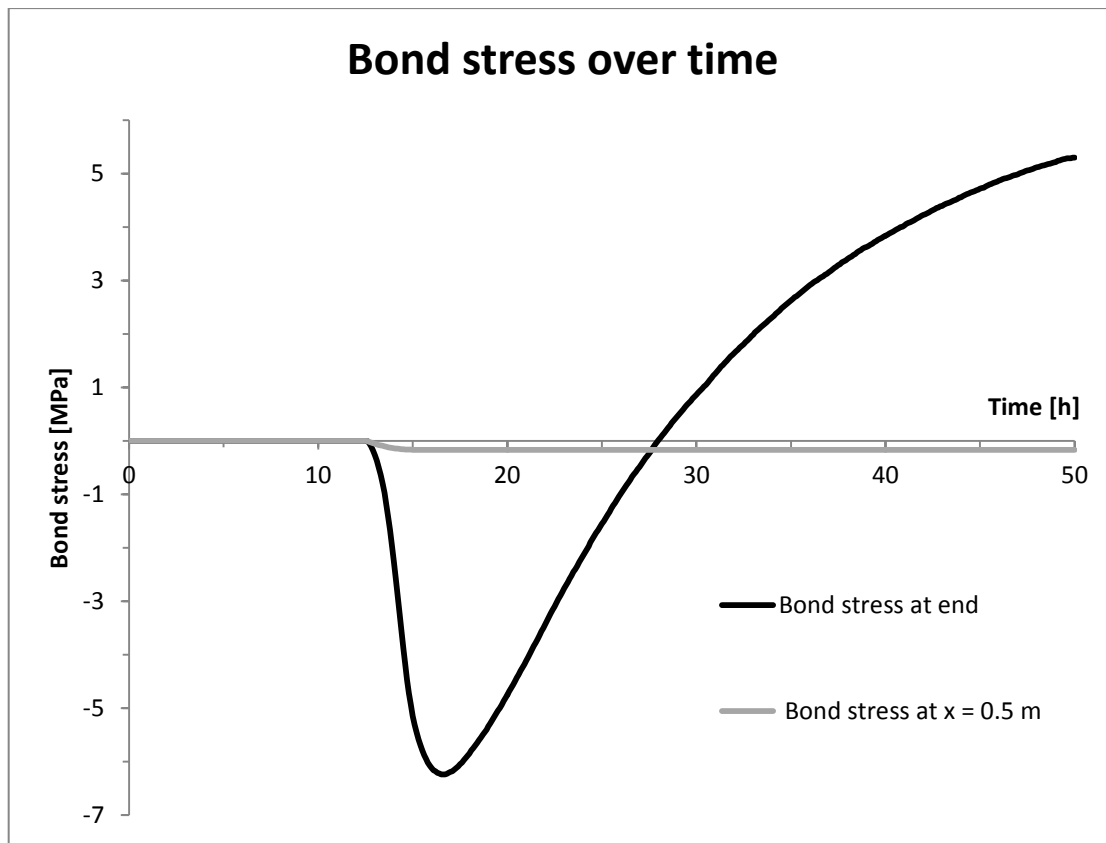
Figure 6.6. *Bond stresses as a function of time at the active end in Vislanda.*

As can be seen, the maximum bond stress obtained in the analysis was 6.2 MPa at the very end. Thus, bond failure took place at that position and stresses would be redistributed to the nearby elements. Thus, the prestress loss at 0.5 m from the edge could be slightly larger due to this. However, since the difference between 6.2 and 5 MPa was considered to be small, the effect was assumed to be negligible. Figure 6.6 also shows that the bond stresses at 0.5 m from the edge were always very low during the process. Therefore, it was assumed that bond failure will not take place and the results assumed to be reliable, although stresses from the end might be redistributed to some extent.

6.2 Marijampolé

6.2.1 Prestress losses

The results for the prestress loss at 0.5 m from the edge of the concrete at the active end in Marijampolé are presented in Figure 6.7. Measurements at the same position are also presented for comparison. Figure 6.8 shows the results from the modelling without the measurements.
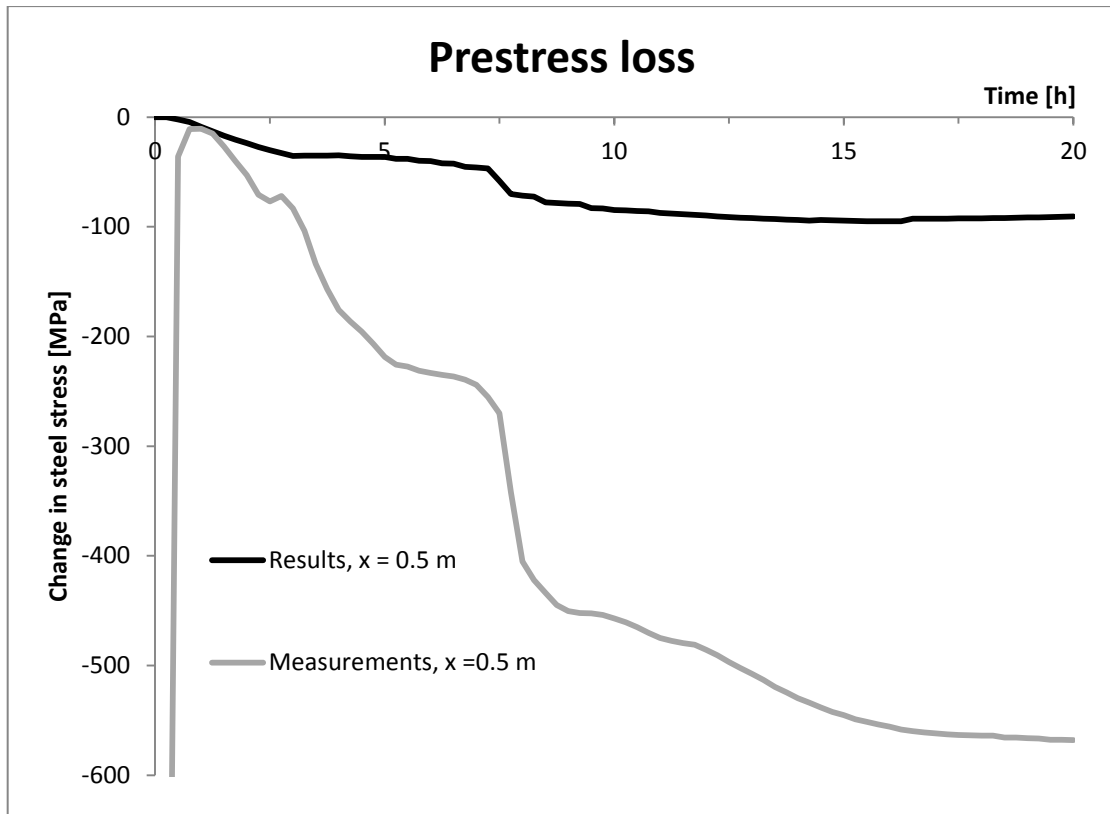
Figure 6.7.   Prestress loss measurements and results obtained for the Marijampolé model at 0.5 m from the concrete edge at the active end.
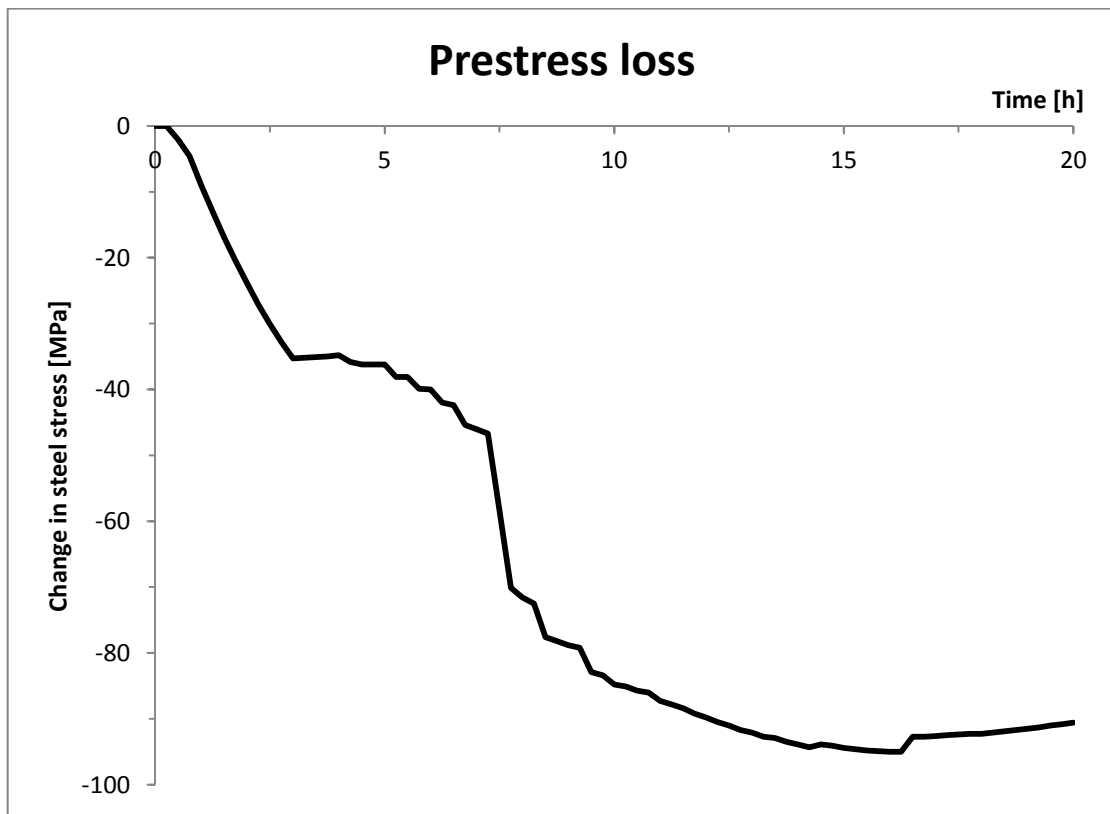
Figure 6.8.   Results for prestress loss in Marijampolé at 0.5 m from the concrete edge at the active end.

Figure 6.7 shows a great difference in magnitude between the measured results and those from the analysis; the measured prestress losses were much larger than was obtained from the FE-model. The reasons for that are still unknown but Figure 6.8 shows a very similar shape of the curve as the measurements.

The analysis results show that before casting, an initial drop occured which was caused by the temperature increase when the concrete was cast. Between 3 h and 7.5 h, a slight prestress drop can be seen. At 7.5 h, the bond was applied at the active end and a very rapid prestress loss can be seen. This drop was most likely caused by the application of the bond, the accumulation effect and the different temperature between different parts of the bed. A parameter study was performed to understand that better, see discussion in Section 7.2. After 7.5 h, the prestress loss continued to gradually follow the temperature curve until the end of the heating phase like in Vislanda. This is to a large extent the same behaviour as can be seen in the measurements.

Figure 6.9 shows the prestress variation along the 100 m long bed at different times.
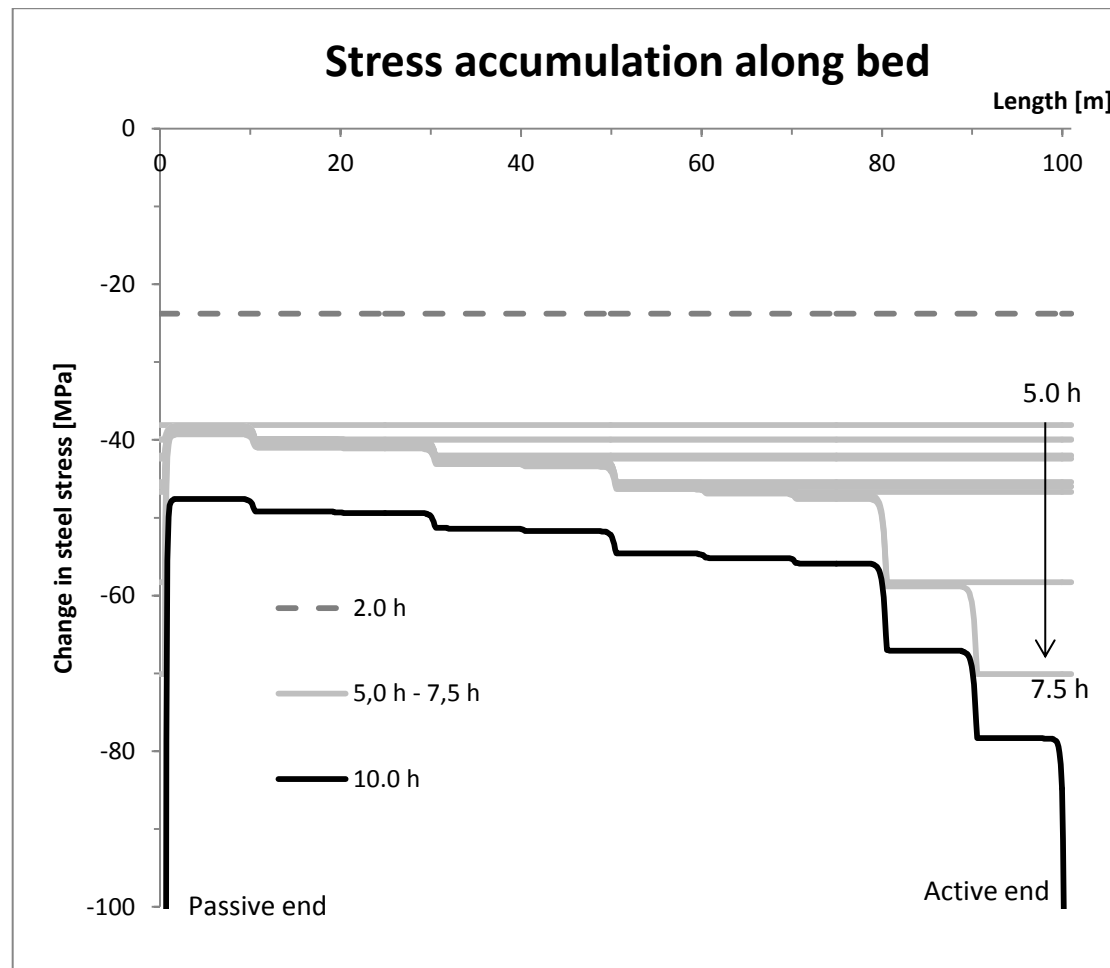
Figure 6.9.   Variation of the steel stress along the bed at different times. Concrete bed is 100 m from 0.5 m to 100.5 m and wire outside the concrete is 0.5 m on each side of the bed.

Figure 6.9 shows, up to a certain extent, similar behaviour as in Vislanda. The prestress difference between the ends is present from 5 h when the bond is applied at the passive end. Then as the process continues, the difference increases for the

application of bond at every part of the bed. The drops between the parts are different of magnitude; in the centre of the bed they are very little while near the active end they are much greater. In Vislanda, the drop size between parts increased gradually from the passive to the active end. This difference between the factories could be due to different temperature input for each part along the bed. In Vislanda, the same temperature curve was applied for every part at different times while in Marijampolé, different temperature curves were applied for every part. This will be discussed further in a parameter study, see Section 7.2. The large drop at 7.5 h in Figure 6.8 can be seen in Figure 6.9 by comparing the prestress at 7 h to 7.5 h at the active end. The curve has dropped quite much during that period, while at the passive end the prestress is almost constant.

The prestress in the "naked" wire as a function of time and the prestress at 0.5 m from the edge can be seen in Figure 6.10.
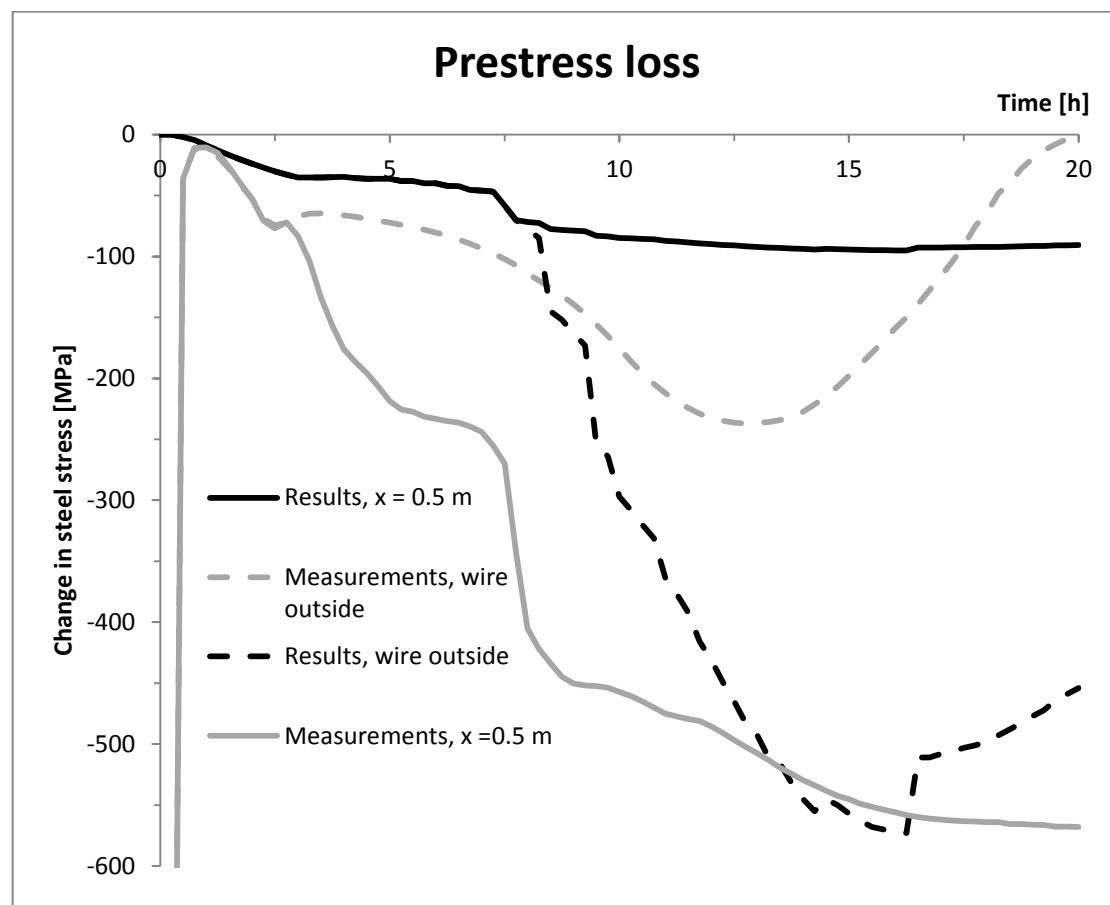
Figure 6.10.   Results and measurements for Marijampolé in the wire outside the bed and at 0.5 m from the concrete edge at the active end.

As in Vislanda, the analysis results for the "naked" wire and the wire at 0.5 m from the edge of the concrete start to deviate when the bond is applied in the active end. That is considered to be a reasonable result since at the application of bond, the concrete and steel start to act as one structure while the "naked" wire is not influenced by the concrete. The measurements from Mariampolé surprisingly enough do not show that behaviour. The two curves start to deviate already at casting and the prestress loss in the "naked" wire is much less than the loss at 0.5 m from the edge. That does not correspond to the measurements in Vislanda or to the results from the modelling. The reasons for this are not known and need to be studied further.

6.2.2 Transmission length and bond stress

Figure 6.11 shows the steel stresses along the bed at 16 h (full bond) into the process and the stresses at the active end have been enlarged to study the transmission length.
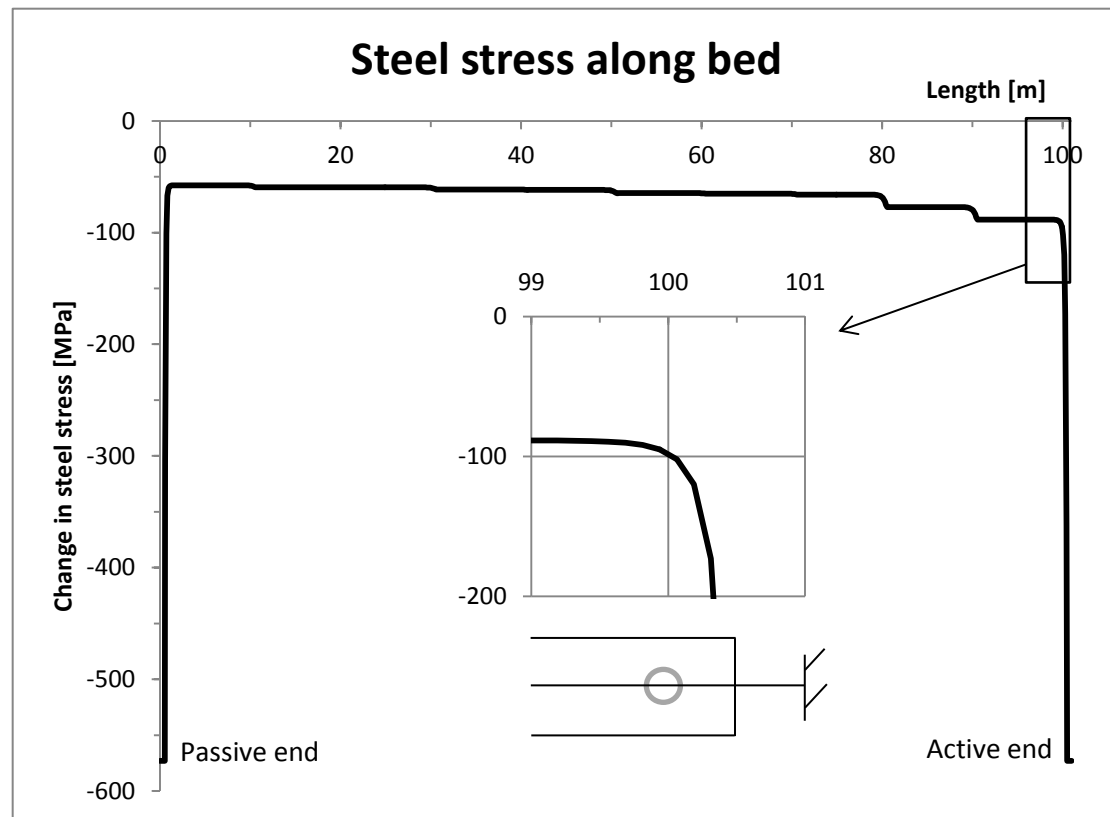
Figure 6.11.   Steel stress change along the bed in Marijampolé at 16 hours.

Equilibrium is reached at approximately 0.5 m from the edge of the concrete where the prestress change is 95 MPa compared to 89 MPa at full equilibrium. The results were obtained at that position and the transmission length does therefore have negligible influence and the results are reliable.

Bond stresses were checked to see if they exceeded the limit of 5 MPa as discussed in Section 5.3. The bond stresses as a function of time at the very end, and at 0.5 m from the edge can be seen in Figure 6.12.
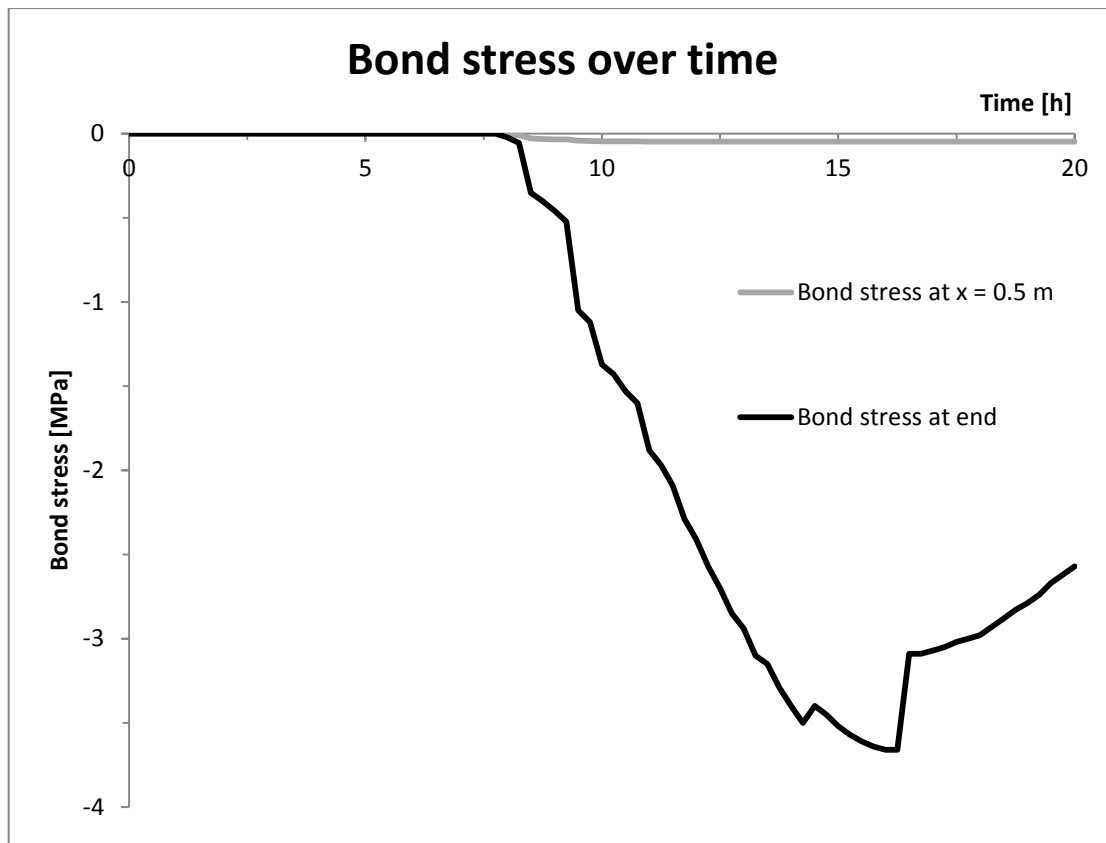
Figure 6.12.   Bond stresses as a function of time at the active end in Marijampolé.

The maximum bond stress obtained in the analysis was only 3.7 MPa at the very end of the concrete. That was under the limit of 5 MPa and therefore no bond failure took place in the process and the results are reliable.

7 Parameter study

A parameter study was performed to increase the understanding of the phenomenon. Analysis with different input for the factory in Marijampolé were carried out and compared to the results in Section 6.2 which will be referred to as the reference results. The Marijampolé model was chosen to study further since the results didn't simulate the measured prestress losses as in Vislanda. The knowledge gained from the parameter study also applies for Vislanda. The following input was varied in the parameter study:

- Process without bond
- Temperature variation along the bed
- Different bond stiffness development along the bed
- Thermal coefficient of the concrete
- Initial temperature of the steel strand
- Starting time for bond development
- Casting time

7.1 Process without bond

In order to see the effect of the bond, an analysis without bond during the whole process was carried out. All other input was the same as in the reference analysis. The prestress losses obtained in the analysis at 0.5 m from the edge of the concrete at the active end are presented in Figure 7.1. Reference values at the active- and passive end are also shown for comparison.
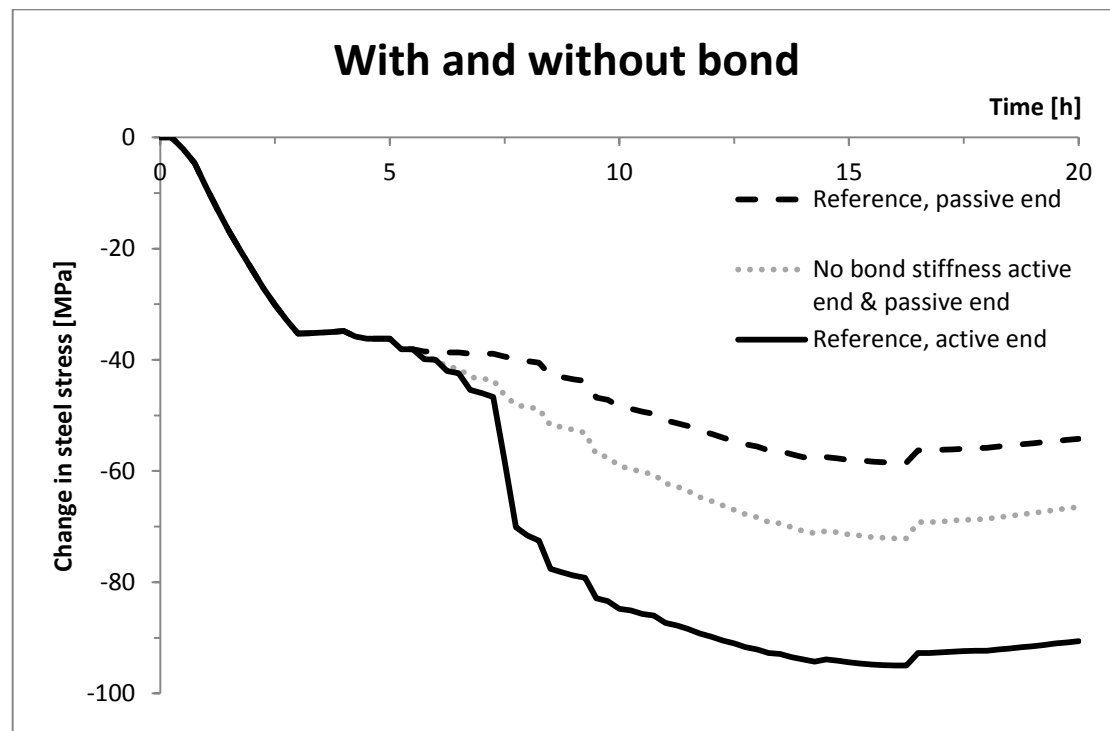
Figure 7.1. Results for the active and passive end with and without bond.

The results clearly showed an effect from the bond on the prestress loss. The curves started to deviate at 5 h in the process, i.e. when the bond was applied at the passive

end. It was interesting to see that the reference prestress loss at the active end was larger than the loss when having no bond, already from 5 hours. This occurred although no bond was present in the reference results at the active end at that time. This indicates that the prestress losses at the active end were increased because of the presence of bond in other parts of the structure, and the prestress losses were accumulated towards the active end. From 5 hours, the reference prestress was higher at the passive end than in the analysis without bond. That is most likely due to the fact that a part of stresses were carried by the concrete after the bond was applied and therefore the prestress loss in the steel was less.

The drop at 7.5 h was not present in the analysis without bond and could only be seen at the active end in the reference results, exactly at the same time as bond was applied there. This indicates that the presence of bond and the accumulation of stresses towards the active end are the key to understand that drop. In order to avoid it, the accumulation effect should be decreased. This will be investigated in more detail in the following sections.

7.2   Temperature variation along bed

The measurements from Marijampolé showed different temperature curves at each end of the bed. The input for the reference results took this into account and linear interpolation of the temperature in between was assumed (see Section 5.2.2). Two separate analyses were carried out to investigate the effect of this. First, the temperature curve at the active end was used for the whole bed. In a second analysis, the temperature curve at the passive end was used; both these analyses took the 2.5 h casting time into account. In the analysis where the passive end temperature was used the bond stiffness development was changed to start earlier and develop faster, corresponding to that temperature curve. The results for the steel stresses at 16 h along the whole bed can be seen in Figure 7.2 which also shows the reference results.

Figure 7.2.   Effects of different temperature and bond input.

The results showed that the difference in prestress between the different parts of the bed was affected by the input. The stress difference between the active- and passive ends were summarized for the three analyses in Table 7.1.

Table 7.1. Accumulation effects due to different temperature and bond input.

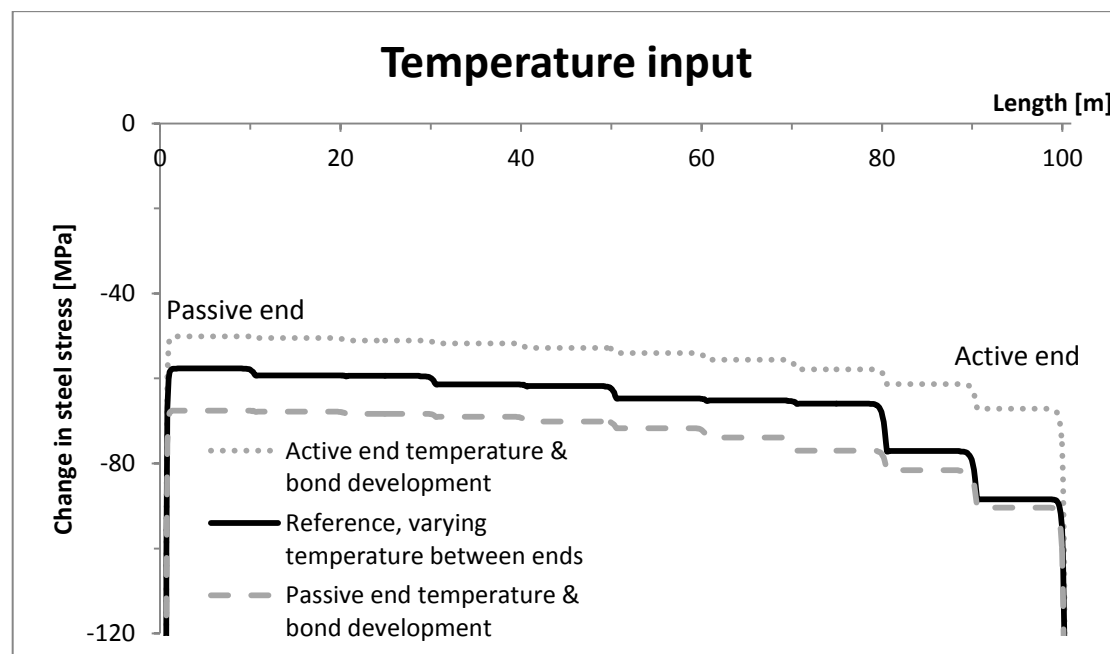| Analysis no.	Temperature curve	Stress difference between ends [MPa]
1	Active end	17
2	Reference	31
3	Passive end	23

The accumulation effect was significantly increased from having the varying temperature along the bed compared to having same temperature curve along the bed. The accumulation was similar in analysis 1 and 3 and the curves in Figure 7.2 have the same shape. The magnitude of the drops between the parts increased gradually from the passive end to the active end in both cases.

The drop magnitude along the bed was assumed to increase towards the active end due to the following reasons:

- At the time of bond application in the passive end, the total temperature increase in the bed was small while at the application of bond in the active end, the total temperature increase was much larger and therefore the drops increased towards the active end.

- The length of the unbounded wire at the active end was assumed to affect the prestress drop because the total deformation of the wire without bond was greater due to shorter length which resulted in more stress decrease.

In analysis 2, the drop magnitude was much greater at the active end than in other parts. This was assumed to occur due to the temperature increase in the active end, at the time of the application of bond, being very small compared to the passive end.

As was discussed in Section 6.2, the drops along the bed which can be observed in all of the graphs in Figure 7.2 occurred when the bond at the different parts was applied. It should be noted that the rapid drop at 7.5 h (which also could be seen in the measurements) only occurred in analysis when the temperature along the bed was varying. When the temperature curve was constant along the bed (analyses 1 and 3), the drop was more gradual and also less. Since the temperature and bond development from the active end (analysis 1) resulted in the least accumulation effects, it can be concluded that a slower temperature increase during the hydration and the same temperature development along the whole bed would be preferable.

7.3   Different bond development along the bed

Section 7.2 proved the importance of giving the correct temperature curve as an input for each part of the model. In Section 5.3, it was assumed that the bond development started when the temperature started to increase and stopped when the temperature reached maximum. Still, the bond development for the whole bed was only based on

the temperature curve from the active end. Hence, a more accurate way of modelling the bond development along the bed would be to make it follow each of the temperature curves that correspond to the different parts. For example, the bond would develop faster at the passive end than the active end because the temperature increased a bit faster at the passive end (see Section 3.2.2). The effect of this was investigated by making the bond develop faster in each part of the bed than at the active end, corresponding to the temperature curve of the part. Figure 7.3 shows the steel stresses at 16 h in Marijampolé obtained from this study and the reference results for comparison.
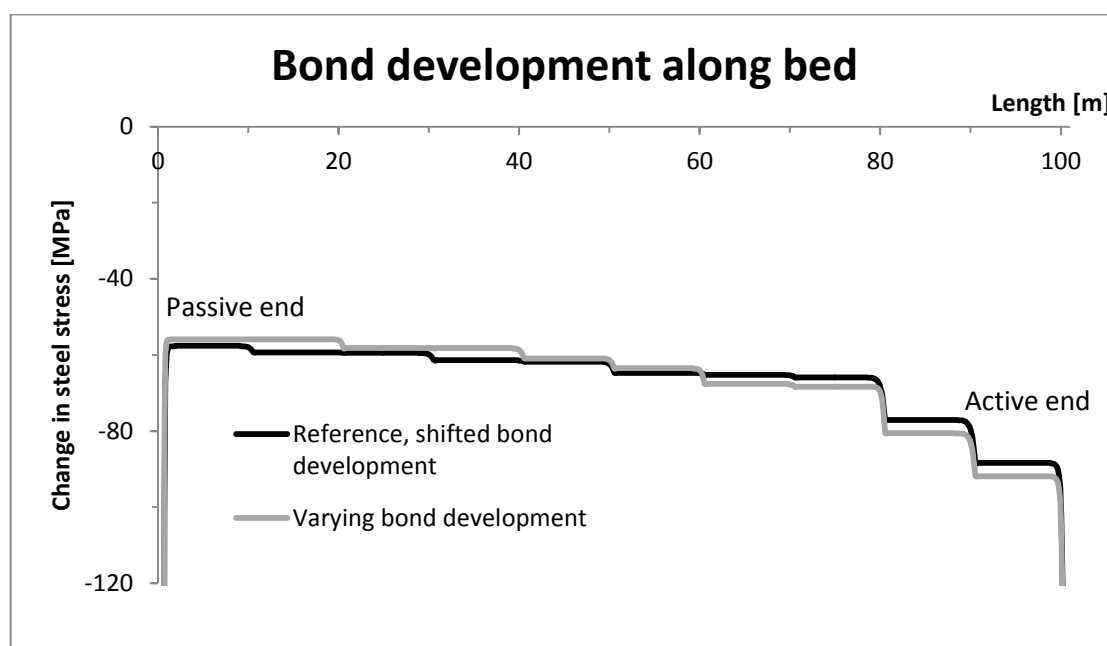
Figure 7.3.   Results from different bond development along bed.

The results showed that the varying bond development caused a slightly more accumulation effect but in general the curves were very similar. Therefore, the assumption of neglecting the effect of including the different bond development along the bed was considered to be acceptable.

7.4   Thermal coefficient of concrete

A graph showing the variation of the coefficient of thermal expansion (CTE) of concrete was presented in Figure 2.6. The graph indicated that the coefficient is very high the first hours after casting of the concrete. In the development of the input for the model, it was assumed that the CTE of concrete would have decreased down to 12 μ/°C when the bond was applied. In Marijampolé, it was therefore assumed that the graph in Figure 2.6 would look differently and the CTE would have decreased down to its final value at around 4.5 hours after casting (7.5 h in the whole process). The effect of this assumption was investigated in a parameter study where the value of CTE of concrete was increased up to a value corresponding to the graph in Figure 2.6. The results for the steel stress at 0.5 m from the edge of the concrete at the active end can be seen in Figure 7.4. The graph is only presented up to 10 hours into the process since such a high CTE is not considered to be realistic longer than that. The reference results and the measurements at the same position are also shown for comparison.
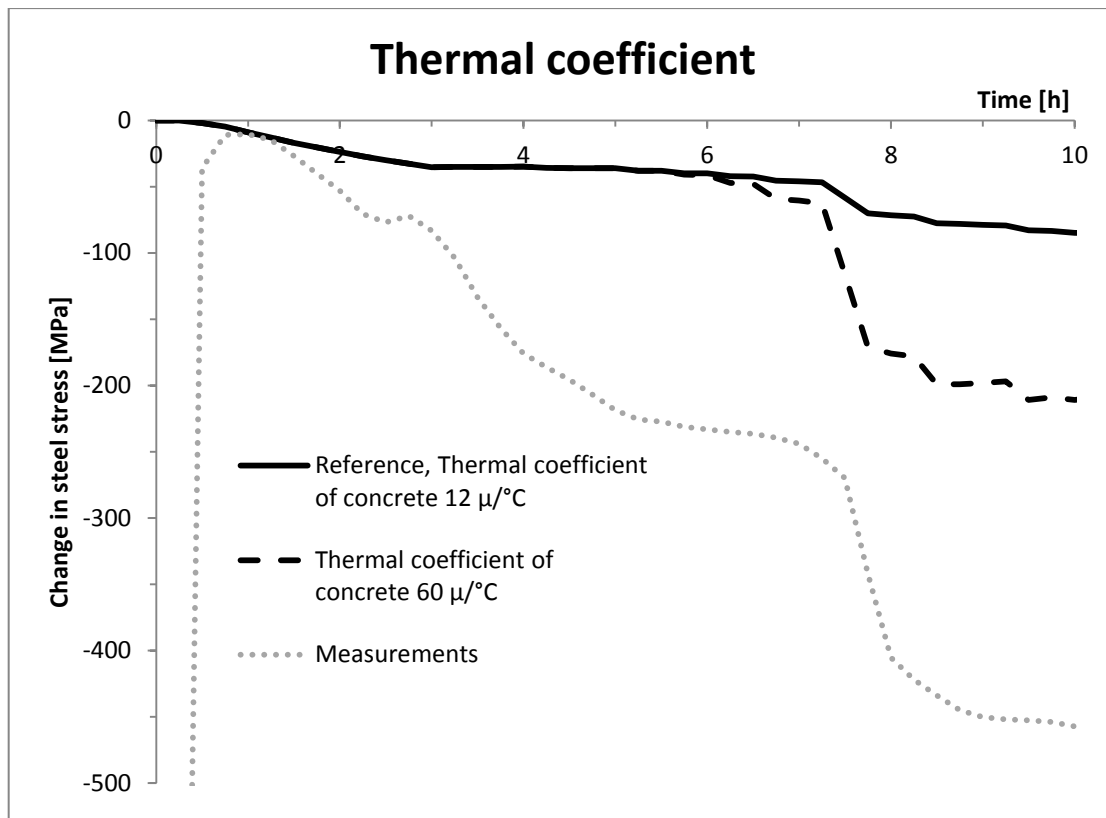
Figure 7.4.   Effects of different thermal coefficient of concrete on the steel stress.

The results showed that the shape of the curve was the same as the reference results but the magnitude increased to a great extent. Before 5 hours, no bond was present in the model and therefore the high CTE didn't have any effect. When the bond was applied, the same drop as before could be seen but the magnitude was then similar to the measurements.

This is a possible explanation for the great magnitude of the prestress losses in Marijampolé. The prestress loss between 3 and 5 hours could then also be explained by a high CTE if a very early bond would be achieved. This still needs to be further studied, since the CTE of concrete most likely decreases more rapidly if the strength development is rapid, as for Marijampolé. The CTE of a liquid is much higher than that for hardened concrete which gives an indication that the main reason for the high CTE in early stages is that the concrete is still in nearly liquid state (Elert, n.d.). If the concrete is in nearly liquid state, it can most likely not develop any bond to the steel so this parameter study is possibly not very realistic. No further literature was studied regarding this but that could be done to gain more understanding on the matter.

7.5   Initial temperature

The surrounding temperature was only around 7°C in Marijampolé while in Vislanda it was 20°C. Due to this, the steel temperature increased in Marijampolé at the casting of concrete (concrete had higher temperature) while it decreased in Vislanda. The effect of this was investigated by varying the initial temperature of the steel strands in Marijampolé and comparing to the reference results.

Two analyses were carried out; in the first one the initial steel temperature was increased so that it was higher than the initial concrete temperature. In the second analysis the initial steel temperature was the same as the initial concrete temperature. This was done for all temperature curves along the bed. As an example, Figure 7.5 shows the temperature curve variations at the active end.
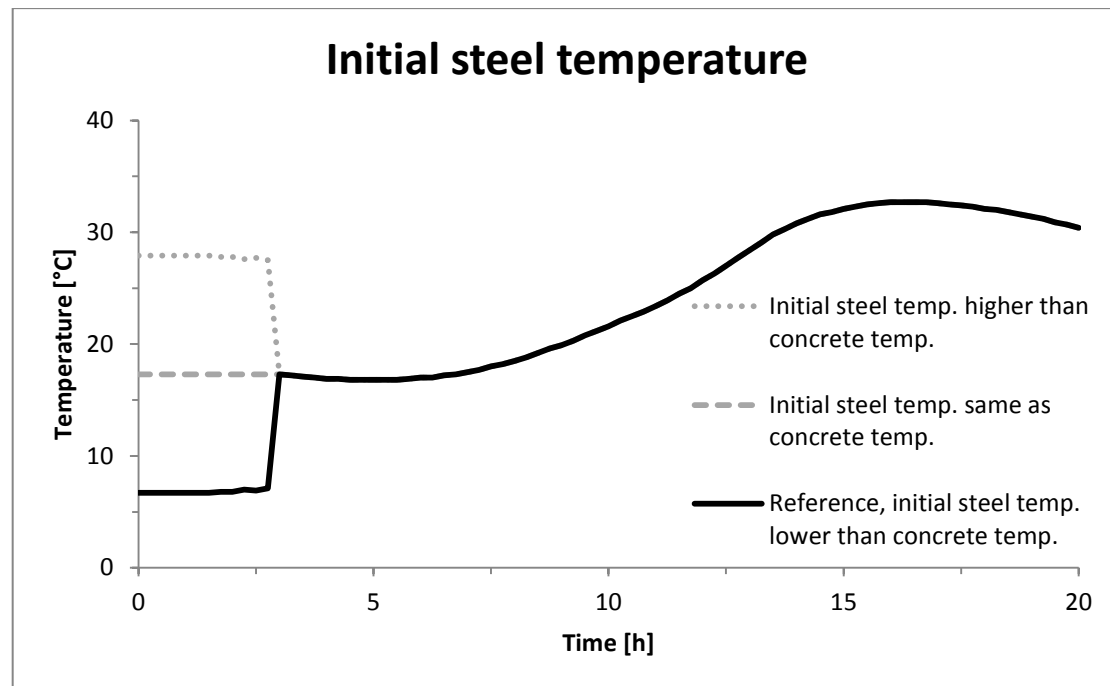
Figure 7.5.   Temperature curves at the active end for varying initial temperature of the steel strand.

The surrounding temperature could have an effect on the hydration development also since hydration occurs faster with higher curing temperature, see Section 2.2.1, but that was not taken into account in these analyses.

The concrete temperature is the same as the reference in these analyses. That could have been varied as well to do the same analyses. Then the whole temperature curve would have been shifted but since the steel stresses only depend on the temperature change over time, which would be the same, that analysis would have given the same information.

The prestress as a function of time at 0.5 m from the edge of the concrete at the active end can be seen in Figure 7.6.
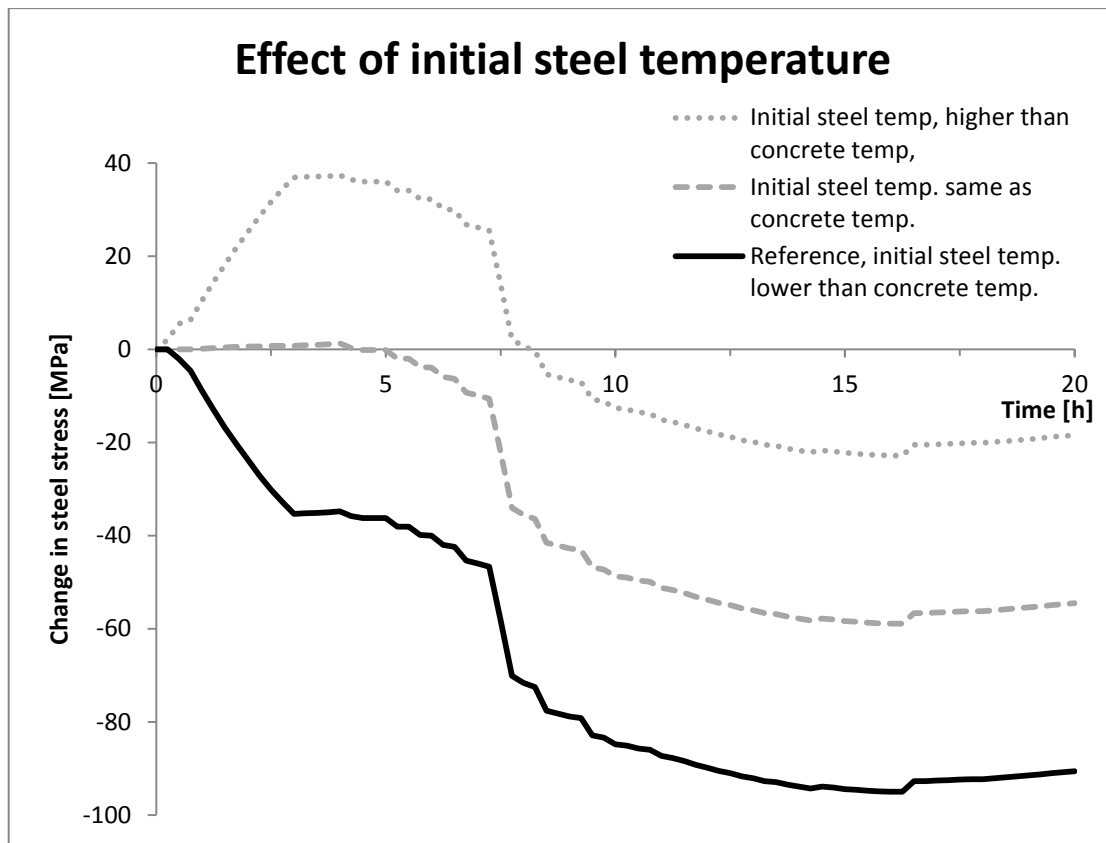
Figure 7.6.   Results for varying initial temperature of the steel strands.

The results showed that the prestress loss during casting was affected to a great extent. After casting (3 hours), the curves are the same but with different starting points.

By increasing the surrounding temperature, an initial prestress increase was obtained as in Vislanda. Then, the total prestress loss was less but the magnitude of this increase was not very high compared to the losses obtained during the hydration in Marijampolé. No prestress change occurred before casting when the steel had no initial temperature change. From this, it can be concluded that the prestress loss in the measurements that can be seen before casting, occurred because of the initial temperature change in the strands when concrete was cast along the whole bed. That resulted in a prestress loss in Marijampolé and a prestress increase in Vislanda.

7.6   Start of bond development

The bond stiffness development at the active end for Marijampolé was assumed to start at 7.5 hours. This was based on that the temperature in the active end started to increase at that point. In the following analyses, the development of the bond stiffness was changed. Figure 7.7 shows the results at 0.5 m from the concrete edge at the active end where the bond development has been shifted to 1 hour earlier and 1 hour later than the reference results.
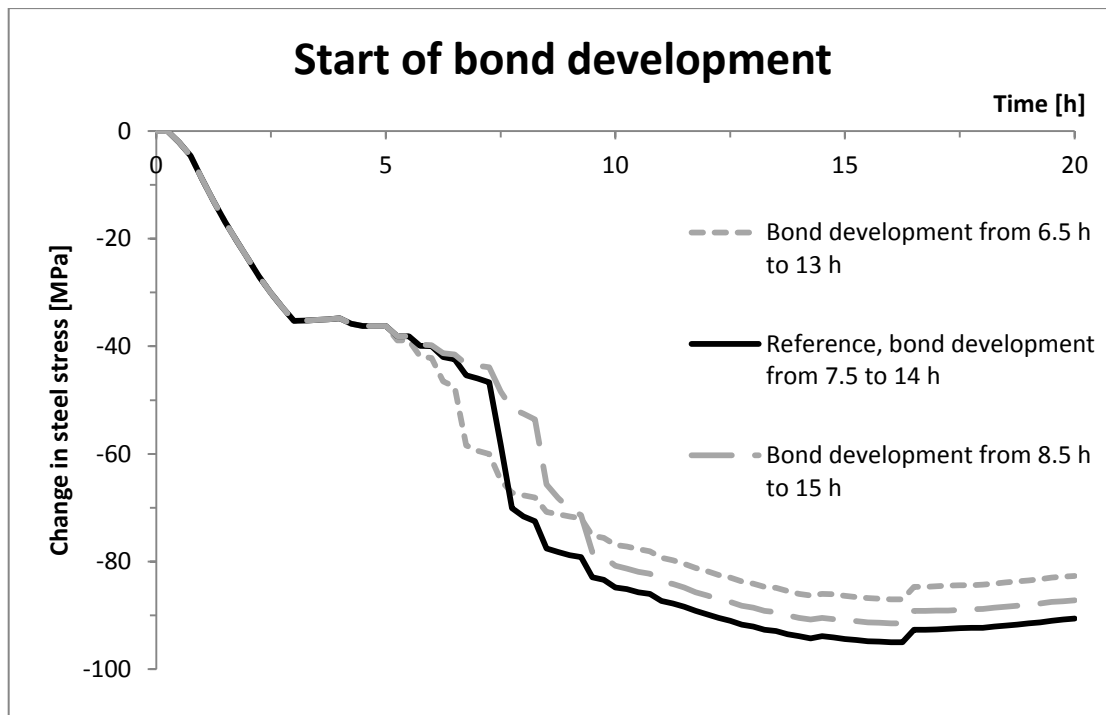
Figure 7.7.   Effects of shifting the bond development 1 hour back and forth.

The results showed that the large drop in steel stress was shifted 1 hour according to the change in the bond development. These results confirmed that the large drop takes place when the bond starts to develop in the active end. It could also be seen that the magnitude of the drop decreased by changing the start of the bond development to 1 hour earlier and the drop became more gradual and also decreased by starting the bond 1 hour later. The reference analysis resulted in the largest prestress loss and the shape of the curve is very similar to the measurements. This indicates that the assumption of the bond development starting at the same time as the temperature increase was correct.

7.7   Casting time

The effect of the casting time in Marijampolé was investigated by carrying out the same analysis as the reference but with a casting time of 1 hour instead of 2.5 hours and another analysis without any casting time, i.e. the concrete was cast everywhere at the same time. The prestress at 0.5 m from the edge of the concrete at the active end can be seen in Figure 7.8 and the prestress along the whole bed at 16 hours in Figure 7.9.
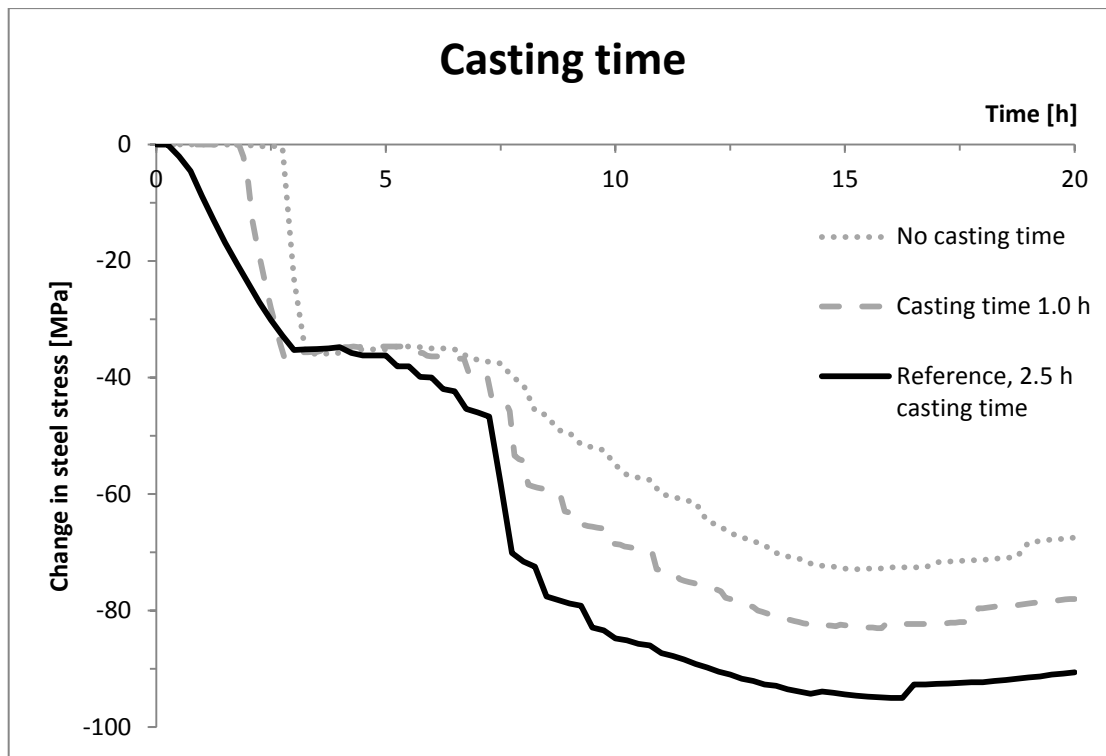
Casting time

Figure 7.8.   Change in steel stress over time with various casting times.

The results showed that the casting time did have an effect on the prestress losses and the accumulation effect. Figure 7.8 showed that the greatest prestress loss was obtained when having the longest casting time, and the smallest loss was obtained when no casting time was assumed. The drop at 7.5 hours could be seen for both the reference- and 1 hour casting time, but it was larger in the reference results. Thus, the behaviour of the prestress losses was the same but the casting time magnified the losses. The curve for no casting time did not show the sudden drop, but only a more gradual.

The three curves have similar amount of prestress change and shape from 7.5 hours on. Hence, the only difference between the curves developed between 5 and 7.5 hours, which was the same time as the bond started to develop along the bed in the reference analysis. That indicates that the casting time only influences the prestress change while the bond is starting to develop along the bed.

It should be observed that the analysis with 1 hour casting time resulted in a longer transmission length than the reference analysis. The reason for that is not known. Due to that, the curve for 1 hour casting time in Figure 7.8 showed larger prestress loss than at equilibrium further inside the bed. The shape of the curve at equilibrium was still the same but the difference between the two different casting times became larger. This can be seen in Figure 7.9.

Effect of casting time along bed
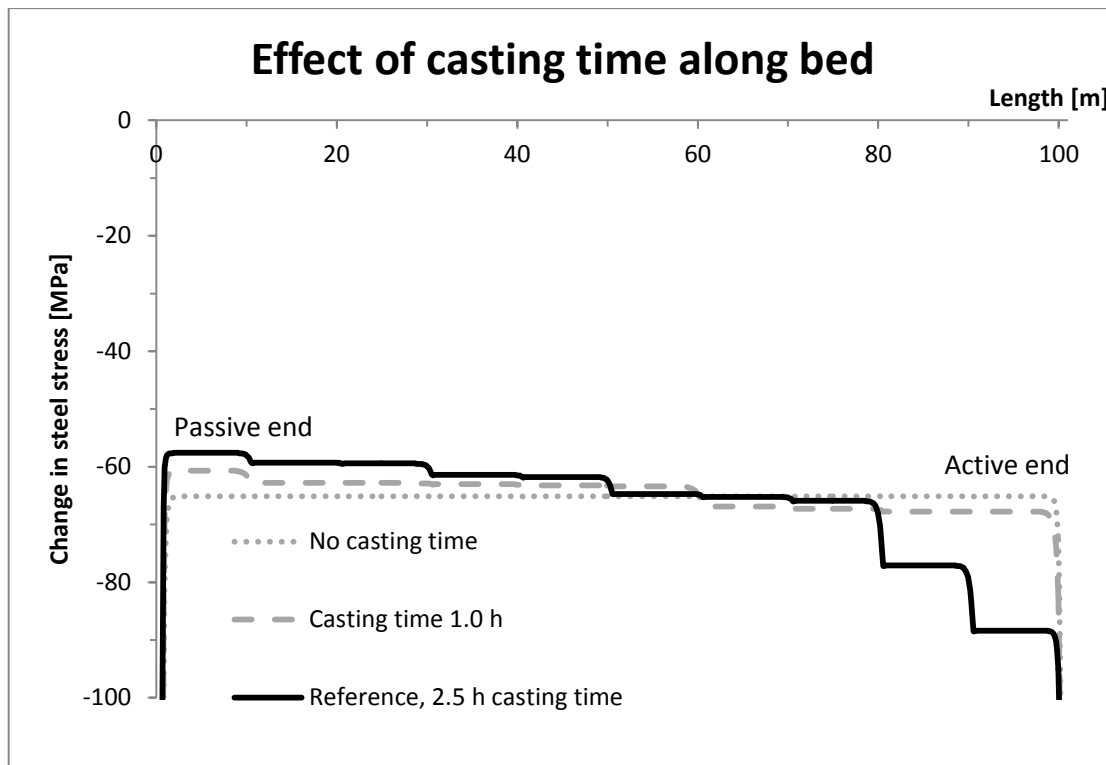
Figure 7.9.   Effect of casting time on accumulation along bed.

Figure 7.9 showed that the stress difference between the ends was greater in the reference analysis than the other two which showed quite similar prestress loss at the active end. It can be seen that the whole curve with 1 hour casting time was quite similar to the reference curve from the passive end to the centre of the bed, i.e. after 1 hour of casting. Then the process in the reference analysis continued and the prestress losses kept on increasing for the rest of the bed while the process was finished in the analysis with only 1 hour casting time and no more losses occurred. The analysis with 1 hour casting time finished before the temperature started to increase much in the passive side of the bed and therefore the prestress losses in the active end were not very great. Since the process in the reference analysis continued further, the temperature at the passive side of the bed had started to increase a lot more at the application of the bond at the active end which resulted in much greater prestress losses.

Therefore, it is assumed that the casting time affects the accumulation of stresses to a great extent because the temperature conditions in the whole bed when the bond starts to develop are very important. Hence, if the bond in all parts of the bed would start to develop before any great temperature increase occurred at the passive side, the accumulation effect would be minimised

8 Final remarks

8.1 Conclusions

Prestress losses that take place in concrete railway sleeper production with the long line method were studied. A numerical model was developed and analyses of the factories in Vislanda and Marijampolé were carried out and compared to measurements. The analyses were able to simulate the measurements from Vislanda quite well, both the shape of the curve and the magnitude of the prestress losses. In the analysis of Marijampolé, the shape of the curve was similar to the measurements but the magnitude of the prestress losses was less. A parameter study was performed which increased the understanding of the involved phenomenon and the following conclusions could be drawn:

- Concrete temperature from the hydration process was shown to be the main parameter affecting the prestress losses. Temperature increase in the system causes prestress loss.
- Initial temperature of the steel strand compared to the concrete temperature when cast on the wire, changes the prestress before the start of the hydration process. It was shown that a wire with a higher temperature than the concrete is a favourable situation.
- Different temperature development between the ends of the casting bed was shown to be an important parameter.
- The development of bond between steel and concrete affects the prestress to a great extent.
- Due to a long casting time, bond- and temperature properties are different between the ends. That was shown to cause accumulation of stresses towards the last cast end. This effect increases the prestress loss. The greatest accumulation occurs when a high temperature increase occurs before the bond starts to develop in the last cast end. For a long casting time, this is more likely to occur. When bond has started to develop in the entire bed, no more accumulation effects take place, and the prestress changes similarly all along the bed.
- When bond is present, a part of the thermal stresses are transferred to the concrete and therefore the prestress changes become less than without bond. For this reason, small prestress changes occur after bond has developed in the entire bed.

An important conclusion is that the difference between the measurements in Vislanda and Marijampolé is most likely due to the long casting time- and different temperature development between the ends in Marijampolé.

8.2 Further studies

Further studies are needed to understand why the magnitude of the measured prestress losses in Marijampolé is so large. Since only one measurement is available from Marijampolé and the magnitude of the losses is very different from Vislanda, it is advised to perform more measurements to confirm the reliability of the results. The only solution suggested in this thesis to explain the magnitude was that the coefficient of thermal expansion of concrete was large at the start of the bond development and

thereby the magnitude of the prestress loss was increased. However, further studies are needed to confirm the reliability of that.

The numerical model did not include the friction that the concrete experiences from the casting moulds. The friction is believed to affect the stress in the wire outside the concrete and therefore the results from the FE model in the wire outside are much higher than the measurements show. These high stresses are assumed to affect the transmission length which could therefore be longer than in reality. Further studies are needed to include the friction and solve this problem.

Not much research has been done regarding the development of bond during the hydration of the concrete. In order to model the bond behaviour more accurately, more experiments are needed.

The bed arrangement in Vislanda was modelled as a continuous bed while the real bed had small parts of "naked" wires between each four sleepers. The effect of this could be studied.

Further parameter studies could be performed using the numerical model developed in this thesis. Examples of interesting things to study could be the following:

- Length of the casting bed
- Variations of the casting sequence like casting from the centre of the bed or from both ends.
- Casting could be performed from the colder end towards the warmer end.
- The length of the "naked" wire could be varied.
- Shrinkage in concrete and relaxation in the steel strands could be included.

9   References

Abetong (2011): *Abetong Concrete Sleepers - The Long Line Method Success,* Abetong AB, Växjö, Sweden, 2011, pp. 1-7.

Andersen, M., Bolmsvik, R. (2011): *Measuring of prestress losses in Vislanda 2010.* Abetong AB, Växjö, Sweden, pp. 3-7.

Andersen, M. (2011): *Monitoring of the sleeper production in Marijampolé - Prestress losses and temperature in concrete.* Abetong AB, Växjö, Sweden, pp. 4-12.

ASM (2002): *Thermal properties of metals*, ASM Internatonal Material Properties Database Committee, Ohio, USA, 11 pp.

Bolmsvik, R. (2013): Personal communucation at a study trip to the Vislanda factory. Sweden, 09/12/2013.

Byfors, J. (1980): *Plain concrete at early ages.* Swedish Cement and Concrete Research Institute, Stockholm, Sweden, pp. 56, 100-104, 119-123, 155-161 230-231.

Carino, N.J., Lew, H.S. (2001): *The maturity method: From theory to application.* Building and Fire Research Laboratory, National Institue of Standards and Technology, Gaithersburg, USA, pp 3-4.

Carlsson, S., Holmbom, E. (2012). *Process induced prestress losses in long bed system for railway sleepers.* M.Sc. Thesis. Chalmers University of Technology, Department of Civil and Environmental Engineering, Publication no. 2012:86, Göteborg, Sweden.

DIANA (2011): *Diana user's manual; Element library.* TNO DIANA BV, Delft, Netherlands.

Domone, P., Illston, J. (2010): *Construction materials; Their nature and behaviour.* Spon Press, Abingdon, England, pp. 87, 90-99.

Elert, G. (n.d.): *Thermal expansion.* The Physics Hypertextbook, available at http://physics.info/expansion/, accessed 23/05/2014.

Engström, B. (2011a): *Design and analysis of prestressed concrete structures.* Chalmers University of Technology, Department of Civil and Environmental Engineering, Göteborg, Sweden, pp. 86-90.

Engström, B. (2011b): *Restraint cracking of reinforced concrete structures.* Chalmers University of Technology, Department of Civil and Environmental Engineering, Göteborg, Sweden, pp. 24, 30-34.

Gustavson, R. (2002): *Structural behaviour of concrete railway sleepers.* Ph.D. Thesis. Chalmers University of Technology, Department of Structural Engineering, Publication no. 02-6, Göteborg, Sweden, pp. 1-5.

Gustavson, R. (2004): Experimental studies of the bond response of three-wire strands and some influencing parameters. *Materials and structures*, Vol. 37, 2004, pp. 97, 105.

Kim, J.K., Kim, K.H., Yang, J.K. (2000): *Thermal analysis of hydration heat in concrete structures with pipe-cooling system.* Elsevier Science Ltd., South Korea, 2 pp.

Li, Z. (2011): *Advanced Concrete Technology.* Wiley, Hoboken, USA, pp. 23, 38-39, 41-42, 53-54.

Lundgren, M. (2005): *Development of strength and heat of hydration of young concrete at low temperature.* Lund Institude of Technology, Division of Building Materials, Lund, Sweden, pp. 11-15.

McCullough, B.F., Rasmussen, R.O. (1998): *Fast track paving: concrete temperature control and traffic opening criteria for bonded concrete overlays,* Vol. I, Transtec, Inc., Austin, USA, pp. 65-68.

Mehta, K., Monteiro, P. (1993): *Concrete; Structure, Properties, and Materials.* Prentice-Hall Inc., New Jersey, USA, pp. 47, 86.

Neville, A.M. (2003): *Properties of Concrete.* Pearson Prentice-Hall, Harlow, England, pp. 8, 12, 15, 17-18, 71-72.

Springenschmid, R. (1998): *Prevention of Thermal Cracking in Concrete at Early Ages.* E & FN Spon, London, England, pp. 84.

Train history. (n.d.): History of rail transport, available at http://www.trainhistory.net/railway-history/railroad-history/, accessed 9/04/2014.

APPENIDX A   ANALYTICAL MODEL

A.1 Matlab input file for analytical model

```
%% Input for verification of small scale model
% Name of file: Verification_input.m
% To be used with "Analytical_model.m", see appendix A.2
% Section 4.3.
% Based on measurements from Vislanda performed at 12/03/2010


%% Time
dt = 0.1;                         % Time step in hours
t_new = 0:dt:50;                  % Time vector [h]
t_cast = 2.5;                     % Time of casting [h]

%% Measured temperature of concrete
% Temperature measurements obtained from file
t = xlsread('Sammanställning av mätvärden 2010-03-12.xls'...
    ,'Blad1','T6:T404');
T = xlsread('Sammanställning av mätvärden 2010-03-12.xls'...
    ,'Blad1','S6:S404');

% Measured temperature adjusted to the time step
for i = 1:length(t_new)
    if t(1)>t_new(i)
        T_new(i)=T(1);
    else
    a = find(t<=t_new(i));
    T_new(i) = T(a(end));
    end
end
T=T_new;
T_max = max(T);                   % Maximumum temperature [°C]

%% Measured prestress
% Prestress measurements obtained from file
t = xlsread('Sammanställning av mätvärden 2010-03-12.xls'...
    ,'Blad1','A6:A4700');
str = xlsread('Sammanställning av mätvärden 2010-03-12.xls'...
    ,'Blad1','K6:K4700');

% Measured prestress adjusted to the time step
for i = 1:length(t_new)
    a = find(t<=t_new(i));
    str_new(i) = str(a(end));
end

si_si = 1343e6;                      % Initial prestress [Pa]
si_meas = si_si*(str_new-100)/100;  % Measured prestress change [Pa]
t = t_new;

%% Geometry
% Cross-sectional area
A_c = 0.2^2;                         % Concrete [m^2]
A_s = 3e-4;                          % Steel [m^2]

%% Young's Modulus of elasticity
E_s = 205e9;                         % Steel [Pa]
E_c = 38e9;                          % Concrete [Pa]
```

```matlab
%% Restraints
% Internal restraint/Bond
R_int = zeros(1,length(t));
% Bond development
t_0_int = 0;                        % Starting point [h]
t_1_int = 12.5;                     % Bond initiated [h]
t_2_int = 17.5;                     % End of bond development [h]
R_int_1 = 0.0;                      % Bond at initiation [ratio]
R_int_2 = 1.0;                      % Bond at end of development [ratio]

% Bond development
for i = 1:length(t)
    if t(i) <= t_0_int
        R_int(i) = 0;
    elseif t(i) <= t_1_int && t(i) > t_0_int
        R_int(i) = R_int_1*(t(i)-t_0_int)/(t_1_int-t_0_int);
    elseif t(i) <= t_2_int && t(i) > t_1_int
        R_int(i) = R_int_1+(R_int_2-R_int_1)...
            *(t(i)-t_1_int)/(t_2_int-t_1_int);
    elseif t(i) > t_2_int
        R_int(i) = R_int_2;
    end
end

% External restraint on concrete/friction to moulds
R_ext = ones(1,length(t));      % For fully fixed [ratio]
% R_ext = zeros(1,length(t));   % For free ends [ratio]

%% Thermal coefficients
TC_c = 12e-6;                       % Thermal coeff. of concrete [1/°C]
TC_s = 12e-6;                       % Thermal coeff. of steel [1/°C]

%% Run "Analytical_model.m"
Analytical_model
```

A.2 Matlab code for analytical model

```
%% Analytical model
% Name of file: Analytical_model.m
% Section 2.5
% Input from file "Verification_input.m", see appendix A.1


%% Case 1 - Concrete heating/cooling
% Input
alpha = E_s/E_c;                        % Ratio of E-modulus
A_I = A_c+(alpha-1)*A_s;                % Transformed concrete section

for i = 1:length(t)
    % Thermal strain
    if i == 1
        eps_cT1 = 0;
    else
        eps_cT1 = TC_c*(T(i)-T(i-1));
    end

    % Internal restraint force
    F_cs1 = -R_int(i)*E_s*eps_cT1*A_s;

    % External restraint force
    N_1 = -R_ext(i)*(eps_cT1*E_c*A_I - F_cs1);

    % Concrete stress change
    si_con1(i) = (N_1+F_cs1)/A_I;

    % Steel prestress change
    si_s1_e(i) = -F_cs1/A_s + R_int(i)*alpha*(N_1+F_cs1)/A_I;

    if i ~= 1
        si_con1(i) = si_con1(i-1)+si_con1(i);
        si_s1_e(i) = si_s1_e(i-1)+si_s1_e(i);
    end
end

%% Case 2 - Steel
for i = 1:length(t)
    % Thermal strain
    if i == 1
        eps_cT2 = 0;
    else
        eps_cT2 = TC_s*(T(i)-T(i-1));
    end

    % Internal restraint force
    F_cs2 = -R_int(i)*E_c*eps_cT2*(A_c-A_s);

    % External restraint force
    N_2 = R_ext(i)*(-eps_cT2*E_c*A_I-F_cs2);

    % Steel prestress change
    si_s2(i) = alpha*(N_2+F_cs2)/A_I;

    % Concrete stress change
    si_con2(i) = -F_cs2/(A_c-A_s) + R_int(i)*1/alpha*si_s2(i);
```

```
    if i ~= 1
        si_s2(i) = si_s2(i-1)+si_s2(i);
        si_con2(i) = si_con2(i-1)+si_con2(i);
    end
end


%% Results

%% Prestress change - Cases combined
% Analytical model results
si_e = si_s1_e+si_s2;                 % Total prestress change [Pa]
plot(t,si_e, 'b')
ylim([-2e8 1e8])
hold on
% Measurements results
plot(t,si_meas, '--k')
% Legend entries
xlabel('Time [h]')
ylabel('Prestress change [Pa]')
legend('Analytical model', 'Measurements', 3)


%% Figure showing input
figure
% Internal restraint/Bond
plot(t,R_int)
hold on
% External restraint
plot(t,R_ext, 'r')
% Temperature
plot(t,T/T_max, 'k')
% Legend entries
xlabel('Time [h]')
ylabel('Ratio')
legend('Internal restraint', 'External restraint', 'Temperature', 4)
```

APPENDIX B   SMALL SCALE MODEL

This appendix includes input files used in the development of the small scale model, including dat-, dcf-, f- and bat-files. Parts of the files have been reduced with "…" due to large amount of nodes and elements.

B.1   Temperature curve (Section 4.2.2)

Dat- file: for S10NSS

FEMGEN MODEL   : S10NSS

ANALYSIS TYPE   : Structural 2D

'UNITS'

LENGTH   M

TIME   HOUR

TEMPER   CELSIU

FORCE   N

'COORDINATES' DI=2

   1   0.000000E+00   0.000000E+00

   2   5.000000E-01   0.000000E+00

…   : Reduction of lines

  20   9.500000E+00   0.000000E+00

  21   1.000000E+01   0.000000E+00

'ELEMENTS'

CONNECTIVITY

  1 L2TRU 1 2

  2 L2TRU 2 3

…

  19 L2TRU 19 20

  20 L2TRU 20 21

MATERIALS

/ 1-20 / 1

GEOMETRY

/ 1-20 / 1

'MATERIALS'

  1 YOUNG   2.050000E+11   : Steel wire

   POISON   3.000000E-01

   THERMX   1.200000E-05

'GEOMETRY'
  1 CROSSE   3.000000E-04
'SUPPORTS'
 / 1 21 / TR   1
 / 1 21 / TR   2
'TEMPER'
NODES
: Temperature presented with time step of 2.5 hours to reduce size,
: real time step was 0.1 hour
   0 2.5 5 7.5 10 12.5 15 17.5 20 22.5 25 27.5 30 32.5 35 37.5 40 42.5 45 47.5 50
/1-21/
    12 12 15 16 18 25 45 43 40 36 33 31 29 27 25 24 23 22 21 20 20
'DIRECTIONS'
   1   1.000000E+00   0.000000E+00   0.000000E+00
   2   0.000000E+00   1.000000E+00   0.000000E+00
   3   0.000000E+00   0.000000E+00   1.000000E+00
'END'

Dcf- file: for S10NSS
*FILOS
 INITIA
*INPUT
 READ FILE "S10NSS.dat"
*END
*NONLIN
 EXECUT TIME STEPS EXPLIC SIZES 0 0.1(500)
: Size of time step and number of timesteps
 OUTPUT FILE "S10NSS"
*END

B.2   Bond between steel and concrete (Section 4.2.3)

Bat- file: for S80SUB, Code for creating the geometry and parameters.

```
UTILITY SETUP UNITS LENGTH METER
UTILITY SETUP UNITS MASS KILOGRAM
UTILITY SETUP UNITS FORCE NEWTON
UTILITY SETUP UNITS TIME HOUR
UTILITY SETUP UNITS TEMPERATURE CELSIUS
GEOMETRY POINT COORD P1 0
```

GEOMETRY POINT COORD P2 10 0
GEOMETRY POINT COORD P3 10 .1
GEOMETRY POINT COORD P4 0 .1
GEOMETRY POINT COORD P5 0 .1
GEOMETRY POINT COORD P6 10 .1
GEOMETRY POINT COORD P7 10 .2
GEOMETRY POINT COORD P8 0 .2
GEOMETRY POINT COORD P9 -.5 .1
GEOMETRY POINT COORD P10 10.5 .1
EYE FRAME
GEOMETRY LINE STRAIGHT L1 P9 P5
GEOMETRY LINE STRAIGHT L2 P5 P6
GEOMETRY LINE STRAIGHT L3 P6 P10
GEOMETRY SURFACE 4POINTS S1 P1 P2 P3 P4
GEOMETRY SURFACE 4POINTS S2 P4 P3 P7 P8
GEOMETRY SURFACE 4POINTS S3 P4 P3 P6 P5
EYE FRAME
MESHING TYPES ALL QU4 Q8MEM
MESHING DIVISION L1 1
MESHING DIVISION L2 80
MESHING DIVISION L3 1
MESHING DIVISION L4 80
MESHING DIVISION L5 1
MESHING DIVISION L6 80
MESHING DIVISION L7 1
MESHING DIVISION L8 1
MESHING DIVISION L9 80
MESHING DIVISION L10 1
MESHING DIVISION L11 1
MESHING DIVISION L12 1
MESHING TYPES L1 BE2 L2TRU
MESHING TYPES L2 BE2 L2TRU
MESHING TYPES L3 BE2 L2TRU
MESHING TYPES S3 IL22 L8IF
MESHING GENERATE

PROPERTY MATERIAL MA1 ELASTIC ISOTROP 38E9 0.2
PROPERTY MATERIAL MA1 THERCONC ISOTROP 12E-6 0
PROPERTY MATERIAL MA2 ELASTIC ISOTROP 205E9 0.3
PROPERTY MATERIAL MA2 THERCONC ISOTROP 12E-6 0
PROPERTY MATERIAL MA3 ELASTIC INTERFAC 7.85E18 10.0E10
PROPERTY PHYSICAL PH1 GEOMETRY PLANSTRS THREGULR 0.2
PROPERTY PHYSICAL PH2 GEOMETRY TRUSCABL 3E-4
PROPERTY PHYSICAL PH3 GEOMETRY INTERFAC LINE BONDSL 0.057
PROPERTY MATERIAL MA4 ELASTIC ISOTROP 205E9 0.3
PROPERTY MATERIAL MA4 THERCONC ISOTROP 12E-6 0
PROPERTY ATTACH S1 MA1
PROPERTY ATTACH S1 PH1
PROPERTY ATTACH S2 MA1
PROPERTY ATTACH S2 PH1

PROPERTY ATTACH S3 MA3
PROPERTY ATTACH S3 PH3
PROPERTY ATTACH L2 MA2
PROPERTY ATTACH L2 PH2
PROPERTY ATTACH L1 MA4
PROPERTY ATTACH L1 PH2
PROPERTY ATTACH L3 MA4
PROPERTY ATTACH L3 PH2
PROPERTY BOUNDARY CONSTRAINT CO1 P9 X
PROPERTY BOUNDARY CONSTRAINT CO2 P9 Y
PROPERTY BOUNDARY CONSTRAINT CO3 P10 X
PROPERTY BOUNDARY CONSTRAINT CO4 P10 Y

Dat- file: for S80SUB

FEMGEN MODEL   : S80SUB

ANALYSIS TYPE   : Structural 2D

'UNITS'

LENGTH   M

TIME   HOUR

TEMPER   CELSIU

FORCE   N

'COORDINATES' DI=2

```
    1    -5.000000E-01    1.000000E-01
    2     0.000000E+00    1.000000E-01
    3     1.250000E-01    1.000000E-01
  …
   81     9.875000E+00    1.000000E-01
   82     1.000000E+01    1.000000E-01
   83     1.050000E+01    1.000000E-01
   84     0.000000E+00    0.000000E+00
   85     1.250000E-01    0.000000E+00
  …
  163     9.875000E+00    0.000000E+00
  164     1.000000E+01    0.000000E+00
  165     0.000000E+00    1.000000E-01
  166     1.250000E-01    1.000000E-01
  …
  243     9.750000E+00    1.000000E-01
  244     9.875000E+00    1.000000E-01
```

```
  245    1.000000E+01    1.000000E-01
  246    0.000000E+00    2.000000E-01
  247    1.250000E-01    2.000000E-01
…
  325    9.875000E+00    2.000000E-01
  326    1.000000E+01    2.000000E-01
'ELEMENTS'
CONNECTIVITY
   1 L2TRU  1 2                          : Steel wire elements
   2 L2TRU  2 3
   3 L2TRU  3 4
…
  80 L2TRU  80 81
  81 L2TRU  81 82
  82 L2TRU  82 83
  83 Q8MEM  84 85 166 165               : Concrete elements
  84 Q8MEM  85 86 167 166
…
 241 Q8MEM  243 244 325 324
 242 Q8MEM  244 245 326 325
 243 L8IF   165 166 2 3                  : Interface elemetns
 244 L8IF   166 167 3 4
…
 321 L8IF   243 244 80 81
 322 L8IF   244 245 81 82
MATERIALS
/ 83-242 /  1
/ 2-81 /  2
/ 243-322 /  3
/ 1 82 /  4
GEOMETRY
/ 83-242 /  1
/ 1-82 /  2
/ 243-322 /  3
'MATERIALS'
```

```
 1 YOUNG    3.800000E+10
  POISON   2.000000E-01
  THERMX   1.200000E-05
 2 YOUNG    2.050000E+11
  POISON   3.000000E-01
  THERMX   1.200000E-05
 3 DSTIF    7.850000E+18   1.000000E+11
  USRIFC   BAGE                                       : Subroutine
:              t_start, t_end
  USRVAL   12.5     17.5                              : Input for subroutine
  USRSTA   0
 4 YOUNG    2.050000E+11
  POISON   3.000000E-01
  THERMX   1.200000E-05
'GEOMETRY'
 1 THICK    2.000000E-01
 2 CROSSE   3.000000E-04
 3 THICK    5.700000E-02
  CONFIG BONDSL
'SUPPORTS'
 / 1 83 /   TR    1
 / 1 83 /   TR    2
'TEMPER'
ELEMEN
  0.0 0.1 0.2 0.3 … 50
/1-80 83-242/                              : Heating of concrete & steel
  19.8 19.8 19.8 … 20.5                    : See temperature curve in Figure 4.5
'DIRECTIONS'
 1   1.000000E+00   0.000000E+00   0.000000E+00
 2   0.000000E+00   1.000000E+00   0.000000E+00
 3   0.000000E+00   0.000000E+00   1.000000E+00
'END'
```

Subroutine code

Subroutine code was constructed to model the development of bond stiffness with time. It was modelled to be zero up to a certain time (USRVAL(1)) and increase linearly to another predefined time (USRVAL(2)) where it reached maximum constant value (DSTIF(2)).
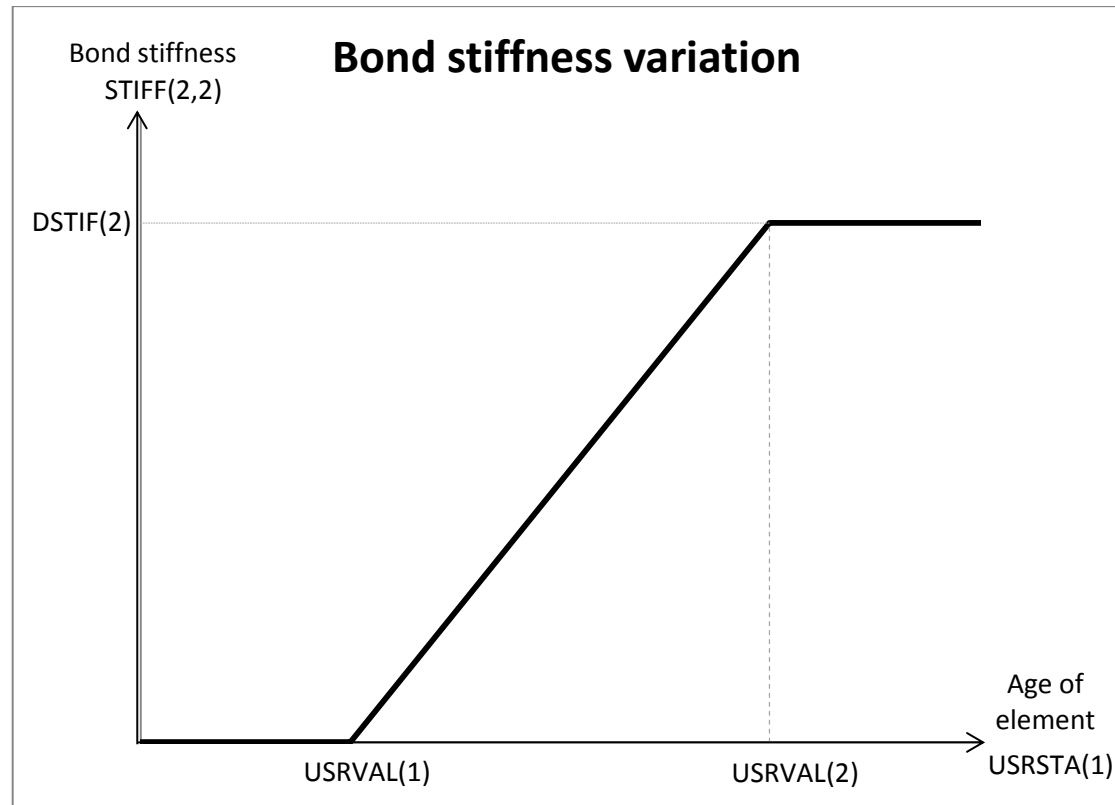
Figure B.1.   Bond stiffness as a function of element age.

*** **Subroutine that varies bond stiffness depending on element age**

```
    SUBROUTINE USRIFC( U0, DU, NT, AGE0, DTIME, TEMP0, DTEMP,
$        ELEMEN, INTPT, COORD, SE, ITER, USRMOD, USRVAL, NUV,
$        USRSTA, NUS, USRIND, NUI, TRA, STIFF )


    INTEGER   NUI, NT, NUV, USRIND(NUI),ELEMEN, INTPT,  ITER, NUS,
$        TE
  CHARACTER*6  USRMOD
  DOUBLE PRECISION    U0(NT), DU(NT), AGE0, TRA(NT), STIFF(NT,NT),
$        USRVAL(NUV), USRSTA(NUS), DSTIF(2)
```

: Check if subroutine is used for correct elements

```
IF (USRMOD .NE. 'BAGE') THEN
  PRINT *, 'No model chosen in the inputfile'
  CALL PRGERR ('USRIFC', 1)
ENDIF
IF (NT .NE. 2 ) THEN
  PRINT *, 'Model can only be used in line interface element'
  CALL PRGERR ('USRIFC', 2)
ENDIF

CALL GTC( '../MATERI/DSTIF', DSTIF, 2 )
STIFF(1,1)= DSTIF(1)
STIFF(2,1)= 0.0
STIFF(1,2)= 0.0

TRA(1) = TRA(1) + STIFF(1,1)*DU(1) + STIFF(1,2)*DU(2)


: Age of element being calculated
          USRSTA(1) = AGE0


: Linear increase of bond stiffness from zero to maximum value
  IF (USRSTA(1) .GE. USRVAL(2)) THEN
    STIFF(2,2) = DSTIF(2)
  ELSEIF (USRSTA(1) .LE. USRVAL(1)) THEN
        STIFF(2,2) = 0.0
  ELSE
        STIFF(2,2) = DSTIF(2)*(USRSTA(1)-USRVAL(1))/(USRVAL(2)-
                  USRVAL(1))
  ENDIF


: Total bond stress
  TRA(2) = TRA(2) + STIFF(2,2)*DU(2)

  CALL PRIVAL(ELEMEN,  'Element number')
  CALL PRIVAL(USRSTA(1), 'Element age')
  CALL PRIVAL(DU(2), 'Relative displacement (slip)')
```

```
      CALL PRIVAL(DTIME, 'Time step')
      CALL PRIVAL(STIFF(2,2), 'Bond stiffness')
      CALL PRIVAL(TRA(2), 'Bond stress')
      END
```

dcf- file: for S80SUB

```
*FILOS
 INITIA
*INPUT
 READ  FILE "S80SUB.dat"
*FORTRAN
 TAKE "usrifc.f"
*NONLIN
 BEGIN EXECUT
   TIME  STEPS  EXPLIC  SIZES 0 0.1(500)
 END EXECUT
 BEGIN OUTPUT
   FILE "S80SUB"
   STRESS  TOTAL  CAUCHY  GLOBAL          : Element stresses
   STRESS  TOTAL  TRACTI  LOCAL           : Bond stresses
 END OUTPUT
*END
```

B.3   Accumulation effects (Section 4.2.7)

The accumulation model used the same bat- dcf- file as the model for bond between steel and concrete.

Dat- file: for S80SUBA. Same dat file as for bond between steel and concrete in B.2 using the following material and temper input.

```
'MATERIALS'
  1 YOUNG    3.800000E+10
    POISON   2.000000E-01
    THERMX   1.200000E-05
  2 YOUNG    2.050000E+11
    POISON   3.000000E-01
    THERMX   1.200000E-05
  3 DSTIF    7.850000E+18   1.000000E+11
```

```
   USRIFC    BAGE
:                 t_start, t_end, First interf. ele., No. of elem. in each step, Casting steps
   USRVAL   12.5   17.5    243              8                          10
   USRSTA   0 0 0
 4 YOUNG    2.050000E+11
   POISON   3.000000E-01
   THERMX   1.200000E-05
'TEMPER'
ELEMEN
   0.0 0.1 0.2 0.3 … 50.0
: Heating of Concrete & Steel x=0-1m (passive end)
/2-9 83-90 163-170/
   19.8 19.8 19.8 …                    : See temperature curves in Figure 4.13
: Heating of Concrete & Steel x=1-2m
/10-17 91-98 171-178/
   19.8 19.8 19.8 …
: Heating of Concrete & Steel x=2-3m
/18-25 99-106 179-186/
   19.8 19.8 19.8 …

…
: Heating of Concrete & Steel x=8-9m
/66-73 147-154 227-234/
   19.8 19.8 19.8 …
: Heating of Concrete & Steel x=9-10m (active end)
/74-81 155-162 235-242/
   19.8 19.8 19.8 …                     : See temperature curves in Figure 4.13
'DIRECTIONS'
  1  1.000000E+00   0.000000E+00   0.000000E+00
  2  0.000000E+00   1.000000E+00   0.000000E+00
  3  0.000000E+00   0.000000E+00   1.000000E+00
'END'
```

Subroutine

This subroutine is structured as the previous subroutine in appendix B.2 see Figure B.1. However this subroutine takes into account the age of the element by its position in the bed, for that reason, age of elements are now USRSTA(3). The model is divided into 10 casting steps (USRVAL(5)), where each part is one time step younger than its part on the left side.

*** Subroutine that varies bond stiffness

*** depending on element age and position in bed

```
   SUBROUTINE USRIFC( U0, DU, NT, AGE0, DTIME, TEMP0, DTEMP,
  $      ELEMEN, INTPT, COORD, SE, ITER, USRMOD, USRVAL, NUV,
  $      USRSTA, NUS, USRIND, NUI, TRA, STIFF )


   INTEGER  NUI, NT, NUV, USRIND(NUI),ELEMEN, INTPT,  ITER, NUS,
  $      TE
   CHARACTER*6  USRMOD
   DOUBLE PRECISION    U0(NT), DU(NT), AGE0, TRA(NT), STIFF(NT,NT),
  $      USRVAL(NUV), USRSTA(NUS), DSTIF(2)


: Check if subroutine is used for correct elements
   IF (USRMOD .NE. 'BAGE') THEN
     PRINT *, 'No model chosen in the inputfile'
     CALL PRGERR ('USRIFC', 1)
   ENDIF
   IF (NT .NE. 2 ) THEN
     PRINT *, 'Model can only be used in line interface element'
     CALL PRGERR ('USRIFC', 2)
   ENDIF


   CALL GTC( '../MATERI/DSTIF', DSTIF, 2 )
   STIFF(1,1)= DSTIF(1)
   STIFF(2,1)= 0.0
   STIFF(1,2)= 0.0
   TRA(1) = TRA(1) + STIFF(1,1)*DU(1) + STIFF(1,2)*DU(2)
```

: Age of element calculated. USRSTA(1) interface element number from 0-799

        USRSTA(1) = ELEMEN - USRVAL(3)

: Position of element, part 1 - 10

        USRSTA(2) = AINT(USRSTA(1)/USRVAL(4)) + 1

: Age of element according to position

        USRSTA(3) = AGE0 + (USRVAL(5) - USRSTA(2)) * DTIME

: Linear increase of bond stiffness from zero to maximum value

        IF (USRSTA(3) .GE. USRVAL(2)) THEN

          STIFF(2,2) = DSTIF(2)

        ELSEIF (USRSTA(3) .LE. USRVAL(1)) THEN

          STIFF(2,2) = 0.0

        ELSE

          STIFF(2,2) = 0.0+DSTIF(2)*(USRSTA(3)-USRVAL(1))/(USRVAL(2)-
                        USRVAL(1))

        ENDIF

: Total bond stress

        TRA(2) = TRA(2) + STIFF(2,2)*DU(2)

        CALL PRIVAL(ELEMEN, 'Element number')

        CALL PRIVAL(USRSTA(1), 'Number of bond element')

        CALL PRIVAL(USRSTA(3), 'Element age')

        CALL PRIVAL(DU(2), 'Relative displacement (slip)')

        CALL PRIVAL(DTIME, 'Time step')

        CALL PRIVAL(STIFF(2,2), 'Bond stiffness')

        CALL PRIVAL(TRA(2), 'Bond stress')

        END

APPENDIX C   FULL SCALE MODEL

C.1   Vislanda model

Bat- file: for FV3-12, Code for creating the geometry and material parameters.

```
UTILITY SETUP UNITS LENGTH METER
UTILITY SETUP UNITS MASS KILOGRAM
UTILITY SETUP UNITS FORCE NEWTON
UTILITY SETUP UNITS TEMPERATURE CELSIUS
GEOMETRY POINT COORD P1 0 0
GEOMETRY POINT COORD P2 0 .1
GEOMETRY POINT COORD P3 0 .2
GEOMETRY POINT COORD P4 0 .1
GEOMETRY POINT COORD P5 10 0
GEOMETRY POINT COORD P6 10 .1
GEOMETRY POINT COORD P7 10 .2
GEOMETRY POINT COORD P8 10 .1

…
GEOMETRY POINT COORD P41 100 0
GEOMETRY POINT COORD P42 100 .1
GEOMETRY POINT COORD P43 100 .2
GEOMETRY POINT COORD P44 100 .1
GEOMETRY POINT COORD P45 -0.5 .1
GEOMETRY POINT COORD P46 100.5 .1


EYE FRAME
GEOMETRY SURFACE 4POINTS S1 P1 P5 P6 P2
GEOMETRY SURFACE 4POINTS S2 P2 P6 P7 P3

…
GEOMETRY SURFACE 4POINTS S19 P37 P41 P42 P38
GEOMETRY SURFACE 4POINTS S20 P38 P42 P43 P39


GEOMETRY LINE STRAIGHT L53 P45 P4
GEOMETRY LINE STRAIGHT L54 P4 P8
GEOMETRY LINE STRAIGHT L55 P8 P12
GEOMETRY LINE STRAIGHT L62 P36 P40
GEOMETRY LINE STRAIGHT L63 P40 P44

GEOMETRY LINE STRAIGHT L64 P44 P46


GEOMETRY SURFACE 4POINTS S21 P2 P6 P8 P4
GEOMETRY SURFACE 4POINTS S22 P6 P10 P12 P8

…
GEOMETRY SURFACE 4POINTS S29 P34 P38 P40 P36
GEOMETRY SURFACE 4POINTS S30 P38 P42 P44 P40


EYE FRAME
MESHING TYPES ALL QU4 Q8MEM
MESHING DIVISION L1 80
MESHING DIVISION L2 1
```

MESHING DIVISION L3 80
MESHING DIVISION L4 1
…
MESHING DIVISION L51 1
MESHING DIVISION L52 80

MESHING DIVISION L53 5
MESHING DIVISION L54 80
MESHING DIVISION L55 80
…
MESHING DIVISION L63 80
MESHING DIVISION L64 5

MESHING DIVISION L65 1
MESHING DIVISION L66 1
…
MESHING DIVISION L75 1

MESHING TYPES L53 BE2 L2TRU
MESHING TYPES L54 BE2 L2TRU
…
MESHING TYPES L64 BE2 L2TRU

MESHING TYPES S21 IL22 L8IF
MESHING TYPES S22 IL22 L8IF
…
MESHING TYPES S30 IL22 L8IF
MESHING GENERATE

PROPERTY MATERIAL MCONC ELASTIC ISOTROP 38E9 0.2
PROPERTY MATERIAL MCONC THERCONC ISOTROP 12E-6 0
PROPERTY MATERIAL MSTEEL ELASTIC ISOTROP 205E9 0.3
PROPERTY MATERIAL MSTEEL THERCONC ISOTROP 12E-6 0
PROPERTY MATERIAL MINT ELASTIC INTERFAC 7.85E18 6.25E10
PROPERTY PHYSICAL PCONC GEOMETRY PLANSTRS THREGULR 0.2
PROPERTY PHYSICAL PSTEEL GEOMETRY TRUSCABL 3.2731E-4
PROPERTY PHYSICAL PINT GEOMETRY INTERFAC LINE BONDSL 0.214

PROPERTY ATTACH S1 MCONC
PROPERTY ATTACH S1 PCONC
PROPERTY ATTACH S2 MCONC
PROPERTY ATTACH S2 PCONC
…
PROPERTY ATTACH S20 MCONC
PROPERTY ATTACH S20 PCONC

PROPERTY ATTACH S21 MINT
PROPERTY ATTACH S21 PINT
PROPERTY ATTACH S22 MINT
PROPERTY ATTACH S22 PINT

…
PROPERTY ATTACH S30 MINT
PROPERTY ATTACH S30 PINT

PROPERTY ATTACH L53 MSTEEL
PROPERTY ATTACH L53 PSTEEL
PROPERTY ATTACH L54 MSTEEL
PROPERTY ATTACH L54 PSTEEL
…
PROPERTY ATTACH L64 MSTEEL
PROPERTY ATTACH L64 PSTEEL

PROPERTY BOUNDARY CONSTRAINT CO1 P45 X
PROPERTY BOUNDARY CONSTRAINT CO2 P45 Y
PROPERTY BOUNDARY CONSTRAINT CO3 P46 X
PROPERTY BOUNDARY CONSTRAINT CO4 P46 Y

Dat- file: for FV3-12

FEMGEN MODEL   : FV3-12

ANALYSIS TYPE   : Structural 2D

'UNITS'

LENGTH   M

TIME   SEC

TEMPER   CELSIU

FORCE   N

'COORDINATES' DI=2

   1   -5.000000E-01   1.000000E-01

   2   -4.000000E-01   1.000000E-01

…

   6   0.000000E+00   1.000000E-01

   7   1.250000E-01   1.000000E-01

   8   2.500000E-01   1.000000E-01

…

 805   9.987500E+01   1.000000E-01

 806   1.000000E+02   1.000000E-01

 807   1.001000E+02   1.000000E-01

 808   1.002000E+02   1.000000E-01

…

 811   1.005000E+02   1.000000E-01

 812   0.000000E+00   0.000000E+00

813	1.250000E-01	0.000000E+00
814	2.500000E-01	0.000000E+00
…		
892	1.000000E+01	0.000000E+00
893	0.000000E+00	1.000000E-01
894	1.250000E-01	1.000000E-01
895	2.500000E-01	1.000000E-01
…		
972	9.875000E+00	1.000000E-01
973	1.000000E+01	1.000000E-01
974	0.000000E+00	2.000000E-01
975	1.250000E-01	2.000000E-01
…		
1053	9.875000E+00	2.000000E-01
1054	1.000000E+01	2.000000E-01
1055	1.012500E+01	0.000000E+00
1056	1.025000E+01	0.000000E+00
…		
…		
3213	9.987500E+01	2.000000E-01
3214	1.000000E+02	2.000000E-01

'ELEMENTS'
CONNECTIVITY
  1 L2TRU 1 2
  2 L2TRU 2 3
…
 809 L2TRU 809 810
 810 L2TRU 810 811
 811 Q8MEM 812 813 894 893
 812 Q8MEM 813 814 895 894
…
2409 Q8MEM 3132 3133 3213 3212
2410 Q8MEM 3133 3134 3214 3213
2411 L8IF   893 894 6 7
2412 L8IF   894 895 7 8

…

 3209 L8IF   3132 3133 804 805
 3210 L8IF   3133 3134 805 806
MATERIALS
/ 811-2410 / 1
/ 1-810 / 2
/ 2411-3210 / 3
GEOMETRY
/ 811-2410 / 1
/ 1-810 / 2
/ 2411-3210 / 3
'MATERIALS'
   1 YOUNG   3.800000E+10
    POISON   2.000000E-01
    THERMX   1.200000E-05
   2 YOUNG   2.050000E+11
    POISON   3.000000E-01
    THERMX   1.200000E-05
   3 DSTIF   7.850000E+18   6.250000E+10
    USRIFC   BAGE
:   t_start, t_end, First interf. ele., No. of elem. in each step, Casting steps
    USRVAL 12.5   17.5   2411   80   10
    USRSTA   0 0 0
'GEOMETRY'
   1 THICK   2.000000E-01
   2 CROSSE   3.273100E-04
   3 THICK   2.130000E-03
    CONFIG BONDSL
'SUPPORTS'
 / 1 811 /   TR   1
 / 1 811 /   TR   2
'TEMPER'
ELEMEN
    0.0 0.1 0.2 0.3 0.4 0.5 … 50.0
: Heating of Concrete & Steel x=0-10m (passive end)

/ 6-85 811-970 /

   19.8 19.8 19.8 …   : See temperature curves in Figure 5.1

: Heating of Concrete & Steel x=10-20m

/ 86-165 971-1130 /

   19.8 19.8 19.8 …

…   : Temperature curves are shifted one time step for each part

: Heating of Concrete & Steel x=80-90m

/ 646-725 2091-2250 /

   19.8 19.8 19.8 …

: Heating of Concrete & Steel x=90-100m (active end)

/ 726-805 2251-2410 /

   19.8 19.8 19.8 …   : See temperature curves in Figure 5.1

'DIRECTIONS'

   1   1.000000E+00   0.000000E+00   0.000000E+00

   2   0.000000E+00   1.000000E+00   0.000000E+00

   3   0.000000E+00   0.000000E+00   1.000000E+00

'END'

Dcf- file: for FV3-12

*FILOS

 INITIA

*INPUT

 READ FILE "FV3-12.dat"

*FORTRAN

 TAKE "usrifc.f"

*NONLIN

 BEGIN EXECUT

  TIME STEPS EXPLIC SIZES 0 0.1(500)

  ITERAT MAXITE 30   : Iterations 30 for each time step

 END EXECUT

 BEGIN OUTPUT

  FILE "FV3-12"

  STRESS TOTAL CAUCHY GLOBAL

  STRESS TOTAL TRACTI LOCAL

 END OUTPUT

*END

C.2   Marijampolé model

The Marijampolé model was created with the same bat- file as the Vislanda model

Dat- file: for FM. Same dat- file as for Vislanda in C.1 but with this material, geometry and temper input.

'MATERIALS'

  1 YOUNG   3.800000E+10

   POISON   2.000000E-01

   THERMX   1.200000E-05

  2 YOUNG   2.050000E+11

   POISON   3.000000E-01

   THERMX   1.200000E-05

  3 DSTIF   7.850000E+18   6.250000E+10

   USRIFC   BAGE

:   t_start, t_end, First interf. ele., No. of elem. in each step, Casting steps

   USRVAL 7.5   14   2411   80   10

   USRSTA   0 0 0

'GEOMETRY'

  1 THICK   2.000000E-01

  2 CROSSE   2.806000E-04

  3 THICK   21.40000E-02

   CONFIG BONDSL

'TEMPER'

ELEMEN

   0.00 0.25 0.50 0.75 1.00 1.25 … 21.50

: Heating of Concrete & Steel x=0-10m (passive end)

/ 6-85 811-970 /

   7.6 7.6 16.0 26.4 …   : See temperature curves in Figure 5.2

: Heating of Concrete & Steel x=10-20m

/ 86-165 971-1130 /

   7.5 7.5 7.5 7.5 25.0 …

: Heating of Concrete & Steel x=20-30m

/ 166-245 1131-1290 /

   7.4 7.4 7.4 7.4 7.4 24….

: Heating of Concrete & Steel x=80-90m

/ 646-725 2091-2250 /

   6.8 6.8 6.8 6.8 6.8 6.8 …

: Heating of Concrete & Steel x=90-100m (active end)

/ 726-805 2251-2410 /

   6.7 6.7 6.7 6.7 6.7 6.7 …   : See temperature curves in Figure 5.2

Dcf- file: for FM

*FILOS

 INITIA

*INPUT

 READ FILE "FM.dat"

*FORTRAN

 TAKE "usrifc.f"   : Include the subroutine

*NONLIN

 EXECUT TIME STEPS EXPLIC SIZES 0 0.25(86)

: Length of time steps and number of time steps

 BEGIN OUTPUT

  FILE "FM"

  STRESS TOTAL CAUCHY GLOBAL

  STRESS TOTAL TRACTI LOCAL

 END OUTPUT

*END